EVALUATION OF LAND, SOIL, WATER, AND VEGETATION-RELATED ECOSYSTEM SERVICES AND TRADEOFFS AT UTLITY-SCALE SOLAR PHOTOVOLTAIC FACILITIES

A Dissertation
Submitted to
the Temple University Graduate Board

In Partial Fulfillment
of the Requirements for the Degree
[DOCTOR OF PHILOSOPHY IN GEOSCIENCES]

---

by
Chong Seok Choi
May 2024

Examining Committee Members:

Sujith Ravi, Advisory Chair, Earth and Environmental Science
Bojeong Kim, Earth and Environmental Science
Nicholas Davatzes, Earth and Environmental Science
Rachel Spigler, Department of Biology

ABSTRACT

Solar photovoltaics are a low-emission electricity source, but utility-scale development of ground-mounted PV may displace natural or agricultural land and compromise the land's ability to provide ecosystem services. Co-locating solar photovoltaics with vegetation (sometimes referred to as "agrivoltaics") could provide a sustainable solution to meet growing food and energy demands while minimizing the land-use impacts of solar energy. Pilot-scale experiments and modeling studies have shown potential for microclimatic alterations by the solar photovoltaics (PV) and the soil-vegetation components of a co-located system to benefit each other. One predicted co-benefit is cooling of PV modules caused by diversion of sensible heat to latent heat for evapotranspiration in the understory vegetation during the growing season. Field experiments that validate the theorized co-benefits within a utility-scale co-located system are less common. Since a large percentage of current and future land use conversions for utility-scale solar energy developments are estimated to occur on farmlands, validation of co-benefits in utility-scale co-located systems are critical for determining the outcome of co-location in a wide range of physical conditions and optimizing the system design for the environmental co-benefits.

In the first study of its kind and scale, three years (2019 – 2021) of microclimate and soil data at three vegetated utility-scale solar plants in Minnesota were tied to the power output data from the corresponding period to examine the influence of ground cover on the PV performance and that of the arrays on the underlying soil and vegetation. Soil moisture, soil temperature, air temperature, relative humidity, wind direction/speed were recorded at a 15-minute interval at three treatments: PV arrays with a vegetated ground cover ("veg

PV"), PV arrays with a bare ground cover ("bare PV"), and a nearby open space with the same vegetation as that in veg PV (control). Solar irradiance and cumulative precipitation were also recorded in the control. While air temperature and relative humidity were not significantly different between the veg PV and the bare PV, soil moisture was lowest in the bare PV treatment and comparable between the veg PV and the control. Soil moisture also varied spatially along the transect perpendicular to the array, though the spatial distribution was not consistent between the treatments and different facilities. Soil temperature was the lowest in the veg PV and the highest in the control, implying that the partial shade from the solar array keeps the underlying soils cooler. Cooler soil temperature in PV arrays could be a buffer for plants during periods of drought, which implies that co-located systems could be implemented in ecosystem restoration projects for climate resilience.

In addition to the microclimate variables, panel temperature was also recorded at veg PV and bare PV treatments and electricity generation data from the corresponding treatments during the study period was provided by the operators of the facilities. Neither vegetation-driven panel cooling nor the increased power output was observed in the veg PV: the bare PV had higher output and panel temperatures than the veg PV in the early mornings, which may imply that the observed difference in output may be due to shading of the panels in the veg PV treatment by the co-located vegetation. The differential of total daily production (bare PV – veg PV) was positive on most days, though the mode in a frequency distribution of the differential was centered around a very small positive value. The lack of panel-cooling in the veg PV was determined to be due to the short rainfall interval (1-2 days) during the study period. Because of the frequent rainfalls, evaporation in the bare PV treatment and evapotranspiration process in the veg PV treatment remained

in an energy-limited stage, and the water would evaporate more rapidly from the bare soil that is more exposed to sunlight and wind. In a drier environment with infrequent rainfalls, evaporation and evapotranspiration would be moisture-limited most of the times, and plants may be able to transpire water from deeper in the soil over a longer period of time to cool the overlying panels, given enough irrigation. The lack of panel cooling in our field sites implies that such environmental co-benefits are likely to be climate dependent, which indicates the need for further study of the influence of the vegetation on the PV operation and vice-versa at large-scale solar facilities in varying climate zones.

Soil samples were also collected for grain size analysis using laser diffraction and nutrient analysis using standard combustion methods. In the sandy soils at the Chisago facility, the bare PV treatment had significantly less clay portion than the veg PV treatment and the control. On the other hand, the clay percentages did not significantly differ among the three treatments in the other two facilities with higher background clay contents (Atwater and Eastwood). The loss in total carbon, nitrogen, and soil cations was also the most pronounced in the bare PV in a facility with the sandy soil. Maintenance of vegetation or re-vegetation while minimizing land grading may protect the soil's ability to store carbon and nutrients, and that effect may be magnified in coarse-textured soils or ones whose carbon and nutrient storage capacity is otherwise compromised. Overall, the field investigation found that the occurrence of some of the environmental co-benefits of co-locating PV with vegetation depended on the climate and soil, prompting a need for case-by-case consideration of these variables to identify which of the co-benefits will be achievable.

Extensive solar PV development to meet energy demand and decarbonize the energy grid will significantly impact the landscape. Co-location offers an opportunity to mitigate the potential negative impacts of utility-scale solar energy, while still meeting sustainable development goals. A system dynamics model is developed to compare the regional land occupation, water usage, carbon emissions, and change in soil carbon storage resulting from solar development using two different development strategies: traditional, in which the land is graded and vegetation is removed, and co-location, in which land grading is minimized and the soil is re-vegetated with native vegetation. The model is applied in two water-sensitive semi-arid regions with high technical potential for solar energy where agriculture is an important element of the local economy. First, Rajasthan, India is undergoing rapid expansion of solar PV to address the growing energy demand while meeting sustainable energy development goals in a developing economy. The results show that at the current growth rate of solar energy in Rajasthan, solar energy will grow to more than 500 GW by 2070 and will occupy a land area equivalent to 20% to 95% of the unused land suitable for solar. Second, the Central Valley of California has a mature power system in a mature economy seeking to decarbonize. The results show that the overall capacity of California's solar energy in 2070 will be less than a fifth of Rajasthan's and occupy at most 10% of California's unused land suitable for solar. Consequently, soil carbon loss due to future solar capacity additions under conventional development strategy will be similarly smaller in California than in Rajasthan. Together, the results show that the opportunity for the mitigation of the negative impacts of energy development may be greater in younger economies with a developing grid network.

ACKNOWLEDGMENTS

I gratefully acknowledge funding provided by the InSPIRE project through the U.S. Department of Energy Office of Energy Efficiency and Renewable Energy (EERE) Solar Energy Technologies Office under award DE-EE00038642, and U.S. National Science Foundation (NSF) CAREER Award # 1943969 for S. Ravi. This work was authored in part by Alliance for Sustainable Energy, LLC, the manager and operator of the National Renewable Energy Laboratory for the U.S. Department of Energy (DOE) under Contract No. DE-AC36-08GO28308. I gratefully acknowledge the contributions of Marcus Krembs, Jacob Fehlen, Jesse Puckett, and Eric Bjorklund (Enel Green Power North America, Inc.) and Jake Janski (Minnesota Native Landscapes) for providing access to field sites and technical guidance.

I would also like to thank the Temple University Graduate School for making this research possible through their funding. Thank you to Dr. Bojeong Kim, Dr. Nicholas Davatzes, and Dr. Rachel Spigler for their guidance and for their serving on the committee. The continued moral support and insight from the members of the InSPIRE team at NREL were also essential for reaching this milestone.

Thank you to my advisor, Dr. Sujith Ravi, for going above and beyond to ensure my growth as a researcher and a person even at times when my progress seemed infinitesimal. In the lab and in the field, Dellena Bloom, Alex Cagle, and Rebecca Bertel have been an unstoppable force and an integral part of my research. I would also like to thank my fellow graduate students Louise Borthwick, Justin Morris, Boyoung Song, Ashleigh Kirker, and my Fall 2016 cohort, who were the best colleagues a graduate student

could hope for. Thank you to Oreo and Somi, who sat with me for countless hours when I was writing in isolation. My parents, my sister, and my brother-in-law never stopped believing in me even when I lapsed into despair. And to my wife G., my love and gratitude for you are boundless.

Thank you.

TABLE OF CONTENTS

ABSTRACT iii

ACKNOWLEDGMENTS vii

Table of Contents ix

LIST OF TABLES xiii

LIST OF FIGURES xiv

CHAPTER

1. INTRODUCTION 1

1.1. Background 3

1.2. Hypotheses and Objectives 9

1.2.1 Hypothesis 1 9

1.2.2 Hypothesis 2 9

1.2.3 Hypothesis 3 9

1.3. To Test These Hypotheses, the Following Research Objectives Were Set: 9

1.3.1 Objective 1 (Chapter 2) 9

1.3.2 Objective 2 (Chapter 3) 9

1.3.3 Objective 3 (Chapters 2 and 3) 10

1.3.4 Objective 4 (Chapter 4) 10

2. ENVIRONMENTAL CO-BENEFITS OF MAINTAINING NATIVE VEGETATION WITH SOLAR PHOTOVOLTAIC INFRASTRUCTURE 11

2.1. Abstract 11

2.2. Introduction 12

2.3. Materials and Methods 14

2.3.1 Site Description 14

2.3.2 Field Measurements 16

2.3.3 Laboratory Methods 17

2.3.4 Statistical Analysis 18

2.3.5 Electricity Production Data 18

2.4. Results 18

2.4.1 Soil Moisture and Temperature 18

2.4.2 Microclimate: Wind Speed, Air Temperature, and Relative Humidity 20

2.4.3 Soil properties: Carbon, Nitrogen, and Grain-Size Distribution 20

2.4.4 Electricity Generation 22

2.5. Discussion 24

2.5.1 Implications for Site Preservation 24

2.5.2 Implications for Developing Agrivoltaic Systems 26

2.6. Conclusions 33

2.7. Supporting Information 33

2.8. Data availability 33

3. MICROCLIMATE AND SOIL INFLUENCE OF VEGETATION AT THREE UTILITY-SCALE SOLAR SITES IN HUMID CONTINENTAL CLIMATE 34

3.1. Abstract 34

3.2. Introduction 35

3.3. Methods 39

3.3.1 Description of the Study Sites and Field Data Collection 39

3.3.2 Laboratory Measurements 41

3.3.3 Analyses 41

3.4. Results 42

3.4.1 PV Temperature and Power Output 42

3.4.2 Microclimate 44

3.4.3 Soil Particle Size Distribution and Nutrients 46

3.4.4 Soil Moisture and Temperature 49

3.5. Discussion 52

3.5.1 PV Temperature and Performance in Co-located Systems 53

3.5.2 Soil-Specific Strategies for Restoration 55

3.5.3 Agrivoltaic Influence on Microclimate and Hydrology and Its Implications for Cropping Geometry and Biodiversity 58

3.5.4 Implications for Climate Change Resilience 60

3.5.5 Future Studies 61

3.6. Conclusion 62

3.7. Supporting Information 63

4. LAND AND WATER FOOTPRINTS FROM EXPANSION OF UTILITY-SCALE SOLAR: A TALE OF TWO STATES 64

4.1. Abstract 64

4.2. Introduction 65

4.3. Background 68

4.3.1 Agricultural Workforce and Economics of Rajasthan and California 68

4.3.2 Solar Resources 68

4.3.3 Historical Capacities and Future Trajectories 69

4.4. Methods 70

4.4.1 Model Boundaries 71

4.4.2 Implementation of Growth Projections from the Literature 71

4.5. Results and Discussions 75

4.6. Conclusion 82

5. SUMMARY 84

BIBLIOGRAPHY ..... **Error! Bookmark not defined.**

APPENDICES

A. SUPPLEMENTAL INFORMATION FOR CHAPTER 2 103

B. SUPPLEMENTAL INFORMATION FOR CHAPTER 3 118

C. COPYRIGHT PERMISSIONS 123

LIST OF TABLES

Table Page

3.1. Comparison of power output between the bare PV and the veg PV treatments using t-test ($p < 0.05$). 44

A.1 Parameter used for the ET model (Penman Monteith with Stewart model) 110

A.2 KS test to compare the soil properties among the relative positions within each treatment 111

A.3 KS tests among the treatments 112

B.1 Details of the three study sites in Minnesota, USA..... 118

B.2 Measured microclimate variables and the measurement locations. 119

LIST OF FIGURES

Figure Page

1.1 Examples of co-location schemes. 7

2.1 Vegetated and bare PV treatment in Chisago, MN 15

2.2 Soil moisture and temperature. 19

2.3 Microclimate. 21

2.4 Soil properties. 22

2.5 Electricity generation. 23

2.6 ET-driven panel cooling effects are site specific. 30

3.1 Daily profile of median DC power output (kW) and median panel temperature (°C) over the growing seasons. 43

3.2 Distribution of air temperature and relative humidity at each treatment over all three growing seasons of the study period. 45

3.3 Wind roses representing frequency of counts (%) by wind direction over the growing periods from 2019 to 2021 46

3.4 Soil Properties 48

3.5 Time series and distribution of the daily mean soil moisture among the treatments and total daily precipitation 50

3.6 Time series and distribution of the daily mean of the soil temperature among the treatments 52

4.1. Historical installed capacity of USSE in California, USA and Rajasthan, India. 70

4.2. Summary of the dynamic recursive model 75

4.3. Growth trajectory of the operating capacity of utility-scale solar energy under different scenarios 77

4.4. Land occupied by solar energy over the modeling period. 79

4.5. Total soil carbon stock in the solar-occupied lands over the modeling period in the decarbonization scenarios 80

4.6. Total water consumption by the solar industry 82

A.1 Location and layout of the study site in Minnesota. 114

A.2 Sensor towers in a. bare PV treatment; b. veg PV treatment; and c. Control. 115

A. 3 The effect of panel temperature on the power output. 115

A. 4 The effect of air temperature on the power output..... 116

B.1 Photos of treatments 120

B.2 Soil properties in all three study locations in Minnesota. 121

B.3 Comparison of soil nutrient contents using ANOVA and Tukey Honestly Significant difference 122

CHAPTER 1.

INTRODUCTION

Solar photovoltaic (PV) technology, backed by the highest technical generation potential among renewable energies, favorable policies, and technological advancement, has been growing rapidly in recent years. It is anticipated that in the next ten years installed capacity is expected to grow five-fold. By 2100, PV will supply 19.9-29.0% of the global total electricity demand (Breyer *et al.*, 2018; Edenhofer *et al.*, 2011; Ellabban *et al.*, 2014; IEA, 2020; Jacobson, 2009; De Marco *et al.*, 2014; U.S. Department of Energy, 2012). Currently, ground-mounted utility-scale solar energy (USSE) dominates the market and is expected to continue to do so for the near future (SolarPower Europe, 2018). On average, ground-mounted solar PV systems have the largest direct land footprint of all renewables except for biomass and hydropower (Trainor *et al.*, 2016). With an average land-use intensity of 3 ha MW_p^{-1} (Ong *et al.*, 2013), ground-mounted solar PV may cause 25 million hectares of land-use change under an optimistic global solar energy deployment scenario (IRENA, 2018). While this number is inconsequential compared to the total global land area, additional solar PV development is likely to be concentrated in areas with attractive characteristics for development, which are areas with high insolation that are flat, dry, unshaded, close to grid infrastructure, and easily accessible for maintenance (Adeh *et al.*, 2019; Grout & Ifft Charles, 2018; Kim *et al.*, 2020). These prerequisites make farmlands attractive potential sites to solar developers, and some farmers in the United States have been leasing their lands to them for a reliable revenue stream that is independent from the volatility of agricultural markets (Maltais, 2019; Nir, 2020).

Even though solar PV is a highly scalable and easily deployable energy source with low greenhouse gases emission, the farmers who lease their lands to solar developers assume a new set of economic and environmental risks: the conventional deployment of utility-scale ground-mounted solar PV in farmland or an ecologically important tract of land precludes any agricultural uses of the land during the facilities' lifetime (30 to 40 years) and may compromise the land's ecological functions (Choi *et al.*, 2020; Hernandez, Easter, *et al.*, 2014; Hernandez, Hoffacker, Murphy-Mariscal, *et al.*, 2015). Subsequently, solar PV's long-term occupation that follows may further disrupt the land's ecological functions or its ability to produce agricultural goods by creating variations in microclimate (Armstrong *et al.*, 2016; Barron-Gafford *et al.*, 2016) and further accelerating erosion (Cook & McCuen, 2013). Though an increasingly seldom part of the construction of ground-mounted solar PV systems, vegetation removal and removal of topsoil decrease the land's ability to produce biomass and sequester carbon by increasing the erodibility of the finer fraction of the soil particles to which soil nutrients (C, N, and P) adhere (Hernandez, Easter, *et al.*, 2014; Larney *et al.*, 2000, 2016; G. H. Zhang *et al.*, 2011). Moreover, the extensive land modification of this practice may extend of the physical impacts on the land past the duration of solar PV occupation (Beatty *et al.*, 2017; Hernandez, Easter, *et al.*, 2014; Hernandez, Hoffacker, Murphy-Mariscal, *et al.*, 2015).

These land impacts may be mitigated by co-locating agricultural activity or native vegetation with solar PV, which is a practice that is sometimes referred to as agrivoltaics. Several modeling and pilot-scale studies have shown that co-location of PV and vegetation can provide mutual benefits that include vegetation-driven cooling of the PV panels for increased PV efficiency, reduction in the solar PV installation and operation costs,

diversified income streams, employment generation, reduction in irrigation water use, and increased crop yields from pollinator services (Adeh *et al.*, 2018; Barron-Gafford *et al.*, 2019; Beatty *et al.*, 2017; Choi, 2019; Elamri, Cheviron, Lopez, *et al.*, 2018; Elamri, Cheviron, Mange, *et al.*, 2018; Hernandez, Easter, *et al.*, 2014; Majumdar & Pasqualetti, 2018; Marrou, Wery, *et al.*, 2013; Marrou, Dufour, *et al.*, 2013; Marrou, Guilioni, *et al.*, 2013; Ravi *et al.*, 2014, 2016). However, equally important to these benefits are whether replanting native vegetation or crops on a solar PV facility can restore the ecological functions of the occupied land to ensure that the landowners have the option to restore agricultural use after the lease. Furthermore, the variations in the physical interaction among different agrivoltaic systems that stem from project-specific factors such as the local climate, soil characteristics, and plant species also need to be considered for a complete estimation of the environmental outcome. To answer this question, detailed field and lab characterization of the microclimatic interaction among the PV arrays, soil, and vegetation of three utility-scale co-located systems in Minnesota, USA was performed. Then, the findings from the research and existing literature were used to create a system dynamic model to project net carbon sequestration and water savings from wide deployment of co-located systems in Rajasthan, India where total installed capacity of solar is growing exponentially.

1.1. Background

Concerns about the current and the future land use impacts of solar energy have been increasing in the last decade with the burgeoning solar energy sector. Many discussions on the topic focus on quantifying environmental impact metrics, such as land transformation or footprint (V. Fthenakis & Kim, 2009; Hernandez, Hoffacker, *et al.*, 2014;

Ong *et al.*, 2013; Wu *et al.*, 2021), water use (Bukhary *et al.*, 2018; V. Fthenakis & Kim, 2010; Mekonnen *et al.*, 2015; Sinha, 2013; Spang *et al.*, 2014; Whitaker *et al.*, 2013), and greenhouse gas emissions (V. M. Fthenakis & Kim, 2011; Hsu *et al.*, 2012; Latunussa *et al.*, 2016; R. Li *et al.*, 2019; Luo *et al.*, 2018; Nugent & Sovacool, 2014; De Wild-Scholten, 2013). Fthenakis and Kim (2009) found that the sum of direct and indirect land transformation over 30 years of lifetime by solar PV was 347-456.4 m^2 GWh^{-1}, which was considerably smaller than that of biomass energy (12,700 m^2 GWh^{-1}), hydroelectric (4,100 m^2 GWh^{-1}), and wind (1,000 to 2,100 m^2 GWh^{-1}) (V. Fthenakis & Kim, 2009). Capellán-Pérez *et al.* (2017) modeled land use requirement for 100% solar electricity scenario and 100% solar energy scenario for 27 EU countries and 13 non-EU countries and found that such scenarios would require more than 100% of total available land in some countries, and that supporting 100% of current energy consumption would require a significant area of solar installations to be located in agricultural areas or biodiversity hotspots (Capellán-Pérez *et al.*, 2017). A recent system dynamic modeling study (van de Ven *et al.*, 2021) suggests that expanding solar energy's share of electricity generation to 25-80% in South Korea, India, Japan, and the EU would require 0.5 to 5% of the total land area in the respective countries. The cumulative carbon emission related to the land-use change would vary significantly with land management practices, which were vegetation removal, maintenance of vegetation, or seeding and management as pastures (van de Ven *et al.*, 2021). In addition, this study also concluded that the USSE typically displaces local cropland or forestry land so that forests and undeveloped arable land outside of the locality would likely be developed for agriculture or forestry (van de Ven *et al.*, 2021).

In addition to the land occupation, USSE may also require large volumes of water, which is also a crucial component of land uses that may compete with USSE (Ringler *et al.*, 2013). While Capellán-Pérez et al. (2017) and van de Ven *et al.* (2021) addressed the intensification of competition for land between USSE and agriculture and managed forests (Capellán-Pérez *et al.*, 2017; van de Ven *et al.*, 2021), the potential conflict over water may be a more urgent issue for regions with abundant land but scarce water resources. For instance, Hernandez *et al.* (2014) found that 183 USSE installation in California are concentrated in the interior regions of southern California and the Central Valley, which is one of the most productive agricultural zones in the world (Hernandez, Hoffacker, *et al.*, 2014; Lo & Famiglietti, 2013). With a land-use efficiency of 16 ha MW^{-1} and maximum water consumption of 4200 L MW^{-1} h^{-1} (Hernandez, Hoffacker, *et al.*, 2014; J. Macknick *et al.*, 2012), a hectare of typical concentrated solar power (CSP) installation in California may require 2 million liters of water annually, which is equivalent to 20% of the annual irrigation for a hectare tomato cultivation in the region (Hooker & Alexander, 1998). Regardless of whether additional USSE installations in the Central Valley will replace agricultural land, it is likely that the added water consumption will put USSE land uses in competition with agriculture over already diminishing water supply (Faunt *et al.*, 2016). Therefore, further discussions on the land transformation by USSE should also examine how much solar energy would compete with other land use activities that require water. At the time of this proposal there are no studies quantify the land and water trade-offs between USSE and agriculture.

At a smaller scale, ground-mounted solar PV's impact on the land has been an active research area: a modeling study found that the bare or gravel often used in solar PV

arrays may increase the peak discharge without lack of proper stormwater-management measures (Cook & McCuen, 2013). They also found that the kinetic energy from the rainwater concentrated to the edges of the PV panels would be greater than that of the direct rainfall, which would cause increased erosion (Cook & McCuen, 2013). A field experiment by Elamri *et al.* (2018) confirmed the concentration of rainfall at the edges of the panel by lining up buckets in a transect perpendicular to solar arrays. Similarly, Choi *et al.* (2020) used spot measurements to confirm that the ground beneath the edges of the solar panels had the highest soil moisture content following rainfall events due to concentration of rain fall (Choi *et al.*, 2020).

Co-locating vegetation with solar PV arrays is a development strategy that was first proposed as a means of co-developing a tract of land for both solar PV and agriculture (Goetzberger & Zastrow, 1982), but the industrial and academic interest in this strategy has been growing due to the growing prevalence of solar development and environmental concerns around it. The theoretical basis for the original proposal was that when the PV panels are installed at 2 meters above the ground or higher, the shading and the radiation under the panels would become more diffused, which is preferable to direct sunlight for photosynthesis (Goetzberger & Zastrow, 1982). This assumption was confirmed by a pilot-scale study in which the development of lettuce, durum wheat, and cucumber under elevated solar panels were not significantly impacted by the presence of the PV panels (Marrou, Wery, *et al.*, 2013). The study also found that air temperature, and vapor pressure deficit at canopy level in the agrivoltaic system were not significantly different from those in the full sun (Marrou, Guilioni, *et al.*, 2013). These findings meant that little adjustments would need to be made for unmechanized crop cultivation in an agrivoltaic system,

provided that the crop of interest had sufficient adaptations for improving radiation interception efficiency in the shade (Marrou, Guilioni, *et al.*, 2013). Examples of co-location schemes are shown in Fig. 1.1.

Figure 1.1 Examples of co-location schemes: re-established native vegetation provides habitats for a. butterflies and b. honeybees; c. string beans are cultivated between rows of PV array; d. vegetated PV arrays provide forage and shelter for grazing sheep. Photos by Chong Seok Choi.

Pilot-scale studies in arid and temperate climates have shown additional environmental co-benefits for both the vegetation and the solar PV panels in an agrivoltaic system: first, the shading from the solar PV panels can minimize the consumptive water use for agriculture by decreasing evapotranspiration by reducing the plant exposure to the full sun, preventing excessive heating and loss of water in plants (Adeh *et al.*, 2018; Barron-Gafford *et al.*, 2019). Additionally, crops grown under panels have shown a significant increase in late season biomass in both arid and non-arid environments (Adeh *et al.*, 2018; Barron-Gafford *et al.*, 2019). Recently, an investigation on soil characteristics at a solar PV facility concluded that revegetation of a PV facility following conventional construction

cannot fully restore ecological functions of the soil, but that the environmental heterogeneity introduced by the solar PV modules may be used to concentrate water to crops or protect certain plants that need to be shielded from direct sunlight (Choi *et al.*, 2020).

A relatively new research area is the vegetation-driven modification of heat fluxes in the solar array: a pilot-scale study on agrivoltaics in Arizona found that PV panels with understory vegetation were cooler than those without, and they attributed this temperature difference to the rerouting of a portion of sensible heat flux to the PV panels to latent heat flux required for evapotranspiration by the understory vegetation (Barron-Gafford *et al.*, 2019). This finding implies that the agrivoltaic system should have higher photovoltaic efficiency and therefore higher output than its conventionally deployed counterpart, but this implication has not been verified with any energy production data (Barron-Gafford *et al.*, 2019). In another study, Adeh *et al.* (2019) found that PV performance would have the greatest potential over croplands (Adeh *et al.*, 2019). However, this study did not confirm the panel-cooling effect with any panel temperature nor energy production data (Adeh *et al.*, 2019). Moreover, neither study was conducted in a commercial solar power plants, so they cannot confirm whether the panel-cooling effect will be present at a larger scale or whether any observed cooling will lead to an increase in electricity output (Adeh *et al.*, 2019; Barron-Gafford *et al.*, 2019). These results provide the basis for five hypotheses needed to determine the potential benefits of co-locating agrivoltaics with PV.

1.2. Hypotheses and Objectives

1.2.1 Hypothesis 1

The compounding effect of PV arrays and vegetation can homogenize soil moisture distribution and provide greater buffer against extreme temperatures.

1.2.2 Hypothesis 2

Reintroducing vegetation can mitigate the impact of construction and operation on the soil properties by maintaining or improving soil carbon and nutrient storage capacity.

1.2.3 Hypothesis 3

The effect of vegetation-induced panel-cooling on electricity generation are site-specific and depend on the background climate and soil properties.

1.3. To Test These Hypotheses, the Following Research Objectives Were Set:

1.3.1 Objective 1 (Chapter 2)

Develop an analytical framework for investigating of the influence of solar PV arrays on precipitation distribution, wind pattern, relative humidity, air temperature, soil nutrients and texture via analysis of continuous environmental data and soil samples. This framework should also inform how these influences would vary between vegetated PV arrays (co-located systems) and PV arrays with bare soil. Use this framework to establish a field study in Minnesota, USA.

1.3.2 Objective 2 (Chapter 3)

Expand the analytical framework to two more sites in Minnesota to evaluate how climate, soil, and ecology will impact the outcomes of the co-location strategy.

1.3.3 Objective 3 (Chapters 2 and 3)

Verify the hypothesized PV panel cooling effect through co-location of solar PV arrays with vegetation through the synthesis of the findings from the microclimate and soil moisture data.

1.3.4 Objective 4 (Chapter 4)

Use the findings from the field study and literature to develop a system dynamics model that estimates the environmental outcomes where the strategy is widely adopted at a regional scale the co-location scheme in the rapidly growing PV installations in Rajasthan, India.

Chapter 2 is a publication from *Earth's Future* that addresses Hypotheses 1 to 4 based on the preliminary data from one of the three field locations and provides framework for Chapter 3, which verifies the findings from Chapter 2 by synthesizing the data from all three field locations. Chapter 3 is in review for publication in *Applied Energy*. Chapter 4 uses the findings from Chapter 2, Chapter 3, and the literature to build a system dynamic model that will estimate the future soil carbon outcome for ubiquitous adoption of co-location scheme for the growing PV capacities in Rajasthan, India.

CHAPTER 2.

ENVIRONMENTAL CO-BENEFITS OF MAINTAINING NATIVE VEGETATION WITH SOLAR PHOTOVOLTAIC INFRASTRUCTURE

(This chapter is published: Choi *et al.*, (2023) *Earth's Future*, 11(6), https://doi.org/10.1029/2023EF003542)

2.1. Abstract

Co-locating solar photovoltaics with vegetation could provide a sustainable solution to meeting growing food and energy demands. However, studies quantifying multiple co-benefits resulting from maintaining vegetation at utility-scale solar power plants are limited. We monitored the microclimate, soil moisture, panel temperature, electricity generation, and soil properties at a utility-scale solar facility in a continental climate with different site management practices. The compounding effect of photovoltaic arrays and vegetation may homogenize soil moisture distribution and provide greater soil temperature buffer against extreme temperatures. The vegetated solar areas had significantly higher soil moisture, carbon, and other nutrients compared to bare solar areas. Agrivoltaics on agricultural areas with carbon debt can be an effective climate mitigation strategy along with revitalizing agricultural soils, generating income streams from fallow land, and providing pollinator habitats. However, the benefits of vegetation cooling effects on electricity generation are rather site-specific and depend on the background climate and soil properties. Overall, our findings provide foundational data for site preservation along with targeting site-specific co-benefits, and for developing climate resilient and resource conserving agrivoltaic systems.

2.2. Introduction

Solar photovoltaics (PV) is one of the fastest growing renewable technologies that is often preferred for its low emission, scalability, and ease of off-grid deployment in rural areas. In the US, solar technologies are expected to account for as much as 45% of the national electricity supply but occupy a maximum land area equivalent to 0.5% of the contiguous U.S. surface and only 10% of suitable disturbed lands (US Department of Energy Solar Energy Technologies Office, 2021). However, due to the suitability of farmlands for PV development (Adeh *et al.*, 2019), competition for these lands may grow as more farmland is converted to PV development to meet the swelling electricity demand (Grout & Ifft, 2018). Extensive landscape modification by utility-scale PV such as vegetation removal, land grading, refilling topsoil, and compaction for the construction of conventional PV plants may have negative impacts on ecological functions and may provide challenges for reintroducing native vegetation or crops during or after the 25-30 year lifetime of solar plants (Hernandez *et al.*, 2014; De Marco *et al.*, 2014; Beatty *et al.*, 2017; Choi *et al.*, 2020). Furthermore, agriculture and energy production coupled with climate change are impacting habitat loss around the world with implications on pollinators and biodiversity loss (Raven & Wagner, 2021). Many native species and pollinators will not be able to migrate in pace with the impacts of climate change (Warren *et al.*, 2018), and habitat fragmentation and alteration from large conventional solar installations may put additional pressure on the biodiversity and insect-pollination activities (Rafferty, 2017).

Co-location of utility-scale PV installations with a competing land-occupying activity such as restoration of native flora or cultivation of profitable crop, fodder, or biofuel is being evaluated as a strategy to minimize the negative consequences of PV

deployment (Dupraz *et al.*, 2011; Macknick *et al.*, 2013; Ravi *et al.*, 2014, 2016; Hernandez *et al.*, 2019; Pascaris *et al.*, 2021). PV - agriculture co-location (Agrivoltaics or Agrophotovoltaics) has the potential to abate the cost of solar power generation with the agricultural income and may also provide several co-benefits, including increased PV cell efficiency from cooler microclimate induced by underlying vegetation, persistent employment generation, rural electrification in remote areas, and renewable electricity sources for processing agricultural products locally (Marrou *et al.*, 2013; Ravi *et al.*, 2014, 2016; Adeh *et al.*, 2018; Barron-Gafford *et al.*, 2019; Weselek et al; 2019; Choi *et al.*, 2021). In addition to creating different microhabitats, PV arrays may also delay and prolong growing season for plants (Graham *et al.*, 2021), which may reduce the chance of phenological mismatch between the plants and the pollinator species (Graham *et al.*, 2021) and increase crop yield and enhance the ability of some crops to expand beyond their current geographical and seasonal range limits (Adeh *et al.*, 2018; Walston *et al.*, 2018; Barron-Gafford *et al.*, 2019). Evapotranspiration (ET) from co-located vegetation may reduce the temperature of the overlying PV system (Barron-Gafford *et al.*, 2019) and increase the PV cell efficiency (Evans & Florschuetz, 1978). While the decreased panel temperature has been observed in a desert setting (Barron-Gafford *et al.*, 2019), it has not been linked to higher PV electricity production in a co-located utility-scale facility.

Several modeling and pilot-scale field experiments that explored the techno-economic and environmental feasibility of co-location approaches have indicated that co-located land uses have higher land use efficiency than the single-component land uses (Dupraz *et al.*, 2011; Marrou *et al.*, 2013; Ravi *et al.*, 2014, 2016; Dinesh and Pearce, 2016; Beatty *et al.*, 2017; Elamri *et al.*, 2018; Adeh *et al.*, 2018; Barron-Gafford *et al.*, 2019;

Majumdar & Pasqualetti, 2019; Trommsdorff et al; 2021). However, field-level investigations on the mutual interactions between PV and underlying soil-vegetation in the context of co-location of crops or native vegetation with utility-scale PV plants are limited (Armstrong *et al.*, 2016; Beatty *et al.*, 2017). No study exists yet to identify and quantify separate contributions of PV arrays and different site management choices at commercial utility-scale solar installations to the soil moisture, microclimate, and soil nutrient characteristics. The scarcity of studies on these topics presents a critical research gap, and the prospect of unforeseen environmental consequences may become a potential roadblock to the widespread implementation of optimally designed co-located systems and deployment of PV in natural or agricultural lands. To address this research gap, we use a combination of sensor data analysis and field and laboratory measurements to investigate the role of site-specific conditions on the environmental co-benefits and trade-offs between PV and underlying vegetation, in the context of designing resource conserving and climate resilient integrated solar energy and food/fodder systems.

2.3. Materials and Methods

2.3.1 Site Description

The study area was a 2.9-acre portion of a 9.5-MW PV plant (located at 45.451148, -92.907255) in Chisago City, Minnesota, USA, that started operating in October of 2016 (Enel Green Power North America (EGP-NA) (Supporting Information S1). This region's climate is characterized as warm-summer humid continental (Köppen climate type Dfb). The panels were installed approximately 2 m above ground (at lowest point) and the distance between the center of the arrays were 7.5 m. Prior to the construction of the PV facility, approximately 74% of the land area was agricultural, and 17% was temperate

forest. The remaining portion of the land was categorized as developed/urban (approximately 6%), recently disturbed/modified (approximately 2%), flooded and swamp forest (approximately 1%), and boreal forest (< 1%). To retain the lands' ability to cultivate crops after the decommissioning of the facility, land grading or any other construction techniques that would remove a significant portion of the topsoil was avoided during the construction of the facility. Native flora was planted in 2018 on the intact soil in a portion of the facility following the construction. To separate the effects of vegetation and PV panels, three treatments were established in the study area. The bare PV treatment was established in the PV arrays where the ground was maintained bare after the construction, whereas the veg PV treatment was in nearby PV arrays that was revegetated with native flora. The control was established in an adjacent area without PV arrays that was revegetated with the same native flora. The entire site was exposed to light sheep grazing for 2-3 weeks per year since 2019. The condition of the vegetated PV and the bare PV treatments are shown in Fig. 2.1 a and b. The list of plant species at the study site is included in Text A.1 in Appendix A.

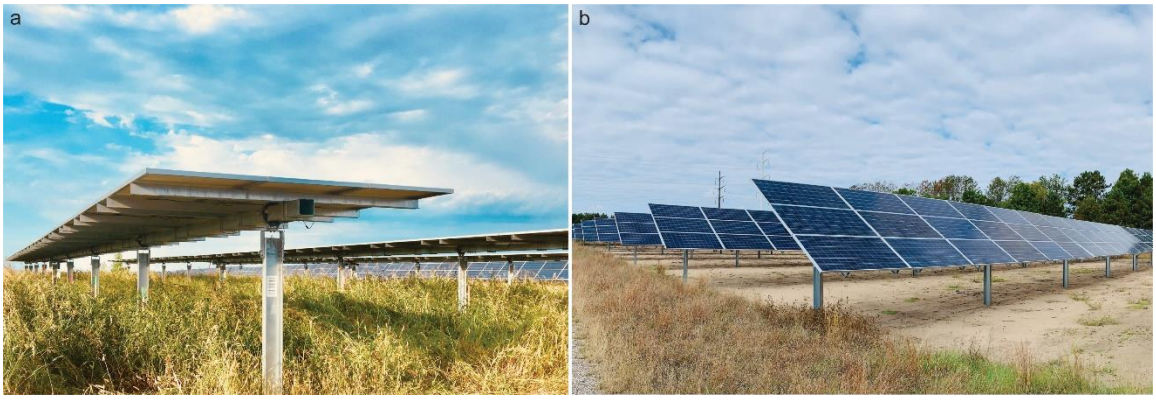

Figure 2.1 a. Vegetated and b. bare PV treatment in Chisago, MN

2.3.2 Field Measurements

The meteorological stations were installed in September of 2018. The analyzed microclimate data were during the growing season of 2019 (May - August). The microclimatic variables, except solar radiation, were measured every 15 seconds and recorded every 15 minutes (Campbell Scientific, USA: CR6 Measurement and Control Datalogger).

The locations of soil moisture and temperature measurements (25-cm depth, Campbell Scientific, USA: CS655 Water Content Reflectometers) at each PV treatment were directly below the center of the PV panel ("BP" for "below panel"), below the western edge ("WE" for "western edge") of the panel, in the central location between two rows of PV panels ("IS" for "interspace"), and finally, below the eastern edge ("EE" for eastern edge) of the adjacent row of panels (Fig. 2.6). Relative humidity and air temperature (Campbell Scientific, USA: EE181 Temperature and Relative humidity probe) were measured at 0.5 meter from the ground at the IS of veg PV and bare PV treatment and also in the control. Relative humidity was sampled and recorded every 15 minutes. Wind speed (minimum, maximum, mean, and standard deviation) and direction (Campbell Scientific, USA: 03002 Wind Sensor) were measured at 1.5 meters from the ground at the IS. PV module temperatures were measured using back-of-the-module temperature sensors (Campbell Scientific, USA: CS240).

Soil moisture and temperature at the control treatment were measured only at two locations that were placed eight meters away from each other along an east-west trending line. Relative humidity, air temperature, wind speed, and wind direction were also measured the same way at the control treatment at the midpoint of the east-west line.

Precipitation depth (Campbell Scientific, USA: TE525 Tipping Bucket Rain Gage) was recorded over 15-minute intervals. Radiation intensity (Campbell Scientific, USA: CS320 Thermopile Pyranometer) was sensed every ten seconds and averaged over an hourly interval.

Soil samples (n=100, top 5-cm) for nutrient and particle size analysis were taken from vegetated (n=40), bare (n=40) and control (n=20) treatments. For the vegetated- and bare PV treatments soil samples were taken from each of the 4 relative positions (n=10 per position). Soil samples for bulk density measurements were taken using a standard 2-inch bulk density cup and cap sampler (AMS, USA).

2.3.3 Laboratory Methods

The air-dried soil samples were sieved using a 2-mm sieve and split into sub-samples using a riffle sampler (Humboldt Mfg. Co. Il, USA). The dry particle size distribution of the soil samples were determined using a laser diffraction particle sizing analyzer (LS 13320 with tornado dry powder system, Beckman Coulter, Inc. CA, USA) with a grain diameter measurement range of 0.4–2,000 μm. Total soil carbon (TC) and total soil nitrogen (TN) were determined with a standard combustion method (McGeehan & Naylor, 1988; Nelson & Sommers, 1996). Other analysis includes pH, Organic Matter, estimated Nitrogen release, Bray I Phosphorus, Exchange Capacity, % base saturation of Cation, Available Nitrogen, and Mehlich III Extractable Phosphorous, Manganese, Zinc, Boron, Iron, Sulfur, Calcium, Magnesium, Potassium and Sodium (Brookside Laboratories, INC. New Bremen, USA).

2.3.4 Statistical Analysis

Analysis of variance (ANOVA) and Tukey post hoc test (at $\alpha = 0.05$) were performed for mean TC, TN, grain sizes, and sorting to detect any significant differences among the bare PV treatment, the veg PV treatment, and the control. Kolmogorov–Smirnov (KS) tests (at $\alpha = 0.05$) were applied to compare distributions of soil moisture, air temperature, air humidity and wind speed from the bare PV treatment, the veg PV treatment, and the control. Both statistical tests were performed with R ver. 4.0.4 (R Core Team, 2021). The results of the KS tests are in Supporting Information Table A.5.

2.3.5 Electricity Production Data

Electricity production data at the PV facility was provided by Enel Green Power North America (EGP-NA). The bare PV treatment and the veg PV treatment each contained an inverter that was linked to 1,044 modules (328.9 kW_p). Production data were recorded every 15 minutes.

2.4. Results

2.4.1 Soil Moisture and Temperature

The compounding effect of PV arrays and vegetation can homogenize soil moisture distribution and provide greater soil temperature buffer against extreme temperatures at vegetated solar sites. The treatment with the traditional management (bare PV) consistently had the lowest average volumetric soil moisture content (25 cm depth), while the treatment with native vegetation (veg PV) and the adjacent undisturbed area (control) had similar average moisture content (Fig. 2.2 a and b). The PV treatments showed heterogeneity in soil moisture distribution among their relative locations with respect to panel position. All locations corresponding to panel edges except for the WE in bare PV had higher soil

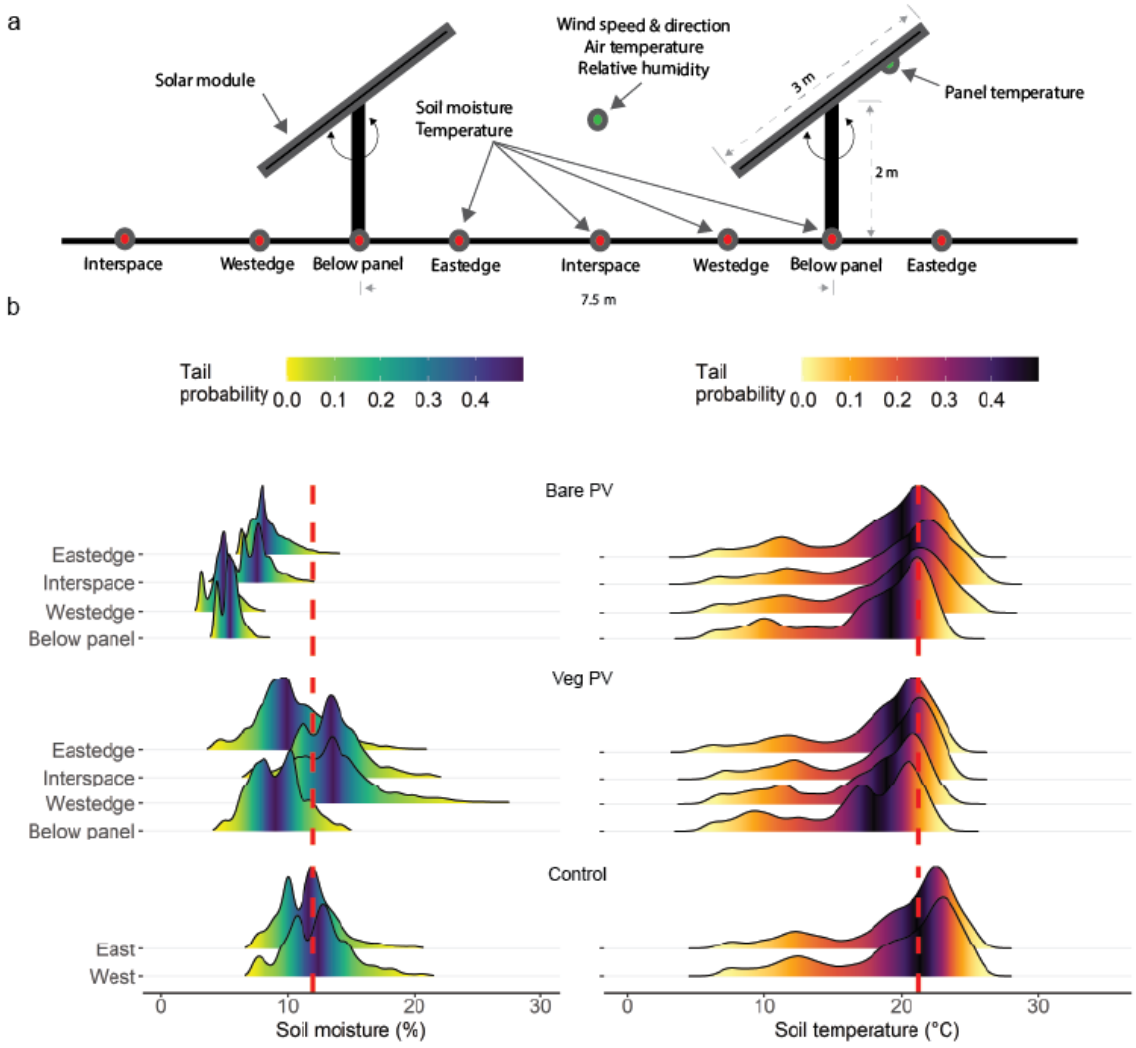

Figure 2.2 Soil moisture and temperature a. Monitoring locations b. Distribution of soil moisture (left) and soil temperature (right) at different relative positions over the experimental period (growing season). The dashed red line indicates the median value at the control.

moisture compared to BP (Fig. 2.2b). Among the three treatments, the control had the highest median soil temperature, and the maximum soil temperature of the two positions of the control were higher than that of all the relative positions in the two PV treatments except the EE, the WE, and the IS in the bare PV treatment (Fig. 2.2b). While the median temperatures of the PV treatments were not significantly different, the bare PV treatment

had a wider range of soil temperatures than did the veg PV treatment. The below panel had the lowest median soil temperature at the bare PV and veg PV treatments.

2.4.2 Microclimate: Wind Speed, Air Temperature, and Relative Humidity

The air temperature, relative humidity and vapor pressure deficits were not significantly different between the treatments (Fig. 2.3 a, b and Supporting information S2). The vegetated solar site showed slower and more homogenous wind speeds over all directions compared to those in the bare solar site (Fig. 2.3c). The distribution of mean, maximum, and minimum wind speeds were significantly different among the treatments ($p < 0.05$). Compared to those in the control, the wind speed was lower in all directions in the vegetated solar site (Fig. 2.3c). The veg PV treatment had the narrowest diurnal variations in soil temperatures (Fig. 2.3d).

2.4.3 Soil properties: Carbon, Nitrogen, and Grain-Size Distribution

The bare PV treatment had significantly ($p<0.05$) lower total soil carbon (TC) and total soil nitrogen (TN) levels than the control and the veg PV treatment (Fig. 2.4a). However, the TC and the TN levels were not significantly ($p>0.05$) different between the veg PV and the control. Also, TC and TN levels were not significantly ($p>0.05$) different between the relative locations both in the vegetated and bare sites. The median soil grain sizes at the bare site were significantly ($p<0.05$) larger than those at the veg PV treatment and the control. The veg PV treatment had the largest variation in grain sizes (φ size-scale = $-\log_2$ (diameter in mm)) and sorting (Fig. 2.4b). Other macro nutrients important for plant growth were significantly higher in the vegetated treatment than in the bare PV treatment compared to the control (Fig. 2.4c). Mean bulk densities of the soil in the bare PV

treatment, the veg PV treatment, and the control were 1.48, 1.27, and 1.39 g $cm^{-3,}$ respectively.

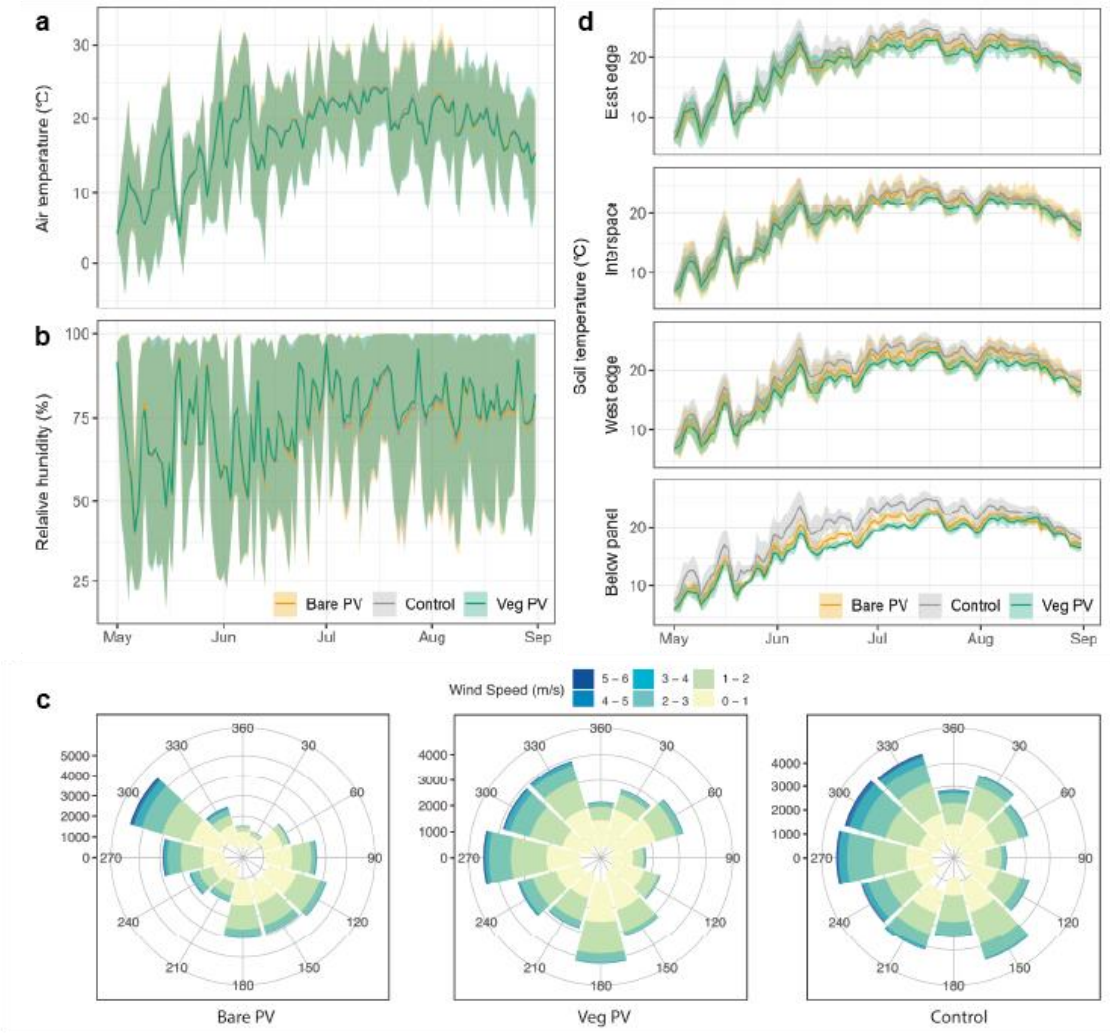

Figure 2.3 Microclimate: a. Air temperature (mean, maximum and minimum) b. relative humidity (mean, maximum and minimum), c. Rose diagram showing distribution of wind directions and speeds over the growing season. Each concentric circle represents number of events and the length of each spoke around the circle indicates the amount of time that the wind blows from a particular direction with that speed range (colors)., and d. soil temperature (mean, maximum and minimum) for the three treatments.

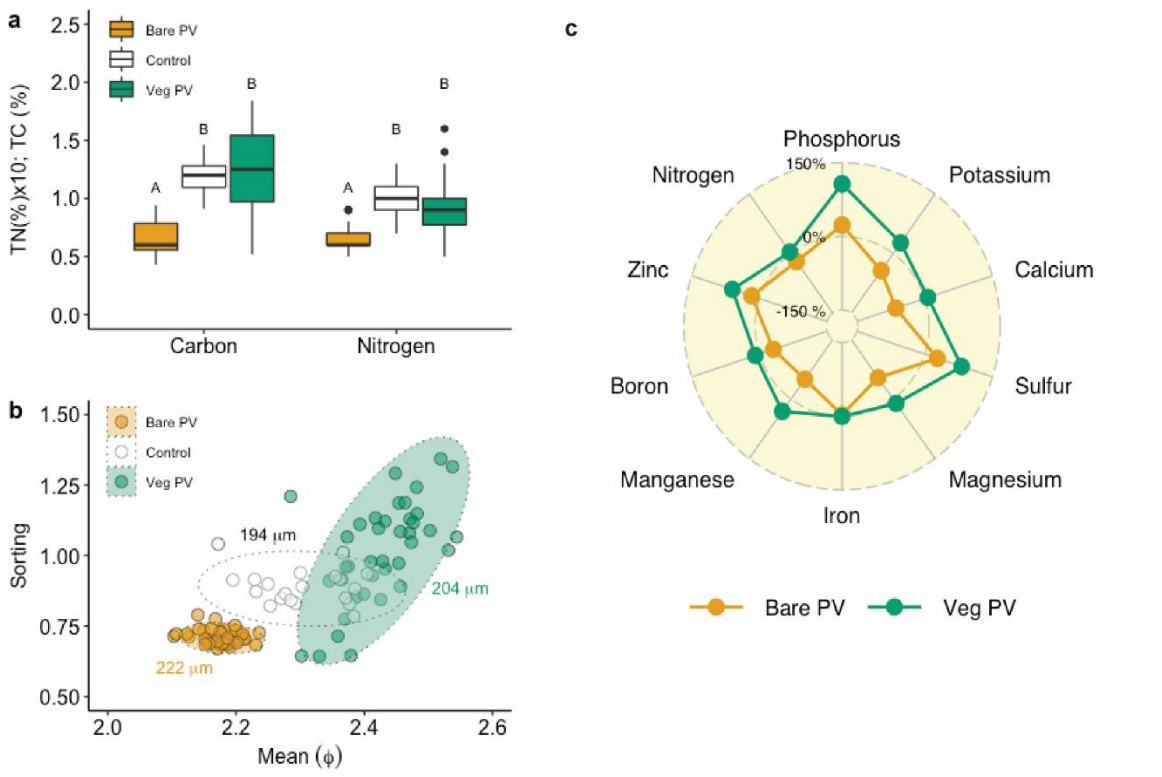

Figure 2.4 Soil properties: a. Total carbon and total nitrogen in soil at the three treatments. The horizontal bar represents the median, and the lower and the upper box boundaries represent the 25th and the 75th percentiles. The whiskers represent the 5th and the 95th percentiles. Treatment categories share letters if pairwise comparisons did not identify significant differences between means; b. Sorting and mean of soil particle size ($\phi = -\log_2 d$, where d is grain diameter in mm) at different sites. The median grain size is shown; and c. Percentage increase (+) or decrease (-) in major soil macro and micronutrients (Phosphorus, Potassium, Calcium, Sulfur, Magnesium, Iron, Manganese, Boron, Zinc, and Available Nitrogen) important for plant growth in the vegetated and bare PV treatments relative to undisturbed control (0%).

2.4.4 Electricity Generation

During the growing season (May – August), the PV arrays in the bare PV treatment produced 198.4 MWh, and the ones in the vegetated PV treatment produced 193.1 MWh, which was equal to 2.7% less electricity generated in the veg PV treatment. The times when the bare PV treatment produced more power than the veg PV treatment were between 6 to 10 and 15 to 18 during the study period, which accounted for 99.3% of the production discrepancy (5.3 MWh) between the two treatments (Fig. 2.5a). Panel temperature was

higher in the bare PV treatment than in the veg PV treatment during the hours 5 to 9 and 14 and 20, which roughly coincide with the times at which the bare PV treatment produced more power than the veg PV treatment.

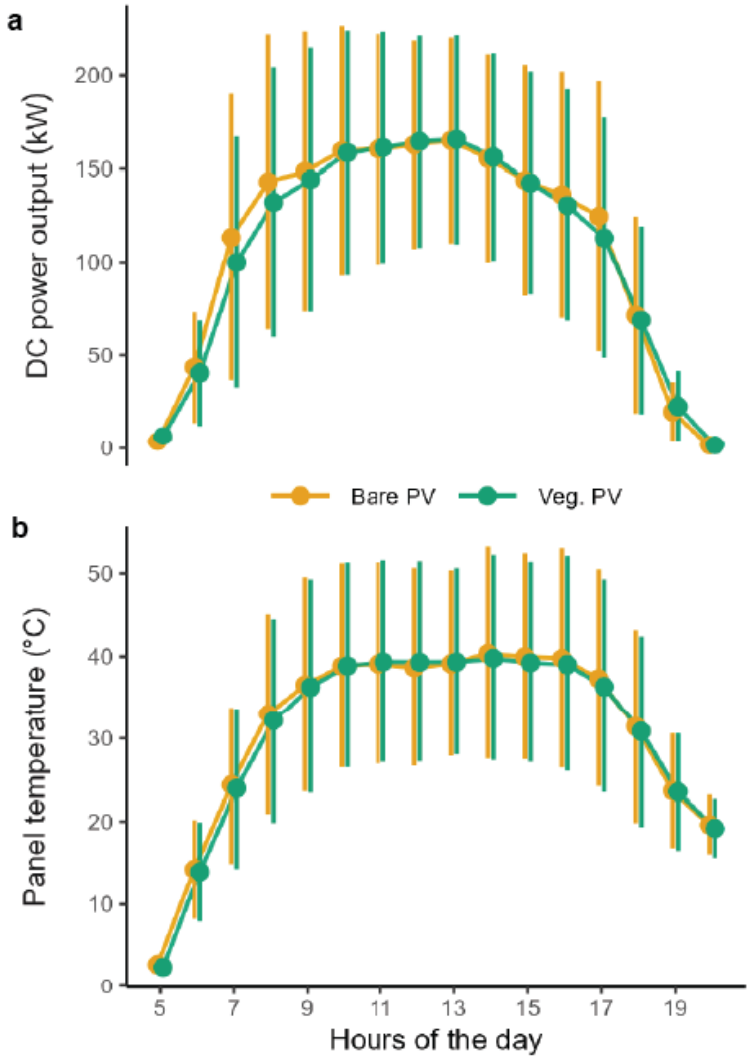

Figure 2.5 Electricity generation: a. Average hourly DC power output (kW) and b. panel temperature (°C). Error bars represent standard deviations, the line and point colors represent treatments, and the blue numbers represent the sample size for each hour. The points that belong to the two treatments are horizontally offset for visibility even though the data from the two treatments are recorded simultaneously.

2.5. Discussion

Our results show that the construction and maintenance of PV arrays can alter soil moisture, microclimate, and soil physicochemical properties. Maintaining natural vegetation on solar sites may mitigate the negative environmental impacts of PV installation and operation on soil conditions and vegetation diversity; such mitigation may also benefit pollinators that comprise an integral part of the landscape. Interestingly, our results demonstrate that the positive impact of ET-induced cooling by vegetation on electricity generation may not be applicable in all climatic zones. Overall, our study provides foundational data on the potential to improve multiple ecosystem services by maintaining native vegetation at PV sites.

2.5.1 Implications for Site Preservation

The elevated soil moisture in the vegetated PV treatment and the control may be a combination of several mechanisms that link vegetation cover with higher soil moisture. First, solar panels intercepted and redistributed precipitation and generated spatial variability of soil moisture (Fig. 2.2b). Positive feedbacks exist between vegetation and soil moisture, leading to transport of water to vegetated areas (Cramer *et al.*, 2017), mostly through soil-water diffusion towards the root zone. Thus underlying vegetation can homogenize or mitigate the soil moisture variability through root uptake of water for transpiration, which can compensate for spatial variability in soil moisture by extracting water from wet regions at a high rate (Breazeale, 1930; Guswa, 2012; Ivanov *et al.*, 2010; Katul *et al.*, 1997). Also, the lower soil moisture levels in the bare PV treatment may be explained by higher soil temperature and less shading that would result in higher evaporation rate from bare soils compared to the vegetated surface in the veg PV treatment

and the control (Li *et al.*, 2016). Furthermore, vegetated soils may retain more water than bare soil because rooted soils have higher suction than do bare soils (Leung *et al.*, 2015). The homogenizing effect of plant uptake on soil moisture can enhance transpiration and ecosystem productivity. These effects are especially significant in water-limited environments (Munson *et al.*, 2011), which presents motivation for similar research on co-located systems in arid climates.

The lower median and maximum soil temperatures and the reduced soil temperature ranges in the PV treatments compared to the control during the growing season are attributed to the interception of incoming shortwave and longwave radiation by the PV panels (Adeh *et al.*, 2018; Armstrong *et al.*, 2014, 2016). Additionally, our comparison between the two PV treatments is in line with previous findings that vegetation can further reduce the median and maximum soil temperature and narrow the range of soil temperature fluctuations (Oliver *et al.*, 1987). Our data shows that compound effect of PV arrays and vegetation may produce even greater temperature buffer against the extreme temperatures than would a native grassland, which may benefit various species of crops whose growth and quality are negatively impacted by thermal stress (Al-Khatib & Paulsen, 1999; Aldous & Kaufmann, 1979; Rivero *et al.*, 2001).

The lower sorting index and the high mean Phi ($\phi = -\log_2 d$, where d is grain diameter in mm) values in the bare PV soil samples imply that the lower TC and TN contents in the soil samples in those soils are likely caused by the preferential loss of fine soil particle that act as substrates for TC and TN from the bare PV treatment in the absence of vegetation (Bashagaluke *et al.*, 2018; Li *et al.*, 2008; Quinton *et al.*, 2010; Sharpley, 1985; Wang *et al.*, 2011; Zhang *et al.*, 2004; Zougmoré *et al.*, 2009). The faster speeds and

homogenized wind directions, as observed in the bare PV, have been linked to increased soil erosion in some systems (Dupont *et al.*, 2014). Assuming a soil bulk density of 1.3 g cm^{-3}, the deficit of 0.6% in TC and 0.03% in TN observed in the bare PV are equivalent to a deficit of 3.9 Mg ha^{-1} of TC and 0.2 Mg ha^{-1} of TN in the top 5-cm of the soil, after the construction of the PV facility in 2016. Over the lifetime of the PV facility with bare soil cover, which may be 20 to 30 years, continued loss of fines in the bare soil may lead to even greater deficit of TC and TN and degrade the soil's ability to retain any added nutrients. Our analysis makes a strong case for vegetating PV sites for site preservation. Land appropriation for intensive farming practices have resulted in substantial loss of carbon from agricultural and grassland soils globally (Sanderman *et al.*, 2017). Improving carbon sequestration in agricultural areas with carbon debt using innovative site management practices such as co-location of PV and perennial native vegetation (often with managed grazing) as in our study sites can be effective climate mitigation strategy along with revitalizing agricultural soils, generating income streams from fallow land, and providing pollinator habitats.

2.5.2 Implications for Developing Agrivoltaic Systems

Possibly favorable microclimatic conditions for the growth of vegetation created by the PV arrays, and the evidence for the erosional buffer created by the presence of vegetation imply that co-locating vegetation with PV arrays are beneficial for PV projects in some climatic zones where conservation of the soil and their potential for biological production is a concern. However, in our study the panel temperature data and the electricity production data from the growing season imply that the co-located vegetation may not always positively impact the performance of the PV arrays in a humid, continental

climate. Therefore, the microclimatic interaction between PV arrays, soil, and vegetation is not consistent across varying landscapes and climates. Consequently, the considerations for co-locating vegetation with PV arrays in any climate should include a site-specific assessment of the tradeoffs between resultant microclimatic determinants stemming from the presence of vegetation.

In our study, since both power production and panel temperature were slightly higher in the bare PV treatment than in the veg PV treatment in the early morning and in the late afternoon (Fig. 2.5 a and b), the panels in the bare PV treatment may have received more solar radiation than those in the veg PV treatment during these times. Had the PV arrays in the two treatments received the same amount of solar radiation, the higher panel temperatures in the bare PV treatment should have coincided with lower power output due to higher cell efficiency (Evans & Florschuetz, 1978), which is not the case. Therefore, it is more likely that the panel temperature in the bare PV treatment is higher because it simply received more solar radiation than did the veg PV treatment. This power output discrepancy may have largely contributed to the veg PV treatment's electricity production deficit over the observation period. A likely explanation for the veg PV treatment's potential solar radiation deficit is shading due to tall vegetation: since the PV arrays are mounted two meters above ground and are three meters along their east-west axis, one-meter-tall plants may have shaded as much as the bottom 0.3 meters of the arrays when they were at a 45°-tilt in the beginning at and at the end of the day. The obstruction from the co-located vegetation can be avoided by choosing plant species that do not grow tall enough to shade the panels, increasing the height on the mounting system, or mowing, though less preferred (Jordan Macknick *et al.*, 2022). Another approach is to open the

facility for sheep grazing, which can increase the soil nutrient content and generate extra revenue without modification of the array mounting system (Towner *et al.*, 2021; Macknick *et al.*, 2022).

Contrary to the previous study that observed lower panel temperatures in arrays with co-located vegetation (Barron-Gafford *et al.*, 2019), distribution of panel temperatures between the bare PV and the veg PV treatments did not differ over the entire daylight hour or during the hours 10 to 15 ($p < 0.05$) (Supporting Information S3), and the distribution of power production in these time windows were also not significantly different between the treatments ($p < 0.05$). While the inverter data cannot conclusively disprove the previously hypothesized benefit of vegetation cover on the PV systems (Barron-Gafford *et al.*, 2019), our analysis of the inverter data suggests that the impact of the vegetation-driven conductive cooling of the PV panels in some temperate climates may not be large enough to overcome the opposing effects, such as slower winds due to increased surface roughness. Furthermore, higher relative humidity in the study area when compared to arid regions (Barron-Gafford *et al.*, 2019) could have decreased the power output of the PV cells by increasing the water vapor and condensed water droplets on the cell surface that scatter solar radiation (Kazem & Chaichan, 2015), which may have negated the elevated cell efficiency from lower panel temperatures.

Another explanation for the lack of significant difference in the panel temperature between the two treatments may be a comparison of ET rates between the two PV treatments. Crop evapotranspiration ET_c can be estimated as per the following equation: $ET_c = ET_{ref} \times K_c$, where ET_{ref} is reference ET, and K_c is crop coefficient (Richard G. Allen *et al.*, 2005). This model of ET divides the ET process into energy-

limited (or atmosphere controlled) Stage 1 and water-limited (soil controlled) Stage 2. For the study sites where the average rainfall interval during the growing season is between 1-2 days and soil surface is consistently wet, K_c for the bare PV treatment can be higher than or comparable to that of a vegetated surface (Fig. 2.6a), and the resulting evaporation may exceed or equal the ET rate in the vegetated PV treatment. The soil surface is consistently kept moist by frequent rainfall events, thereby maintaining evaporation at or near the rate of free-water evaporation. Therefore, in a temperate climate with a wet growing season, the magnitude of ET-driven diversion of net radiation into latent heat in a PV site with a bare soil may be comparable to that of a PV site with underlying vegetation, resulting in slightly higher but still comparable temperatures in the non-vegetated PV. In water-limited environments with long duration between rainfall events, K_c of the bare soil will be significantly lower than that of a vegetated surface (Fig. 2.6a), and the difference in panel temperature will likely be significantly larger in the opposite direction. Vegetation can maintain much higher transpiration rates by utilizing root zone soil moisture even after soil evaporation is drastically reduced (Stage 2) as the surface soil dries out. Even though ET-driven panel cooling was negligible during the study period, crop coefficient during Stages 1 and 2 for the veg PV treatment at this site may increase in the future growing seasons as the vegetation becomes more established (increase in leaf area index), which may result in a cooling effect large enough to create a discernible increase in the productivity of the overlying PV arrays. This possibility prompts the need for a multi-year study with a similar experimental design.

Recent pilot-scale studies have demonstrated the effect of vegetation on PV panel cooling, however the actual benefits to electricity generation and irrigation requirements

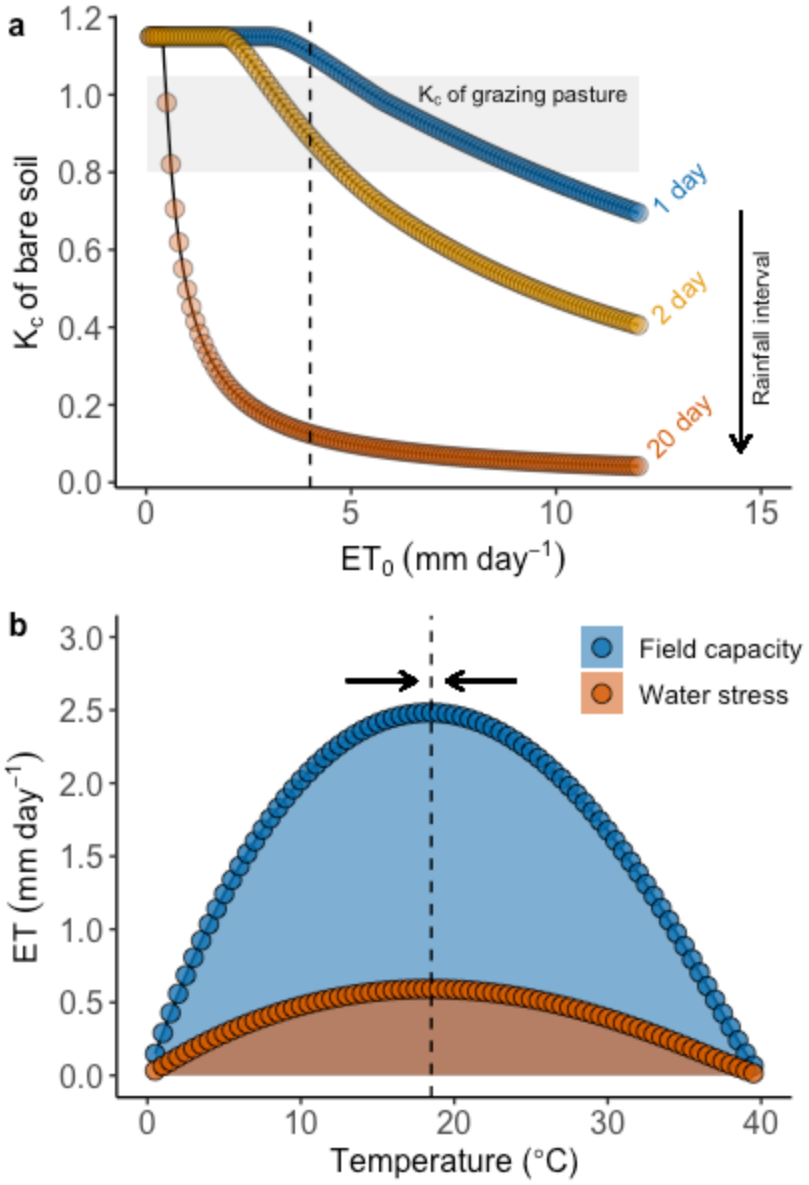

Figure 2.6 ET-driven panel cooling effects are site specific: a. Crop coefficient (K_c) of bare soil as a function of reference ET depth and rainfall intervals. The shaded area represents the typical range of K_c for grazing pastures, and the vertical dotted line represents an example daily value of growing season reference ET in the study region (modified from Allen et al (2005)); b. Evapotranspiration as a function of air temperature at high soil moisture (field capacity) and water stress conditions (Penman–Monteith equation combined with Stewart (1988) model of leaf conductance to include environmental controls on canopy resistance). The vertical dotted line represents the optimal air temperature for ET.

need to be investigated. To determine whether co-location is worth the cost of irrigation and soil quality improvements in arid regions, one should consider its benefits to the

vegetation (shading, water use efficiency) and the extent of improvement in electricity generation. To demonstrate the effects of water limitations and temperature on crop ET, we used the Stewart model (Stewart, 1988) of leaf conductance and the Penman–Monteith model (Dingman, 2015) to compare the transpiration rate from the canopy for soil-moisture deficits. Even though the leaf conductance nonlinear functions for environmental controls on canopy conductance (incident short-wave radiation, specific humidity deficit, air temperature and soil moisture deficit) used in this example are not specifically for grassland species, it is instructive to visualize the significance of water limitations and temperature on ET (Fig. 2.6b). The detailed description and inputs of the model are provided in the Appendix A. In arid and semiarid systems, maintaining higher vegetation ET may result in panel cooling and potential increase in electricity generation. However, bringing the soil to field capacity to maximize the ET in such an arid climate will require additional irrigation (Fig. 2.6b), which also comes at a cost in water-limited systems. Further, water for cleaning panels and for dust suppression can be a significant component of the water budget of solar facilities in desert regions (Ravi *et al.*, 2014), and it may place a major demand on the already scarce local water resources.

The fact that the soil temperatures were lower in the veg PV and the bare PV treatments than they were in the control site during the growing season (Fig. 2.2b) implies that the shading from the PV arrays may cool the underlying soil-vegetation. Since photosynthesis declines at temperatures exceeding 30° C for C_3 plants and 35° C for C_4 plants and stops increasing at solar radiation exceeding certain threshold, partial shading by the PV panels may benefit the vegetation. It is well understood that partial shading can increase yield, nutritional quality, and/or survival rate of some crops, such as lettuce,

tomatoes (Wolff & Coltman, 1990a, 1990b), cherry tomatoes (Rosales *et al.*, 2011), while this is untrue for other crops, such as broccoli (Kläring *et al.*, 2001), or peanuts (Wolff & Coltman, 1990b). The variability in shade response across different types of plants imply that the selection of suitable vegetation or crop for co-location as consistent with the background condition is essential for the viability of co-location. As with the panel-cooling effect, the shading from the PV panels may be more beneficial for vegetation in arid and semi-arid regions with high air temperature and abundant solar radiation, and utility-scale PV facilities may even be used to expand areas with temperature range and radiation intensity that are ideal for certain crops. Further, shading by panels can decrease ET and thereby increase irrigation water use efficiency. In our study the vegetated solar sites had lower diurnal variations in soil temperatures even though the vapor pressure deficits were not significantly different between the treatments. On the other hand, the partial shading from the PV arrays may decrease crop yields in temperate regions which have considerably less net radiation than arid regions, and the only way to increase plant-available solar radiation in these areas may be to increase the spacing between the PV arrays or the PV panels. However, lower PV density will result in lower energy production and a reduced ground-cover ratio, which can affect economic viability as profit margins for PV are currently higher than most agricultural crops. Therefore, our findings show that agrivoltaics in temperate regions may be suited for maintaining the multiple ecological functions of the soil with native vegetation or providing supplemental income with cultivation of shade-tolerant crops or pastoral activities.

2.6. Conclusions

Agrivoltaics in areas with soil carbon debt can be an effective climate mitigation strategy along with revitalizing agricultural soils, generating income streams from fallow land, and providing pollinator habitats. The compounding effect of PV arrays and underlying vegetation may homogenize soil moisture distribution and provide greater soil temperature buffer against extreme temperatures. The effect of vegetation-induced panel cooling on electricity generation are rather site-specific and can be predicted using background climatic parameters and soil properties. We expect the temperature buffering and panel cooling effects to be greatly amplified in arid and semi-arid regions and may provide opportunities to expand agriculture to marginal lands, but with additional investments for irrigation and improving soil quality. Our findings provide foundational data for site preservation and for optimizing agrivoltaic designs by targeting site specific co-benefits and highlight the need to target site specific ecosystem services.

2.7. Supporting Information

Supplementary information is available in Appendix A.

2.8. Data availability

All data used in our work can be found online (https://figshare.com/s/05ad6d8ea5449979a67e).

CHAPTER 3.

MICROCLIMATE AND SOIL INFLUENCE OF VEGETATION AT THREE UTILITY-SCALE SOLAR SITES IN HUMID CONTINENTAL CLIMATE

(This chapter is in postprint for publication in *Applied Energy*)

3.1. Abstract

Concerns over the land use changes impacts of solar photovoltaic (PV) development are increasing as PV energy development expands. Co-locating utility-scale solar energy with vegetation may maintain or rehabilitate the land's ability to provide ecosystem services. Previous studies have shown that vegetation under and around the panels may improve the performance of the co-located PV and that PV may create a favorable environment for the growth of vegetation. While there have been some pilot-scale experiments, the existence and magnitude of these vegetation benefits has not been confirmed in a utility-scale PV facility over multiple years. In this study, we use measured power output coupled with microclimatic measurements in temperate climates to assess these potential benefits. This study combines multi-year microclimatic measurements to analyze the physical interactions between PV arrays and the underlying soil-vegetation system in three utility-scale PV facilities in Minnesota, USA. No significant cooling of PV panels or increased power production was observed in PV arrays with underlying vegetation. Fine soil particle fraction was the highest in soils within PV arrays with the vegetation which was attributable to the lowest wind speeds from the compounding suppression of wind by vegetation and PV arrays. Soil moisture and soil nutrient response to re-vegetation varied between PV facilities, which could be attributed to differing soil

texture. No statistically significant vegetation-driven panel cooling was observed in this climate. This finding prompts a need for site-specific studies to identify contributing factors for environmental co-benefits in co-located systems.

3.2. Introduction

Installed capacity of solar photovoltaics (PV) has been rapidly growing due to decreasing costs, increasing policy support, and the burgeoning demand for energy with low carbon emissions: In the US alone, the annual capacity additions of utility-scale solar energy (USSE) have increased from lower than 1 GW $year^{-1}$ to more than 20 GW $year^{-1}$ over the past decade (Boligner *et al.*, 2019; Chaturvedi & Malyan, 2021; L. Gill *et al.*, 2021; US Energy Information Administration, 2022). Similarly, increasing numbers of farmers are investing in on-farm PV systems to power their farming operations or alternatively, leasing out their lands for USSE development to provide a reliable revenue stream independent from the volatility of agricultural markets (Beckman & Xiarchos, 2013; Maltais, 2019; Nir, 2020; US Department of Energy, n.d.). While PV has low greenhouse gas (GHG) emission rates and may be sited on degraded lands (Hoffacker *et al.*, 2017), USSE construction and operation on an ecologically or agriculturally important land can affect ecological functions and agricultural productivity in multiple ways.

First, conventional construction practices of USSE modifies the landscape, which can include vegetation removal, soil removal, grading, and compaction of soil from the use of heavy machinery= (Bureau of Land Management (BLM) & US Department of Energy (USDOE), 2012). Removal of soil and vegetation decreases gross primary productivity and carbon sequestration capacities (Bureau of Land Management (BLM) & US Department of Energy (USDOE), 2012; Choi *et al.*, 2020; Larney *et al.*, 2000, 2016). Decreased carbon

sequestration and soil organic carbon stock may result in reduced aggregate stability of the soil, which may accelerate erosion and further loss of soil nutrients (Bronick & Lal, 2005). Soil compaction has been shown to limit rooting depth and root density in experiments that compacted soils to varying degrees by driving tractors over them (Raghavan *et al.*, 1979). In some construction practices, topsoil is moved into a stockpile and then redistributed so the underlying earth material can be graded without damaging the topsoil, but even this practice can cause reductions in organic carbon, nitrogen, and soil aggregate stability (Wick *et al.*, 2009). Second, maintenance of un-vegetated USSE plants can further degrade ecosystem services: Cook & McCuen (2013) has concluded that the operation and maintenance of solar facilities on a bare or gravel ground cover may increase peak stormwater discharge and soil erosion rates at the base of the PV panels by concentrating the intercepted rainwater into a flow with a higher kinetic energy (Cook & McCuen, 2013), which was corroborated by a field study (Choi *et al.*, 2020). Soil erosion, especially of fine particles, may cause long-term damage to the soil's ability to retain life-supporting nutrients (J. Li *et al.*, 2007; Matus, 2021). Additionally, Lovich and Ennen (2011) has suggested that the operation and maintenance of the PV facilities may cause habitat fragmentation and obstruct gene flow (Lovich & Ennen, 2011). In short, the modification of the landscape from the construction of PV sites and the operation of un-vegetated USSE facilities can compromise the ecosystem services of the land. These potential environmental impacts may be a cause for concern for landowners who wish to use the land for farming or conservation efforts following the lease to solar developers, if they are not appropriately mitigated. These concerns can be addressed by investigating the

influence of PV arrays on the surrounding environment and the underlying soil, then using the findings to develop or refine mitigation strategies.

One strategy to reduce the land-use impacts of USSE is co-location of PV with beneficial vegetation, which was first proposed in 1982 as a technique for modifying the PV operation to grow crops from PV-occupied lands (Goetzberger & Zastrow, 1982). Studies have shown that a co-located system with proper crop selection for partial shading has potential to increase the land equivalent ratio compared to cropland or a ground-mounted PV system of equivalent land area (Marrou, Guilioni, *et al.*, 2013; Marrou, Wery, *et al.*, 2013) as well as create microclimatic zones with favorable temperatures that can extend the growing season for some crops (Armstrong *et al.*, 2016; Barron-Gafford *et al.*, 2019; Graham *et al.*, 2021; Pregitzer & King, 2005). Co-location practices that focus on restoring or maintaining native plants instead of crop production are sometimes referred to as "ecovoltaics", and they have the potential to improve the lands' ability to provide ecosystem services such as carbon sequestration and pollination, which may even benefit neighboring farmlands (Walston *et al.*, 2018, 2021). Furthermore, experiments in PV facilities co-located with native plants have shown only minimal reduction in aboveground net primary production and evapotranspiration underneath the panels despite significantly reduced light, implying that re-established plants may sufficiently grow even in the dynamic shading environment within PV arrays (Beatty *et al.*, 2017; Kannenberg *et al.*, 2023; Sturchio *et al.*, 2022). However, impact of PV construction may have lasting impacts on the soil: a study on the soils in an agrivoltaic site in Colorado, USA saw that fine fraction of the soil particles and total soil carbon (TC) and nitrogen (TN) contents in a conventionally constructed PV facility had not recovered to the reference levels after a

decade even with sufficient vegetation cover in the array (Choi *et al.*, 2020). In contrast, another study in Minnesota, USA showed PV arrays with minimized land modification and reestablished native vegetation experienced reduced erosion of the fine soil particle fraction and retained total soil carbon and nitrogen to the reference levels in nearby undisturbed soil, while PV arrays with bare soil underwent loss in fine particle fraction, TC, TN, and various soil cations (Choi *et al.*, 2023). The relative abundance of these variables in the vegetated array may have been due to the avoidance of land modification as well as re-vegetation. Therefore, the extent of mitigated soil alteration due to avoided land grading needs investigation.

Studying the influence of PV arrays on the soil-vegetation component of agrivoltaics also provides opportunities to investigate the influence of vegetation on PV performance, the studies of which are relatively scarce. Barron-Gafford *et al.* (2019) observed lower panel temperatures and diurnal panel temperature fluctuations in agrivoltaic arrays compared to those in an adjacent PV array at a test site and concluded that the added evapotranspiration by the co-located vegetation increases the portion of incoming solar radiation that is converted to latent heat, thereby decreasing the sensible heat flux to the PV panels for an irrigated system in an arid region (Barron-Gafford *et al.*, 2019). The findings of this study provide motivation for similar research in USSE installations, which currently represents the majority of ground-mounted PV installations (Solar Energy Industries Association, 2022). Furthermore, vegetation-driven panel-cooling has not been observed in environments other than drylands, and the resulting increase in efficiency is yet to be confirmed by electricity production data from other climates. To address this gap, this study links multi-year microclimate and power

production data in three USSE facilities in Minnesota, USA. Additionally, this study combines soil chemistry and particle size analyses of the soil samples from the PV facilities with the microclimate data to study the physicochemical impact of the PV arrays on the underlying soil-vegetation complex and its potential to conserve or improve the native productivity of the soils after the construction of PV arrays.

3.3. Methods

3.3.1 Description of the Study Sites and Field Data Collection

Meteorological and soil data and samples were collected in three utility-scale solar PV facilities owned and operated by Enel Green Power North America (EGP-NA) located in Minnesota, USA (Fig. B.1b). Details of the three facilities (Atwater, Chisago, and Eastwood) are listed in Table B.1 (Appendix B) in supporting information. Each facility contained three treatments: PV arrays on soil that was re-vegetated with native grasses, referred in this study as "vegetated PV" (veg PV), PV arrays with bare ground cover, or bare PV, and an adjacent undisturbed open-sky area with similar native grasses and forbs as the control. Part of the bare PV treatment at Chisago and the veg PV treatment at Atwater was graded, but the topsoil was removed and stockpiled on site prior to grading and redistributed after the fact. Due to the timeline of the study, soil data prior to the construction of the facilities was not available. However, because the control was adjacent to the treatments but outside of the direct construction, the soil conditions and other physical attributes of the control were considered a valid representation of those in the two treatment areas prior to the construction. Therefore, the soil and other physical data taken post-construction in the other two treatments would reflect the combined effects of the construction and the treatments.

In the veg PV and the bare PV treatments, soil moisture data measured as volumetric water content and soil temperature measurements were collected at a 25-cm depth in four locations: below the western edge (WE) of one of the PV arrays, in the interspace (IS) between the two rows of the arrays, below the eastern edge (EE) of the other PV array, and in the area below one of the PV trackers (BP) (Fig. B.1d). In veg PV and bare PV, six 5-cm soil cores were randomly sampled from areas underneath the PV panels (area between a WE and EE of the same row) and another six from areas between the rows of PV panels with open sky. Six 5-cm soil cores were also sampled from the control as well. This depth was chosen to examine the effect of soil erosion and the resulting change in the soil nutrients. In addition to the 5-cm cores, three bulk core samples were collected from each treatment at all three facilities. The samples from the veg PV treatment and the bare PV treatments were taken in areas at least a meter away from posts or buried cables. Soils in areas directly under the panel edges, gaps between panels within a row where evidence of concentrated rainfall impact was observed were also not sampled.

Electricity production data from the bare PV and the veg PV treatments in all three facilities were provided by Enel Green Power North America (EGP-NA). The bare PV treatment and the veg PV treatment each contained an inverter that was linked to 1,044 modules (328.9 kWp), whose total surface area was 2,026 m^2. Production data were recorded every 15 minutes from January 1st, 2019 to December 31st, 2021. The power data (W_{dc}) were normalized by the solar irradiance (W m^{-2}) and the total surface area of the PV (m^{-2}). Any power data that coincided with the solar irradiance ≤ 0 were filtered out. Due to equipment failure, inverter data from Chisago before 2021 and between May 1st and June

10th in 2021 and those from Eastwood between May 30th and September 31st in 2021 were excluded from analysis.

3.3.2 Laboratory Measurements

The soil samples were tested for a suite of soil nutrients including total soil carbon (TC), and total soil nitrogen (TN) with a standard combustion method, and also for phosphorus (P), potassium (K), calcium (Ca), magnesium (Mg), manganese (Mn) using Mehlich III (Brookside Laboratories, INC. New Bremen, USA) (Ross & Kettering, 2011). For statistical procedures, any soil nutrient content that was reported as below detection limit was removed from analyses. In addition to the nutrient content, particle size distribution (PSD) of the collected soil samples was determined with a laser diffraction particle sizing analyzer (LS 13320 with aqueous liquid module, Beckman Coulter, Inc. CA, USA) with a grain diameter measurement range of 0.4 – 2000 μm. Prior to the PSD analysis, the samples were disaggregated (but not pulverized) with a soil crusher and sieved through a 2 mm sieve. Organic matter was removed from the samples by submerging the sample in a sodium hypochlorite solution (100 mL 2M HCl to 1 liter of sodium hypochlorite, 12.5%) for 24 hours.

3.3.3 Analyses

The electricity production data of the PV modules in the veg PV treatment and those in the bare PV treatment was compared using the DC power record from the inverter data. Malfunctioning solar tracking system may put the PV array at a suboptimal angle, which may significantly decrease the power production of the array. To account for the tracking system malfunction, outliers ($1.5 \times IQR$) were removed to account for large differences in the power output due to instances in which the sunlight tracking systems malfunctioned

in one of the two treatments. The exact timing of the tracking system malfunctions was unknown, so the data within the time window of tracker malfunction had to be visually identified and removed.

Since t-test on autocorrelated data may yield a type I error, a modified t-test was used to compare the means of continuous time series of DC power output from bare PV and veg PV treatments (O'Shaughnessy & Cavanaugh, 2015). The t-test was performed on the data above the 10^{th} percentile to exclude the readings during low sunlight periods and on those above the 50^{th} percentile to focus on high insolation periods. Before performing the t-test, the Durbin-Watson (D-W) test was performed on the data to determine whether they constituted AR(1) time series (O'Shaughnessy & Cavanaugh, 2015).

Analysis of variance (ANOVA) and Tukey post hoc test (at $\alpha = 0.05$) were performed to determine the difference in the soil nutrient content among the treatments.

3.4. Results

3.4.1 PV Temperature and Power Output

Over the three growing seasons, power output and panel temperature were similar in both treatments throughout the day. The times of the day when the difference in either were the most pronounced was in the early mornings (hours 6 - 9) and late afternoons (hours 14 – 18), and the power output and the panel temperature difference occurs in the same direction (Fig. 3.1a) The median difference in in daily electricity output (output difference = bare PV output – veg PV output) was positive in all three facilities, which meant that the bare PV produced more electricity in all three facilities (Fig 1b). However, the t-test showed no significant difference ($p < 0.05$) in electricity output from the PV

arrays between the bare PV and the veg PV treatments under all, 50th percentile, or 90th percentile of the irradiance levels (Table 1).

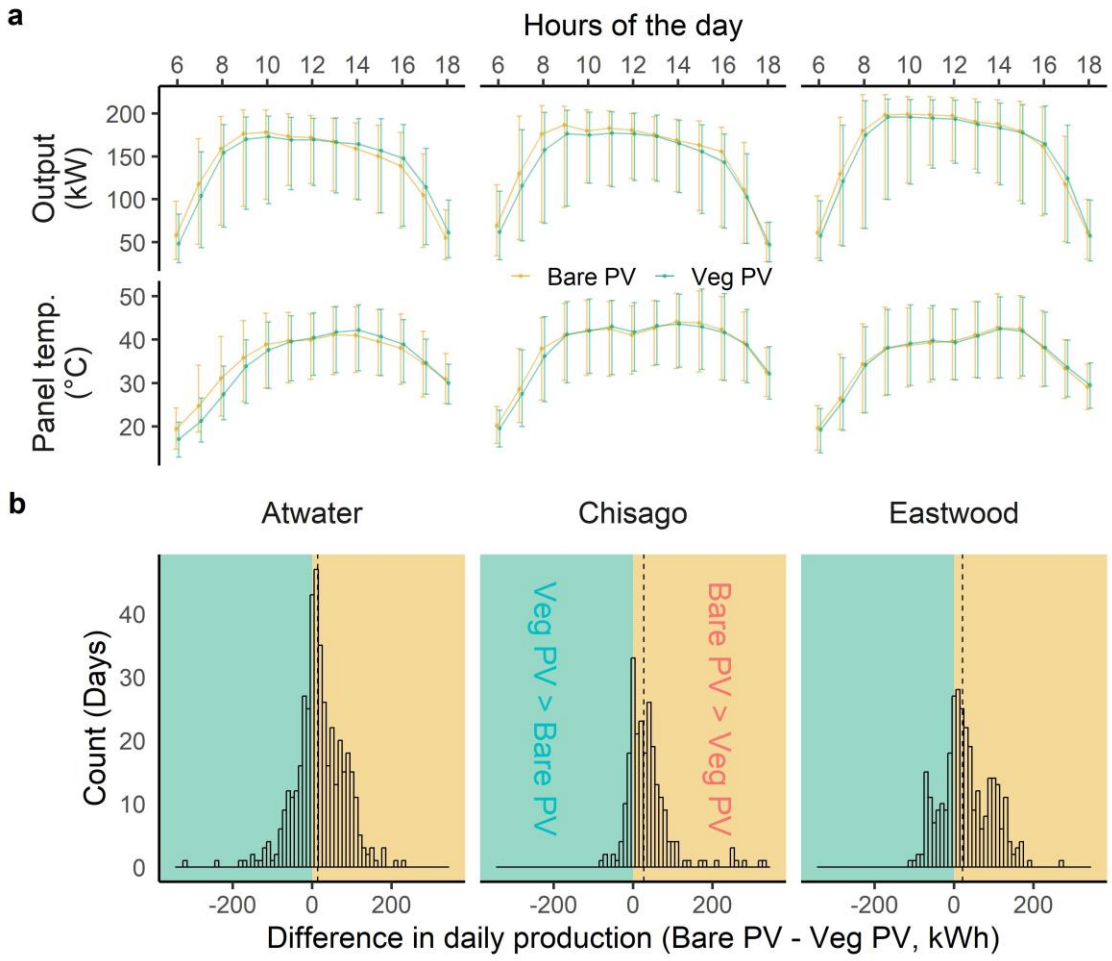

Figure 3.1 a. Daily profile of median DC power output (kW) and median panel temperature (°C) over the growing seasons (between May and September of the years 2019, 2020, and 2021). The whiskers represent the 25th and the 75th percentiles; b. Histogram of raw difference (kWh) in daily production between Bare PV and Veg PV (Bare PV – Veg PV), separated by facility. The vertical dashed line represents the median, and the colored area represents the range in which the daily production of a treatment exceeds that of the other treatment type. Throughout, Bare PV is tan and Veg PV is cyan.

Table 3.1. Comparison of power output between the bare PV and the veg PV treatments using t-test ($p < 0.05$).

Facilities		**Atwater**			**Chisago**			**Eastwood**		
	Compared treatments	**2019**	**2020**	**2021**	**2019**	**2020**	**2021**	**2019**	**2020**	**2021**
Power output (kW_{dc}) at top 10% irradiance	Bare PV - Veg PV	0.7495	0.8650	0.7279	0.7834	0.9448	0.7163	0.3950	0.9278	0.6942
Power output (kW_{dc}) at top 50% irradiance	Bare PV - Veg PV	0.6032	0.8795	0.5564	0.8335	0.8143	0.9315	0.2297	0.9363	0.2228
Power output (kW_{dc}) at all irradiance levels	Bare PV - Veg PV	0.7361	0.9385	0.8618	0.7416	0.9709	0.8933	0.3151	0.9639	0.8662

3.4.2 Microclimate

Overall, air temperature and relative humidity were not significantly different among the treatments in all facilities (Fig. 3.2). However, the median of the daily minimum temperatures was slightly higher in the bare PV treatment than in the veg PV treatment and the control, whereas the median of the daily minimum relative humidity was the lowest in the bare PV treatment. Additionally, the median of the daily maximum air temperature was slightly higher in the veg PV treatments than in the other two.

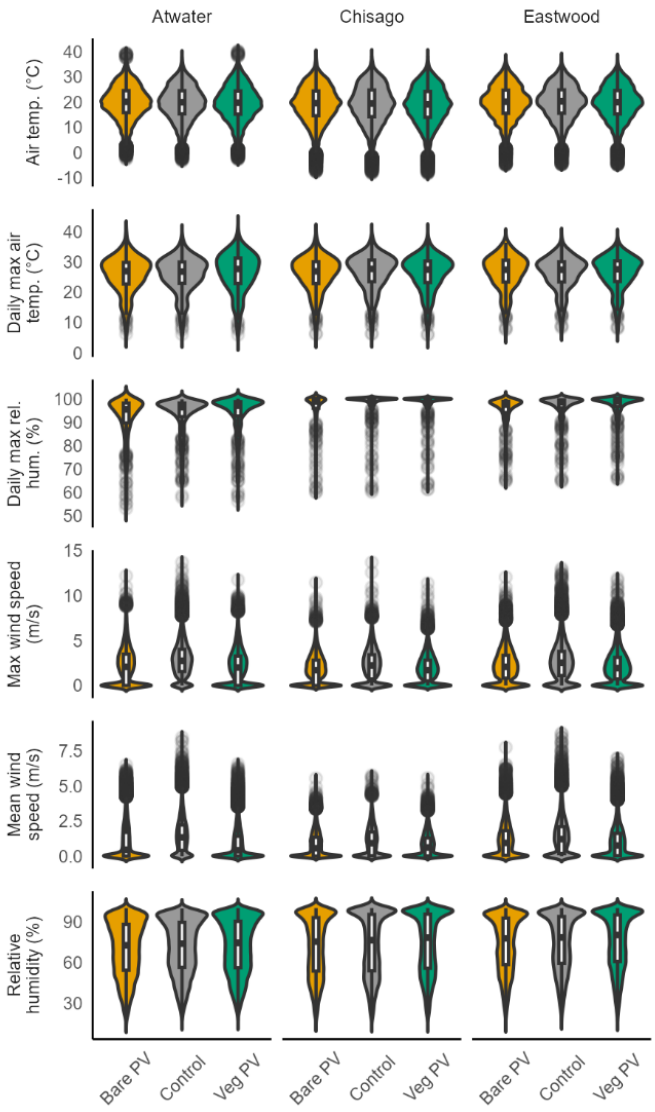

Figure 3.2. Distribution of air temperature and relative humidity at each treatment over all three growing seasons of the study period. The color under the curve indicates tail probability, which is 0 at the darkest and 50% (median) at the highest.

Higher wind speeds were more frequently recorded in the control than in the other two treatments in all three facilities over the growing seasons, and the veg PV treatment experienced the least frequent higher wind speed observations (Fig. 3.2 & 3.3). The bare PV and the veg PV treatments had lower mean wind speed and higher percentage of calm

periods compared to the control. Between the bare PV and the veg PV treatments, the bare PV experienced higher wind speeds more frequently than the control in Atwater and Eastwood, while the opposite was true in Chisago.

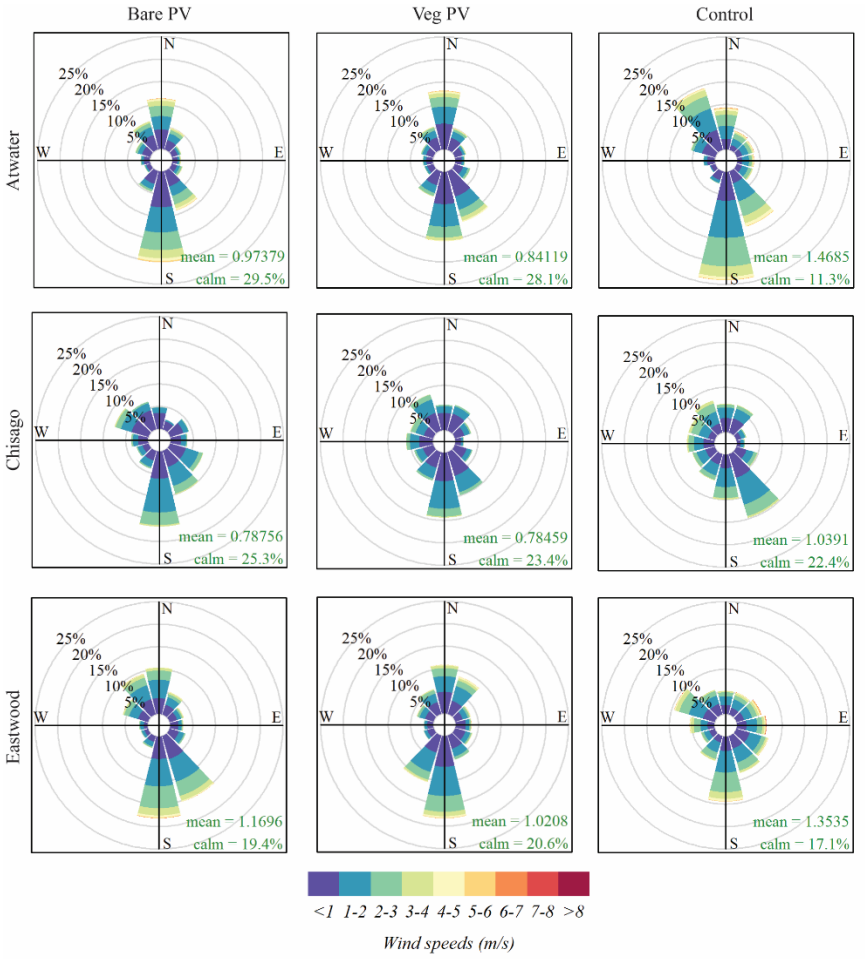

Figure 3.3. Wind roses representing frequency of counts (%) by wind direction over the growing periods from 2019 to 2021. The thickness of the bands represents frequency of measurement, and the colors represent average wind speeds (m/s). The data is separated by facilities and treatments. Calm percentage represents the percentage of measurements for which the wind speed was lower than the minimum sensible speed of the wind speed measuring equipment.

3.4.3 Soil Particle Size Distribution and Nutrients

Overall, Chisago had the coarsest soil texture (sand), while Atwater (a sandy loam) and Eastwood (a silt loam) had finer soil textures (Fig. 3.4a, B.2a, B.2c). Eastwood had the

highest total carbon (TC) and total nitrogen (TN) on average, and Chisago had the lowest at approximately half of those of Eastwood (4b). In all three facilities, the bare PV and the veg PV treatments had higher mean phosphorus (P) and zinc contents (Zn), but no other consistent pattern in the relative abundance of macro and micro soil nutrients emerged (Fig. 3.4c).

In Atwater, the control had the highest and the most variable mean grain sizes, and the bare PV and the veg PV had similar mean grain sizes, while sorting was similar in all three treatments (Fig. 3.4a). The TC and TN contents were similar in the bare PV and veg PV treatments but significantly higher in the control (Fig. 3.4b). The mean of the total exchange capacity (TEC) and the manganese (Mn) content were similar in all three treatments (Fig. 3.4c). The bare PV treatment had the highest mean potassium (K), phosphorus (P), and sulfur (S) contents. The mean zinc (Zn) content was higher in the bare PV and veg PV treatments compared to the control.

In Chisago, the bare PV treatment had the most homogenous grain size distribution (low sorting) and slightly higher mean grain size than the veg PV treatment and the control. The TC content in the control and the veg PV were similar but significantly lower in the bare PV treatment. The TN content was the highest in the control and the lowest in the bare PV treatment. In Chisago, the mean TEC was similar between the veg PV treatment and the control, but the veg PV had higher mean content of K, Mn, P, S, and Zn than the control did. The bare PV treatment had the lowest TEC, iron content, K, Mg, and Mn, but its P, S, and Zn contents were still higher than those of the control.

In Eastwood, the control had the largest mean grain size and the largest variation in grain sizes (highest sorting). The bare and the veg PV treatment had similar mean grain

sizes, but the bare PV treatment had the most homogeneous grain sizes (lowest sorting). The TC and TN contents were similar in all three treatments. The bare PV treatment had significantly higher mean Zn content and around 400% of the mean P content of that of the control. Conversely, TEC and other mean soil nutrients contents (Cu, K, Mg, Mn, and S) were lower in the bare PV than those in the control. The Fe content was similar in the bare PV treatment and the control. As in the bare PV treatment, the mean Zn and P contents in the veg PV were higher than those in the control, while the mean Cu, Fe, K, Mg, Mn, and S contents, and the TEC were lower than those in the control.

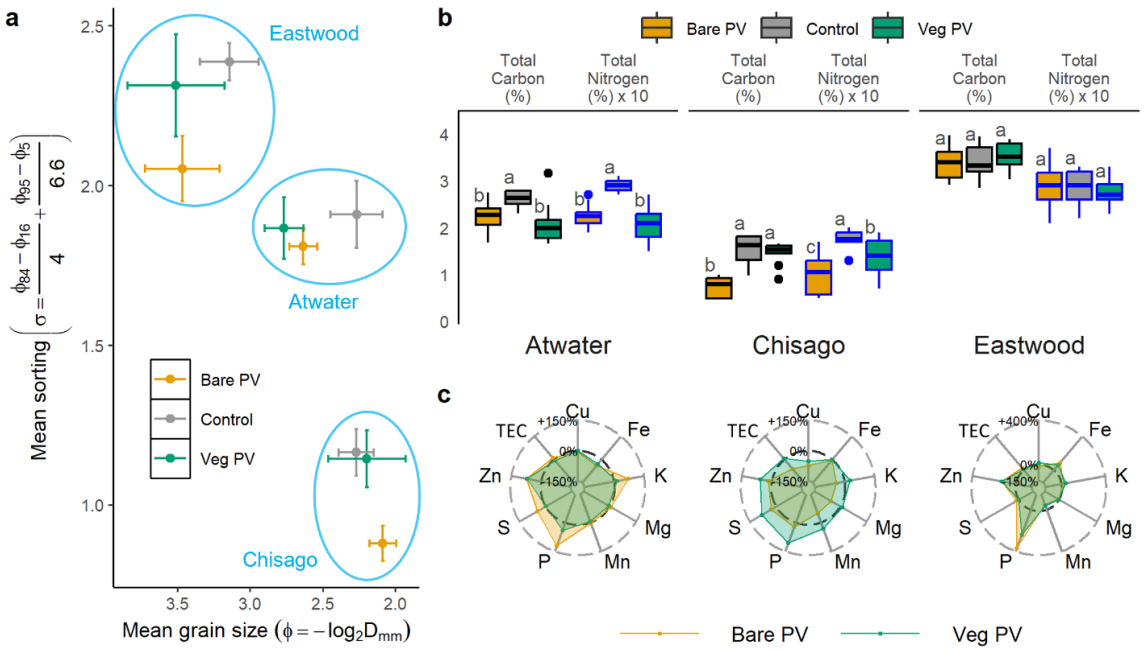

Figure 3.4 a. Mean grain size against mean sorting with the whiskers extending to one standard deviation; b. Boxplots of total carbon (% by weight) and total nitrogen (% by weight × 10). The letters next to the boxes show the result of Tukey's honest significance test, and the differing letters represent significant difference among treatments within a facility. The middle notch represents the median, the bottom and the top of the box represent the first and the third quartiles, and the whiskers extend to 1.5 times the interquartile range. The colors represent treatments, and the boxes bordered with black lines show total carbon data while the boxes with blue lines show the total nitrogen data; c. radar plots of the percent difference in soil cations and cation exchange capacity between a corresponding treatment and the control. 0% signifies no deviation from the

control. Axis label key: TEC = total exchange capacity; Cu = copper; Fe = iron; K = potassium; Mg = magnesium; Mn = manganese; P = phosphorus; S = sulfur; Zn = zinc.

3.4.4 Soil Moisture and Temperature

Every subsequent growing season, precipitation decreased in frequency and depth, and the local minima of the soil moisture in the veg PV and the control prior to a precipitation event also decreased over the years (Fig. 3.5a). Within each treatment, the soil moisture distribution was heterogenous among the relative positions along the transverse profile through the solar arrays (Fig. 3.5b), but the pattern was not consistent in magnitude or direction across the treatments. On the other hand, the heterogeneous distribution of soil temperature among the relative position was consistent across both PV treatments and all three facilities. In Chisago and Eastwood, the soil moisture was higher in the veg PV treatment and the control than in the bare PV treatment, but Atwater showed higher soil moisture in the bare PV treatment and the control than the veg PV treatment (Fig. 3.5a and b). The soil moisture measurements in the vegetated PV treatment and the control drifted downwards over the three years, which is apparent in some of the time series in Fig. 3.3a but also in the corresponding curves that are wide and multimodal. This downward drift of the soil moisture measurements was less prominent in the bare PV treatment of all three facilities (Fig. 3.5a), whose corresponding distribution curves were narrower and more unimodal (Fig. 3.5b). The distribution of soil moisture varied among the relative positions within each treatment for the bare PV and the veg PV treatments in all three facilities, but the pattern of variation among the relative positions was not consistent across different treatments or facilities. For instance, interspace (IS) and east edge (EE) had higher median soil moisture than did west edge (WE) and below panel (BP) in the bare PV treatment of Atwater and Chisago, but the same was not true in the bare PV treatment in Eastwood nor

was it for the veg PV treatment. The only pattern that was consistent in both the bare PV and the veg PV treatments of all three facilities was that the IS had the highest soil moisture.

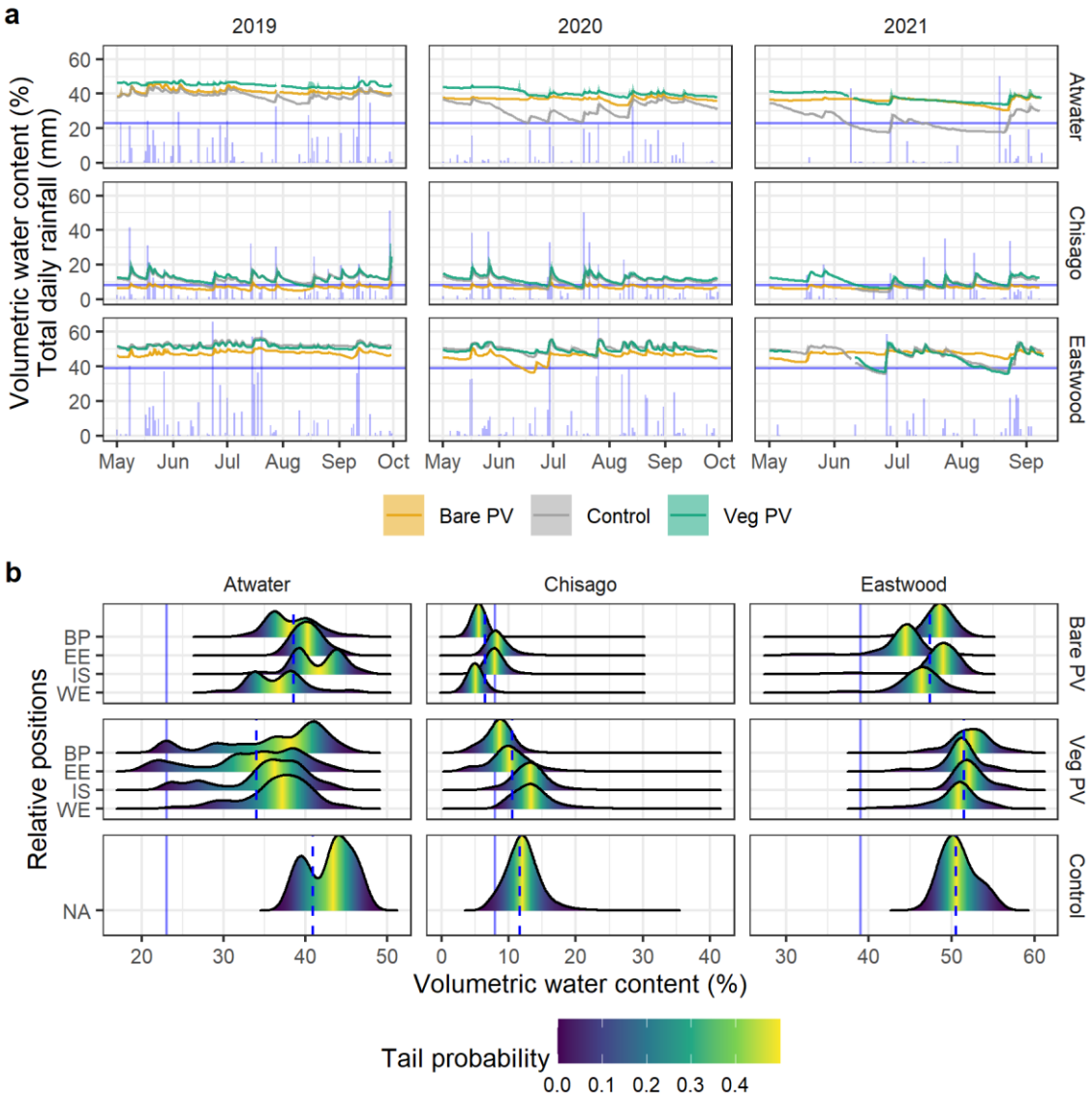

Figure 3.5 a. Time series of the daily mean soil moisture (unitless) among the treatments and total daily precipitation (mm), separated by year and facility; the daily mean soil moisture has been averaged across the relative positions; the solid vertical blue line represents soil moisture at field capacity based on the average soil texture at each facility (Tsoar, 2005); b. frequency distribution of the soil moisture over all three growing seasons; the curves are separated by the relative positions, and the plotting area is separated by facility, year, and treatment; the colors represent tail probability, and the dashed blue lines represent the median soil moisture across all sensors in the respective

treatments. The solid horizontal blue line represents soil moisture at field capacity, as in part a.

The daily mean soil temperature was the highest in the control during most of the growing seasons at all three facilities, and it was the lowest in the veg PV treatment at all facilities every growing season (Fig. 3.6a). As whole, the median soil temperature was the highest in the control and the lowest in the veg PV treatment (Fig. 3.6b). The difference in average soil temperature between the veg PV and the other two treatments is also the largest in the higher temperatures. Among the relative positions, the IS had the highest median soil temperature, and the BP had the lowest while the those of the WE and the EE's were in the middle.

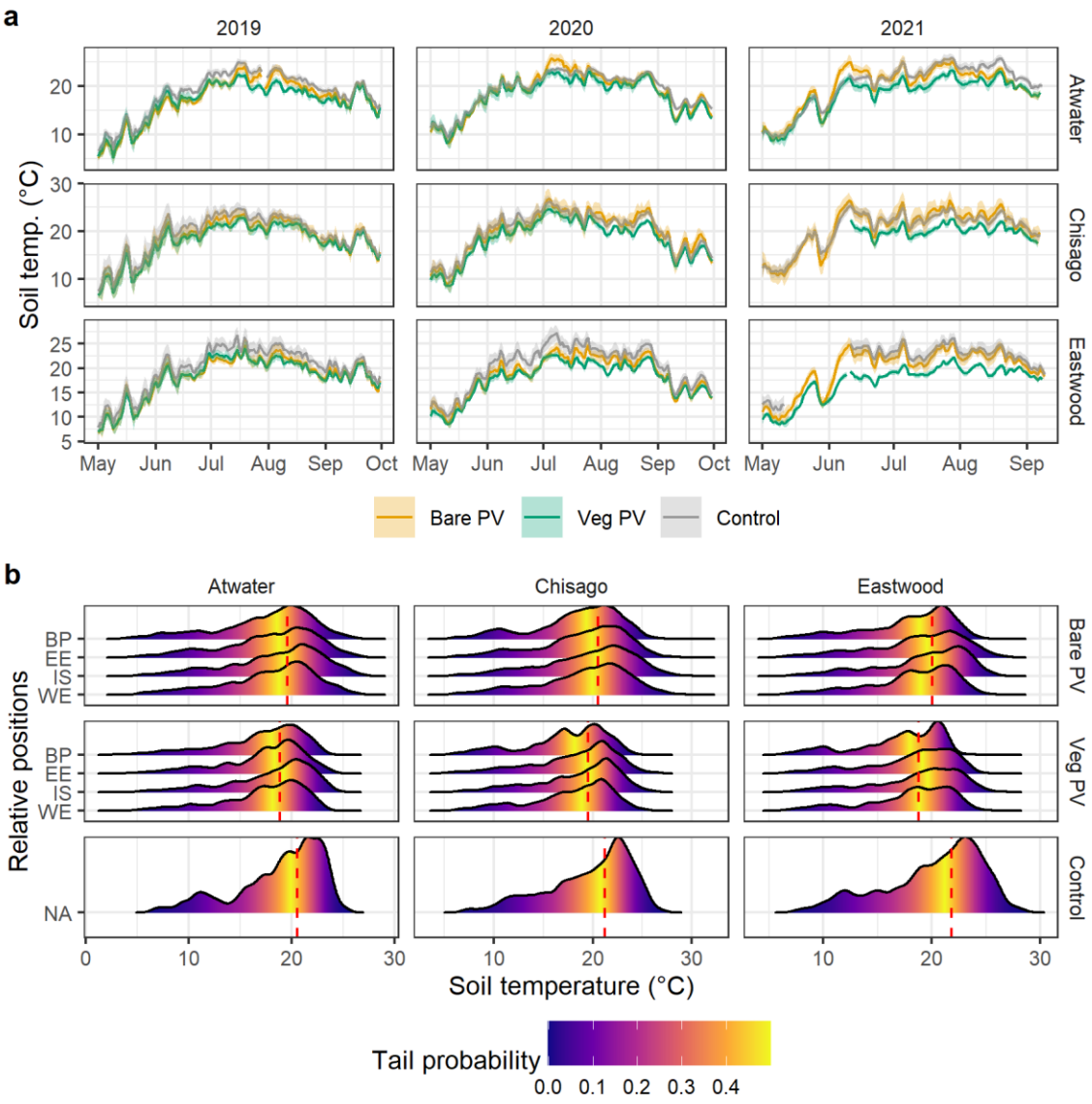

Figure 3.6 a. Time series of the daily mean of the soil temperature (°C) among the treatments, separated by year and facility; the daily mean soil temperature has been averaged across the relative positions; b. frequency distributions of the soil temperature measurements over all three growing seasons; the curves are separated by the relative positions, and the plotting area is separated by facility, year, and treatment; the colors represent tail probability, and the dashed red lines represent the median soil temperature across all sensors in the respective treatments.

3.5. Discussion

Our results indicate that, in this humid temperate climate with these soil types, vegetation under PV arrays without irrigation may not cool the overlying panels or improve

their performance to a statistically significant degree. The lack of difference in panel temperature between the bare PV and the veg PV treatments is explained by the similar lack of difference in the air temperature and relative humidity.

The combined influence of PV arrays and vegetation may decrease wind speeds and heterogeneous distribution of soil moisture and temperature in all three facilities, but the treatment responses in soil nutrient, grain size distribution, and hydrology were inconsistent across the facilities and with existing literature. Some of these discrepancies can be explained by the variation in soil characteristics and climate, which imply that the nature and the magnitude of environmental co-benefits of a co-located system are contingent on at least the soil characteristic and the climate. Therefore, site-specific knowledge of the climate and the soil is required to identify which co-benefits can be attained by a potential co-located system and maximize them.

3.5.1 PV Temperature and Performance in Co-located Systems

In humid temperate climates such as this one in Minnesota, vegetating PV arrays may not decrease the operating temperature of the overlying panels or increase their performance to a statistically significant degree. The lack of statistically significant difference in the power output and in the panel temperatures between the bare PV and the veg PV treatments (Fig. 3.1a, b, and Table 3.1) was consistent in all three facilities over every growing season at different irradiance levels. This is consistent with observations from a previous study (Choi *et al.*, 2023), but contrasts with a significant difference in panel temperature observed in an agrivoltaics study in drylands (Barron-Gafford *et al.*, 2019).

Higher frequency of rainfall and relative humidity in Minnesota compared to the dryland study may explain this lack of panel temperature difference: generally, a vegetated surface has a longer roughness length than a bare soil surface which leads to increased aerodynamic resistance to water vapor diffusion and decreased potential evapotranspiration (R. G. Allen *et al.*, 1998; Richard G. Allen *et al.*, 2005). On the other hand, because evaporation over a saturated bare soil is limited only by energy availability in the early stage of evaporation, the evaporation rate from a bare soil shortly after rain events is comparable to or higher than the evapotranspiration rate of its vegetated counterpart (Richard G. Allen *et al.*, 2005). Because all three facilities experienced frequent rainfalls over the growing seasons, the evaporation rate in the bare PV treatment was likely comparable to or higher than the evapotranspiration rate of the veg PV for most of the growing seasons. The lack of significant difference in air temperature or relative humidity between the bare PV and the veg PV treatments and the fact that the relative humidity was close to 100% most of the time (Fig. 3.2) also imply that any additional evapotranspiration in veg PV is unlikely to result in practically significant cooling of the panels that would translate into measurably improved power production. However, if the effects of the climate change were to increase the periods between rainfalls in Minnesota in the future, the prolonged evapotranspiration in the vegetated PV arrays may cause a significant difference in the temperature and the performance of the PV arrays, but irrigation may be required to maintain the cooling effect, which may not be financially practical (Choi *et al.*, 2023).

3.5.2 Soil-Specific Strategies for Restoration

Slower wind speeds caused by the co-location of PV and vegetation may protect the soil from erosion (Fig. 3.2), but the original texture of the soil and construction history may have had the strongest influence on the soil nutrient and texture response to the treatments. While minimizing land modification during PV construction is beneficial for all soils, those with higher clay fraction and carbon content may be less susceptible to the change in soil texture and nutrients from land modification than those with lower clay fraction and carbon content.

The consequence of mechanically disturbing the topsoil through stockpiling/replacement or leaving the topsoil exposed through de-vegetation was more pronounced in soils with less clay content (S. G. Baer *et al.*, 2010). In the bare PV treatment in Chisago, the stockpiled topsoil of the bare PV had lesser clay and silt fraction in the bare PV treatment than in the veg PV treatment and the control (Fig. B.2a), as well as less TC, TN, TEC, Cu, K, Mg, Mn, and OM (Fig. 3.4b, c & B.2a). Since soil organic matter provides structural stability to soil, and clay provides surface for adhesion of organic matter (Chaney & Swift, 1984; Chenu *et al.*, 2000), loss of either OM or clay fraction may cause the loss of the other and result in a significant drop TEC and anion concentrations. In contrast, the stockpiling and replacing the topsoil in the veg PV treatment in Atwater did not result in a lower TEC than the control (Fig. 3.4a) despite the loss in OM (Fig. B.3). The unexpectedly higher fraction of silt and clay in the removed-then-replaced veg PV treatment compared to both the bare PV treatment and the control may be attributed to the disaggregation of silt and clay from the removal and re-distribution of the topsoil (Wick *et al.*, 2009). Increased TEC contributions from the disaggregated clay and silt fractions also explain why the veg

PV's TEC was comparable to that of the control despite its comparatively low TC and OM content (Fig. 3.4c & B.3): on top of freeing silt and clay particles, the breakdown of aggregates may expose the previously occluded OM and increase the rate of carbon and nitrogen loss through respiration (De Freitas *et al.*, 1999; Hevia *et al.*, 2007). The breakdown of soil aggregates also correlates with decreased water retention in soils (Zibilske & Bradford, 2007), which may be the reason the soil moisture reaches levels lower between rainfalls in the veg PV treatment than those in the control (Fig. 3.4a). Overall, no consistent pattern in relative abundance of soil ions and TEC emerged, which may be due to the fact that TEC was calculated by totaling the cation concentrations and that the soil ions may have been incorporated in plant biomass when the samples were collected (Ross & Kettering, 2011).

The lower median average wind speeds and median max wind speeds in the bare PV and the veg PV treatments (Fig. 3.2) imply that PV arrays may decrease wind speeds, which corroborates the findings of a previous study (Armstrong *et al.*, 2016). Furthermore, the lower mean and max wind speeds in the veg PV treatment compared to that of the bare PV treatment (Fig. 3.2) implies a compounding wind suppression effect from the co-location of PV arrays and vegetation. In Eastwood, the lower clay fraction in the bare PV treatment (Fig. B.2a) in absence of any topsoil stockpiling may indicate loss of clay fraction from the bare PV treatment due to increased exposure of the bare soil. Conversely, the comparatively higher clay fraction in the veg PV treatment alludes to a possibility of unloading of aeolian sediments within the veg PV treatment because of compounding suppression of the wind from the vegetation and PV as well as sufficient mitigation of erosion the vegetation (Gonzales *et al.*, 2018; J. Li *et al.*, 2008). However, aeolian

entrainment and saltation mechanisms of clay particles in frequently wet soils in humid climates need to be examined to further quantify the avoided erosion of the clay particles.

The contrasting effects of stockpiling in Chisago and Atwater are in line with previous findings on re-vegetation, which show that the capacity to accumulate carbon is more heavily impacted after a disturbance in coarser soils than in finer soils (Choi *et al.*, 2020). While re-vegetating the modified soil with native vegetation can prevent further erosion of the finer soil particle fraction, it may take decades before the soil carbon content returns to the levels seen in prairie grasslands (S. G. Baer *et al.*, 2010; McLauchlan, 2006). Considering all three facilities were built on prior farmlands that had already been heavily altered from prairie grasslands, re-vegetating PV arrays for the duration of the project may continue increase the soil carbon stock beyond the pre-construction levels and the timeline of this study. While additional soil data are required to separate the effects of soil stockpiling and absence of vegetation, this finding underpins the importance of re-vegetation or preservation of existing vegetation as well as soil during construction. Suggested construction practices that may minimize soil impact such as avoiding land grading or using alternative torque tube designs to accommodate for undulating surfaces with fewer piles (B. A. Gill & Meydbray, n.d.; Sinha *et al.*, 2018; Yavari *et al.*, 2022), and the lack of research in the physical viability, insurability, and financial viability of such changes is a research opportunity that may address many environmental concerns about general PV deployment beyond agrivoltaics.

3.5.3 Agrivoltaic Influence on Microclimate and Hydrology and Its Implications for Cropping Geometry and Biodiversity

Atwater and Eastwood had higher soil moisture content than Chisago (Fig. 3.5a) due to relatively higher clay and silt contents in Eastwood and Atwater (Fig. B.2a), which may have resulted in high porosity but low hydraulic conductivity (van Genuchten, 1980; R. Zhang, 1997). For this reason, the soil moisture of the bare PV treatment in Atwater and Eastwood remained higher and fluctuated much less than that of the other two treatments between rainfall events and dry periods. The interannual decrease in the local maxima and minima of soil moisture in the veg PV treatment and the control is likely caused by the decreasing frequency and intensity of rainfall events, but also aligns with decrease in soil moisture due to increased plant uptake that has been observed in other re-vegetation studies (Bin Bin Li *et al.*, 2021; X. R. Li *et al.*, 2004). In contrast, the water outputs from soil in the bare PV treatment without plant transpiration is downward infiltration and evaporation, but infiltration in Atwater and Eastwood to is limited due to the higher clay content (Genuchten, 1980), and evaporation rate would fall off quickly compared to the evapotranspiration rate in vegetated counterpart (Richard G. Allen *et al.*, 2005; Richard G Allen *et al.*, 2005). Therefore, the bare PV treatment maintains soil moisture comparable to or higher than that of the veg PV treatment and the control in Atwater and Eastwood even during the long rainfall intervals in 2021 (Fig. 3.5a).

The difference in the soil moisture and temperature profile among the relative positions in the bare PV and the veg PV treatments show that while PV panels may alter the distribution of both soil moisture and heat, the distribution of soil moisture will be more site-specific than that of soil heat distribution. The contrast in the spatial distribution of the

two variables may be a result of the following: First, it is possible that the lateral transfer of heat through the soil is less susceptible to the effects of spatial heterogeneity in the soil than porosity or hydraulic conductivity. Second, the raindrops do not always fall on the soil surface at a right angle because of the wind, allowing the raindrops to reach parts of the soil that lie directly below the PV modules. Therefore, the distribution of soil moisture across the relative positions will vary among the facilities as does the distribution of wind speed and direction (Fig. 3.3). In contrast, wind does not control solar incidence angles, and the range of solar incidence angles are sufficiently predictable to allow estimation of irradiance without field data (Andres *et al.*, 2023; Dupraz *et al.*, 2011; Veldhuis & Reinders, 2012). Therefore, the direction of soil temperature differences among the relative positions and between the treatments are consistent across the facilities (Fig. 3.6a and b). When considering the placement of native vegetation or crops in a sun-tracking agrivoltaics system, the soil moisture distribution profile resulting from the wind pattern, soil heterogeneity, and rainfall may introduce more uncertainty than the transverse soil temperature profile given that the facility or the system in question has the mounting height, width (perpendicular to the tracking axis), and the distance between rows that are similar to other facilities or systems in the region. Therefore, considering the historical data of local wind speed and wind direction in addition to the solar resources may be important for understanding water availability for plants in different relative positions of within co-located systems.

The disturbance and the heterogeneity maintained by PV occupation may drive biodiversity under the certain conditions: in prairie grasslands such as those of our study sites, C3 plants are the main drivers of biodiversity but are often shaded and outcompeted

by the taller C4 graminoids, which result in community convergence despite the heterogeneity in soil nutrient and moisture (Sara G. Baer *et al.*, 2005, 2020). However, because C3 forbs can adapt to a wider range of shade conditions than C4 graminoids, persistent shade conditions and potential destabilization of the grass-dominated prairie community from long-term occupation of PV arrays may provide an opportunity for C3 forbs to take advantage of the soil nutrient and moisture heterogeneity and increase the biodiversity (Sara G. Baer *et al.*, 2020; Kubásek *et al.*, 2013; Y.-T. Li *et al.*, 2021; Lin *et al.*, 1998; Turner & Knapp, 1996). In addition to the light requirement, the cooler temperatures and soil moisture levels in the relative locations can be compared with the water requirement of the plant species to select the planting location. The compounding heterogeneity created by the light and moisture conditions in these areas may provide varying niches around PV arrays, and repeated measurements in different climates and soils may be used to model resulting niches during the design stage of a co-located system.

3.5.4 Implications for Climate Change Resilience

Our soil temperature data indicate that the combination of vegetation and PV arrays may provide compounding thermal protection against the effects of climate change. Global average temperature increase since pre-industrial levels will likely reach 1.5 °C and possibly 2.0 °C even in low anthropogenic radiative climate forcing scenario (Diffenbaugh & Barnes, 2023). As these thresholds are reached, mean temperature in Minnesota may increase by 1.5-2.0 °C, and maximum temperature may increase over 2.0 °C in relation to the 1995-2014 levels (Gutiérrez *et al.*, 2021; Iturbide *et al.*, 2021). While the yield may gradually increase with the warming, both cool- and warm-season plants may experience sharp, non-linear decrease in yield beyond the threshold temperatures of 29-32 °C

(Feldhake & Boyer, 1986; Nóia Júnior *et al.*, 2018; Schlenker & Roberts, 2009). Furthermore, with the shift in the average soil temperature, the growing season for cool-season plants may be shortened or shifted, causing a phenological mismatch with other organisms that rely on the affected plant species. The soil temperature in every location of veg PV plots were cooler than that of that in the control (Fig. 3.6b) which suggests that PV arrays buffer the soil temperature response to the increasing air temperature and lengthen the growing season in a future climate where the limiting factor may be extreme heat. Therefore, reduction of soil temperature (Fig. 3.6b) and insulation from the PV panels may buffer the effects of the climate change and give more time for landowners and organisms to adapt its outcome.

3.5.5 Future Studies

The concentration of soil ions and TEC by extension were not a very reliable measure of soil health. The environmental processes within agrivoltaic system are a relatively new field of study, and there is a critical scarcity of data from varying different climates and soils that limit general conclusions that can be made from the accumulating body of research. While research with data on many variables may be more capable of analyzing complex relationships between different factors, experiments in utility-scale PV facilities are likely constrained by funding, timing, access to the study sites, and bureaucratic but necessary procedures that may influence any of the above. In consideration of these obstacles and the need for abundance of agrivoltaic data around varying environments, future studies may benefit from limiting their scope to a few variables, such as total carbon, nitrogen, soil particle fractions, and OM. Soil particle size distribution is an especially important as it is the key determinant of soils' capacity for

retaining OM and TEC by extension (Matus, 2021; Tang *et al.*, 2009). Rather than performing a complete suite of tests for soil nutrients and TEC, focusing on soil particle size distribution may allow additional samples and a more statistically robust analysis. In addition to the above, analyzing soil for clay mineralogy may be useful for in calculating the soil's true cation exchange capacity than calculating the TEC by the summing up the cations, whose concentration may vary seasonably (Ross & Kettering, 2011).

3.6. Conclusion

In Minnesota and regions with similarly wet growing seasons, co-located vegetation may not generate additional evapotranspiration large enough to result in statistically significant panel cooling or higher PV output, which is corroborated by the lack of difference in panel temperature and power output as well as in air temperature and relative humidity between the vegetated array and its unvegetated counterpart. However, panel cooling and increased PV performance may be possible with irrigation if the effects of climate change were to increase the period between rain events in Minnesota. Additionally, co-locating native vegetation with PV may offer other benefits: compounding microclimatic influence of PV arrays and co-located vegetation may preserve the soil's ability to store nutrients, sequester carbon, and host organisms by providing protection against erosion and the excessive increase in soil temperature due to climate change. These benefits may be magnified in soils with smaller clay fractions which have reduced ability to retain soil carbon and therefore more vulnerable to further loss of the clay particles. Lastly, the shade conditions evidenced by the spatial variation in soil temperature in the PV arrays may act as a persisting disturbance to the dominant grass population in prairie grasslands, increasing the likelihood that shorter plant species may establish, but this has

yet to be verified with ecological data. Overall, our study shows that some expected benefits of co-locating native vegetation with PV arrays may vary not only at a regional scale with climate but also at a finer scale with soil texture and near-surface hydrology. Not all the previously reported environmental co-benefits may be achievable in a single co-located system, and case-by-case considerations of the climate, soil properties, and plant communities may help identify which environmental benefits are achievable for a potential development location and maximize them.

3.7. Supporting Information

Supplementary information for this chapter is in Appendix B.

.

CHAPTER 4.

LAND AND WATER FOOTPRINTS FROM EXPANSION OF UTILITY-SCALE SOLAR: A TALE OF TWO STATES

4.1. Abstract

Utility-scale solar energy (USSE) has been an attractive option for meeting the growing energy demand. However, USSE developments have also targeted arid regions with high insolation, as does agricultural. Therefore, meeting the expanding energy demand with limited land and water resources in arid and semi-arid regions may be a major challenge for the future. As two arid regions with drastically different socioeconomic profiles, California, USA and Rajasthan, India provide interesting case studies on the land use and water consumption by USSE generation under current and future energy demand scenarios with implications for local and regional food security. Using dynamic recursive simulation, we estimated the water consumption of USSE in California, USA and Rajasthan under different policy scenarios and land management practices, from present to 2070. USSE's water consumption was compared to that of competing land-use practices such as residential and agricultural use as well as non-renewable thermoelectric power generation. At a regional scale, our analyses indicate that USSE's water consumption would never be larger than 1% of the total agricultural water consumption, and that USSE's land occupation would not exceed 2% of the present total agricultural area. However, a significant portion of new USSE deployments would be concentrated in agriculturally important areas and incur land and water footprints that represent a significant portion of those from local agricultural and domestic activities. Per unit volume of consumed water, USSE would generate more electricity than conventional thermoelectric power generation

and more profit than some agricultural land uses. The results also show that integrating USSE into agricultural uses may decrease the land transformation due to solar and even transform arid and semi-arid areas into arable or productive lands. This hybrid deployment strategy may allow a larger portion of migrant farmworkers to retain their employment in the off-season, which may improve migrant children's access to education. Overall, the study indicates that increasing USSE developments will not impose a significant burden on the land and water resources regionally, and that local impacts could be largely mitigated by integrating the USSE infrastructure to existing agricultural activities.

4.2. Introduction

Utility-scale solar energy (USSE) is driven by the highest technical generation potential among renewable energies, technological advancement, and decarbonization policies from many countries (Edenhofer *et al.*, 2011; Ellabban *et al.*, 2014; IEA, 2020; Jacobson, 2009; U.S. Department of Energy, 2012). On average, ground-mounted solar photovoltaics (PV) systems have the largest direct land footprint of all renewables except for biomass and hydropower (Trainor *et al.*, 2016). At an average land-use intensity of 3 ha MW_p^{-1} (Ong *et al.*, 2013), ground-mounted PV may cause 25 million hectares of land-use change under an optimistic global solar energy deployment scenario (IRENA, 2018). While this number is inconsequential compared to the total global land area (13 billion hectares), additional PV development is likely to be concentrated in areas with attractive characteristics for development, which are areas with high insolation that are flat, dry, unshaded, close to grid infrastructure, and easily accessible for maintenance (Adeh *et al.*, 2019; Grout & Ifft Charles, 2018; Kim *et al.*, 2020). These prerequisites make farmlands attractive potential sites to solar developers, and some farmers have been leasing their lands

to them for a reliable revenue stream that is independent from the volatility of agricultural markets (Maltais, 2019; Nir, 2020).

However, farmers who lease their lands out to solar developers assume a new set of economic and environmental risks: despite PV low greenhouse gases emission (V. Fthenakis, 2009; V. Fthenakis & Kim, 2010; V. M. Fthenakis & Kim, 2011; Leccisi *et al.*, 2016; Turney & Fthenakis, 2011), conventional deployment of utility-scale ground-mounted PV in farmland or an ecologically important tract of land precludes any agricultural uses of the land during the facilities' lifetime (30-40 years) and may compromise the land's ecological functions (Choi *et al.*, 2020; Hernandez, Easter, *et al.*, 2014; Hernandez, Hoffacker, Murphy-Mariscal, *et al.*, 2015). Vegetation removal and topsoil grading that are sometimes part of the conventional construction of a PV facility decrease the land's ability to produce biomass and sequester carbon by increasing the erodibility of the finer fraction of the soil particles to which soil nutrients such as nitrogen, phosphorus, and other soil cations adhere (Hernandez, Easter, *et al.*, 2014; Larney *et al.*, 2000, 2016; G. H. Zhang *et al.*, 2011). PV's long-term occupation following the construction may further disrupt the land's ecological functions or its ability to produce agricultural goods by creating variations in microclimate (Armstrong *et al.*, 2016; Barron-Gafford *et al.*, 2016; Choi *et al.*, 2020) and further accelerating erosion (Cook & McCuen, 2013). Moreover, the extensive land modification will extend the duration of the physical impacts on the land past the duration of PV occupation (Beatty *et al.*, 2017; Choi *et al.*, 2020; Hernandez, Easter, *et al.*, 2014; Hernandez, Hoffacker, Murphy-Mariscal, *et al.*, 2015). Lastly, operation of solar thermal (ST) facilities and that of PV facilities may divert water from agricultural activities, which could exacerbate any pre-existing local water

stress in the area. The overlapping prerequisites for USSE and agriculture and USSE's potential to compromise concurrent and future agricultural use of the land may be concerning to countries that heavily rely on expansion of the USSE capacities to decarbonize their power sector. These negative impacts may be mitigated by co-locating agricultural activity or native vegetation with PV. Several modeling and pilot-scale studies have shown that agrivoltaics can provide mutual benefits that include vegetation-driven cooling of the PV panels for increased PV efficiency, reduction in the PV installation and operation costs, diversified income streams, employment generation, reduction in irrigation water use, and increased crop yields from pollinator services (Adeh *et al.*, 2018; Barron-Gafford *et al.*, 2019; Beatty *et al.*, 2017; Choi, 2019; Elamri, Cheviron, Lopez, *et al.*, 2018; Elamri, Cheviron, Mange, *et al.*, 2018; Hernandez, Easter, *et al.*, 2014; Majumdar & Pasqualetti, 2018; Marrou, Wery, *et al.*, 2013; Marrou, Dufour, *et al.*, 2013; Marrou, Guilioni, *et al.*, 2013; Ravi *et al.*, 2014, 2016).

As a case in point, India is an emerging economy and the third-largest carbon-emitter that has rapidly increased its national USSE capacity. India is one of the markets on track to lead the increase in PV: under stated policies, growth of India's PV generation capacity may account for more than 23% of the global increase in PV generation and 15% of the increase in global electricity generation and between 2020 and 2050 (BP Energy, 2020; Cozzi & Gould, 2021). As the state with the largest solar potential India, Rajasthan may receive a significant portion of the future USSE capacity. Since Rajasthan is a severely water-stressed region where more than half of the land area is used for agriculture, the potential for competition for land and water resources between the growing USSE and the pre-existing agriculture needs to be examined.

This study examines the land use change and water use implications of the Rajasthan's rapidly expanding solar industry and the extent of land use and water use for solar that can be mitigated by wide implementation of dual land-use for agriculture and energy production. As a case comparison, the same analysis is performed for California, USA, who has similar environmental resources.

4.3. Background

4.3.1 Agricultural Workforce and Economics of Rajasthan and California

Rajasthan's economy depends significantly on agriculture, which accounts for 30% of the state gross domestic product (GDP) and the livelihood of more than 60% of the state's population of 69 million (Gulati *et al.*, 2020). Of the available labor, 10.5% is estimated to be surplus, and from 6 to 20% is estimated to be seasonally migrant (Singh Rajput *et al.*, 2022). On the other hand, agriculture only comprises 2.1% of California's state GDP in 2020 and employs only about 1% of the population of 39 million (Bureau of Economic Analysis, 2021; Employment Development Department (EDD), 2021; US Census Bureau, 2021). Therefore, the potential land-use interaction between USSE and agriculture may have a larger socioeconomic impact in Rajasthan than in California, which highlights the importance of analyzing the land and water footprint of the growing USSE sector.

4.3.2 Solar Resources

Rajasthan's global horizontal irradiation (GHI) ranges from 4.91 to 5.65 kWh/m^2 and the average and the median values were 5.38 and 5.43 kWh/m^2, respectively. Direct normal irradiance (DNI) ranges from 3.48 to 5.45 kWh/m^2 and the average and the median values of 4.48 and 4.51 kWh/m^2 (ESMAP, 2021a). Out of 342,870 km^2 of grassland, salt

marsh, scrubland, and other types of wasteland, 80,300 km^2 is deemed suitable unused land for PV, and this land area can provide 1000 – 4200 TWh/yr of generation potential and 600 – 1000 GW of capacity potential depending on the land use factor assumptions (Deshmukh *et al.*, 2019).

In California, GHI ranges from 4.17 to 6.04 kWh/m^2 and the average and the median values are 5.39 and 5.41 kWh/m^2. DNI ranges from 4.41 to 8.18 kWh/m^2 and the average and the median values are 6.79 and 6.74 kWh/m^2, respectively (ESMAP, 2021b). Hernandez, Hoffacker & Field (2015) found that area available for solar development that were close to road and transmission infrastructure and also met other land-use and environmental criteria[1] amounted to 81,334 km^2 that could provide 32,756 TWh/yr of generation potential (Hernandez, Hoffacker, & Field, 2015).

4.3.3 Historical Capacities and Future Trajectories

India launched the National Solar Mission in 2010, which has set the solar deployment target of 100 GW by 2022 (MNRE, 2021a), and the national solar capacity is at 45.6 GW as of August of 2021 (MNRE, 2021b). Despite the short history of the solar energy industry in India, Rajasthan's USSE capacity is comparable to that of California (Figure 4.1). CEEW projects that India will need 5600 GW additional capacity by 2070 to meet its net zero carbon emissions (Chaturvedi & Malyan, 2021).

Under the recently-passed Senate Bill 100 (SB100), California's grid is required to meet 100% of its retail electricity demand by 2045 with sources that meet the standard for renewable energy portfolio, which are PV, solar thermal, on/offshore wind, geothermal,

[1] Areas that do not coincide with federally protected lands or areas with low insolation, open water and perennial ice or snow, development, high slope, endangered or threatened species

bioenergy, hydrogen fuel cells, and small hydropower, and the ones that meet the zero-carbon criteria, which are pre-existing nuclear and large hydropower (L. Gill *et al.*, 2021).

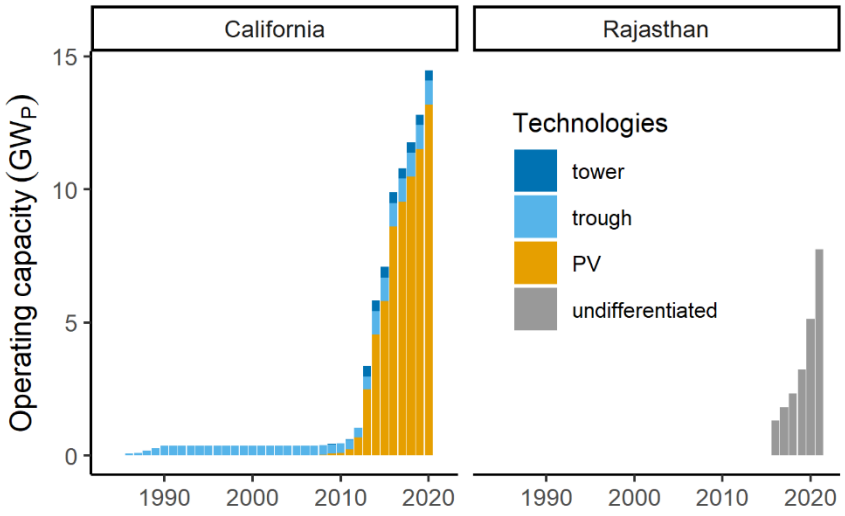

Figure 4.1. Historical installed capacity of USSE in California, USA and Rajasthan, India. USSE capacities before 2016 and the types of solar technology were unavailable.

4.4. Methods

The land footprint, water consumption, and the soil carbon stock were modelled as a function of the projected growth in the USSE capacity using a dynamic recursive model in VenSim (Ventana Systems, Inc., MA). This model is a variant of one that was previously used to study the energy balance of the PV industry (Dale & Benson, 2013). The model structure is outlined in Figure 4.2. In each region, the USSE growth is simulated under two scenarios:

- a Business-as-Usual (BAU) scenario, in which the grid mix stays similar to the present,
- and a decarbonization scenario, in which each region transitions to a mostly-renewables future.

The definitions of these scenarios are different between the two regions, and these differences are explained in Section 3.2.

4.4.1 Model Boundaries

The simulation period spans from 2021 to 2070. This model does not consider developments of new energy technology or improvements on existing technology such as hydrogen fuel or carbon capture and storage (CCS) in the role of mitigating carbon emissions. The only solar energy technologies considered are PV, parabolic trough (PTs) with wet or dry cooling technology, and solar power tower (or tower).

4.4.2 Implementation of Growth Projections from the Literature

We used growth projections described above to determine the USSE capacity in operation in 2070. Since the two regions are taking different approaches to decarbonizing their respective grids over different timelines, implementing the respective USSE growth scenarios required distinct approaches.

For Rajasthan, the transition scenario in which net-zero grid emission is achieved by 2070 without CCS and low hydrogen fuel use (Chaturvedi & Malyan, 2021) serves as the basis for the USSE growth projection under the decarbonization scenario, and the reference scenario from the same report is used for the projection under the BAU scenario. Rajasthan represents approximately 47% of India's utility-scale PV capacity and two-thirds of the concentrated solar power (CSP) capacity (Deshmukh *et al.*, 2019). Because the USSE capacity projection under the net-zero scenario (5630 GW) (Chaturvedi & Malyan, 2021) exceeds India's total capacity potential (5200 GW) (Deshmukh *et al.*, 2019), we assume that Rajasthan's USSE capacity will be fully utilized. Thus, Rajasthan's operating USSE capacity at the end of the modeling period ($FinCap_{raj}$) is simply calculated as:

$$FinCap_{raj} = FinCap_{india} \times 0.47, \quad \textbf{Eq.1}$$

where $FinCap_{india}$ is the total operating capacity of USSE in 2070 and 0.47 is Rajasthan's share of India's USSE potential. Likewise, Rajasthan's total USSE capacity under the BAU scenario is calculated as 0.47 multiplied by CEEW's projection of USSE growth (657.6 GW) under the reference scenario (Chaturvedi & Malyan, 2021).

As a basis for the USSE growth projection in California under the decarbonization scenario, this study uses the projected USSE growth in transition from current grid mix to 100% renewable portfolio standard by 2045 described in a joint report by the California Energy Commission (CEC), the California Public Utilities Commission (CPUC), and the California Air Resources Board (CARB) (L. Gill *et al.*, 2021). The reference case from the same report with a 60% renewable portfolio standard (L. Gill *et al.*, 2021) was the basis for the BAU scenario. Because the joint agency report's simulation period ends in 2045 (L. Gill *et al.*, 2021), the simulated growth of USSE in California had to be extrapolated to 2070 for an equitable comparison of USSE growth between the two regions. California's final operating USSE capacity ($FinCap_{ca}$) was not explicitly given in the source literature, it was determined by extrapolating the reported average annual build rates (BR_{avg}) for the decarbonization scenario (2.8 GW yr^{-1}) and the BAU scenario (1.8 GW yr^{-1}) as:

$$FinCap_{ca} = BR_{avg} \times \left(year_{final} - year_{initial}\right) + InCap_{ca}, \quad \textbf{Eq.2}$$

where $year_{initial}$ is the starting year of the modeling period, $year_{final}$ is the final year of the modeling period, and $InCap_{ca}$ is the initial capacity of USSE in California at $year_{initial}$.

For both regions, annual build rate of USSE was incrementally increased annually to negotiate the discrepancy between the capacity additions in the year prior to this study and the BR_{avg} required for meeting the projected $FinCap_{region}$. The subscript "$region$" is a placeholder for the shorthand of the region (raj = Rajasthan; ca = California), and the term described by the subscript placeholder is defined identically for both regions henceforth. The incremental increase in the capacity addition (ΔGR_{region}) is calculated as:

$$\Delta GR_{region} = \frac{GR_{max,region} - GR_{initial,region}}{year_{final} - year_{initial}}, \quad \textbf{Eq.3}$$

where $GR_{max,region}$ is the maximum growth rate of USSE over the modeling period and $GR_{initial,region}$ is the initial growth rate of the USSE at the beginning of the modeling period. $GR_{initial,region}$ is equal to the last reported capacity additions on record for the respective regions. $GR_{initial,region}$ as of 2021 is 2.35 GW yr^{-1} for Rajasthan (MNRE, 2021a) and 1.67 GW yr^{-1} for California (US Energy Information Administration (EIA), 2021) $GR_{max,region}$ is calculated as:

$$GR_{max,region} = 2 \times GR_{avg,region} - GR_{initial,region}, \quad \textbf{Eq.4}$$

where $GR_{avg,region}$ is the average annual growth rate of USSE, which is defined as:

$$GR_{avg,region} = \frac{FinCap_{region} - InCap_{ca}}{year_{final} - year_{initial}} \quad \textbf{Eq.5}$$

$CapConst_{1,region}$, or capacity that is in the development stage or at the beginning stage of construction (scheduled to be added in the following year)

$$CapConst_{1,region} = GR_{initial,region} + \Delta GR_{region} \times (year_{current} - year_{initial}) + CapDecom_{region}, \quad \textbf{Eq.6}$$

where $year_{current}$ is the current time step (in years) and $CapDecom_{region}$ is the USSE capacity under decommission after its lifespan of 25 years. $CapDecom_{region}$ is added to the growth rate to acknowledge that decommissioned USSE capacities need to be replaced so that the rest of the expression reflects net growth in the total USSE capacity.

The operating capacity $CapOp_{region}$ equals the last reported operating capacity for the respective regions at the beginning of the model and the incremental increase to $CapOp_{region}$ is determined as below for the following years:

$$\Delta CapOp_{region} = CapAdd_{region} - CapDecom_{region}, \quad \textbf{Eq.7}$$

where $CapAdd_{region}$ is the capacity added to $CapOp_{region}$ and equals $CapConst_{1,region}$ from the previous year.

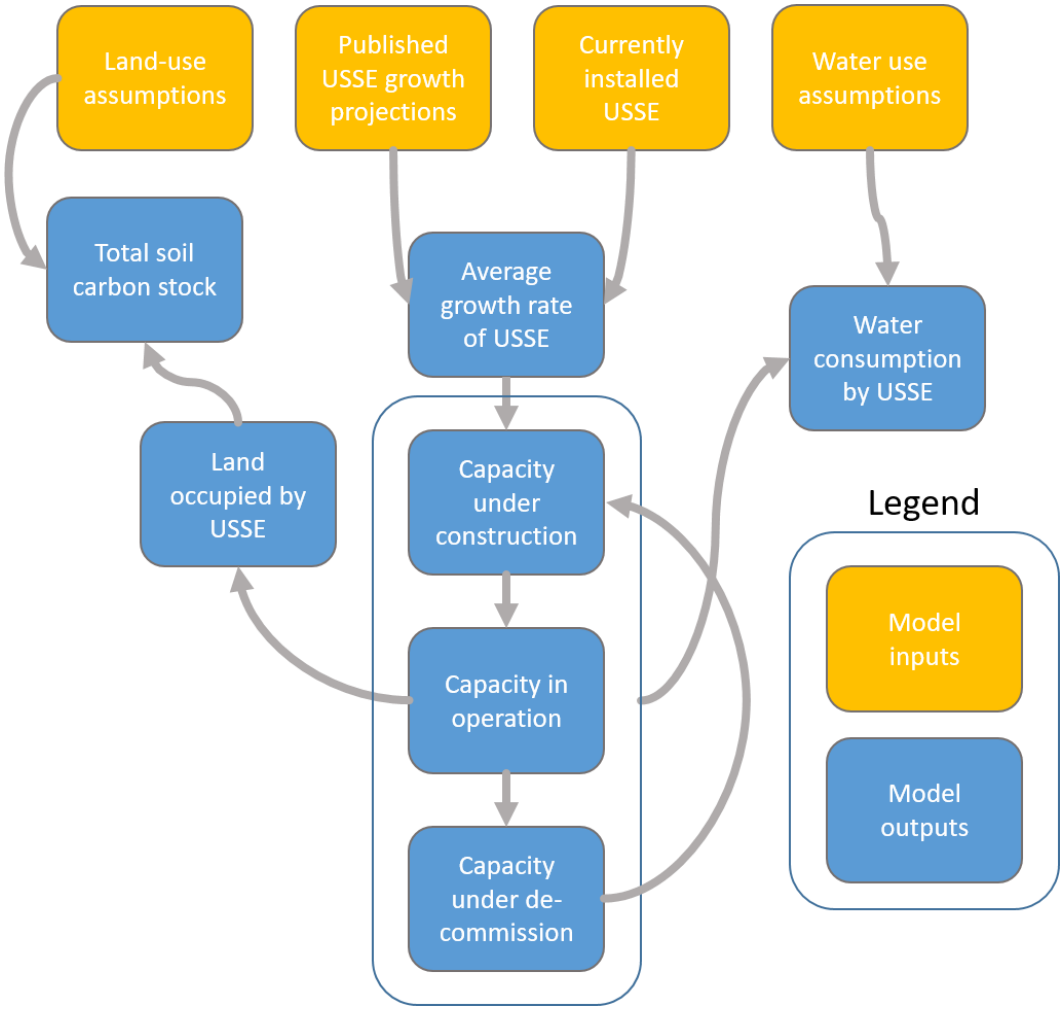

Figure 4.2. Summary of the dynamic recursive model.

4.5. Results and Discussions

Rajasthan's operating capacity at the end of the period is 558 GW for the BAU scenarios and 2260 GW for the decarbonization scenarios (Figure 4.3). In contrast, California's operating solar capacity remains significantly low at the end of the modeling period in both the BAU (113.36 GW) and the decarbonization (158.75 GW) scenarios. The disparity between the USSE growth trajectories of the two regions is due to the fact that

CEC's projected trajectory for the growth of solar industry in California has a very low average annual capacity additions (1.8 GW for the BAU and 2.8 GW for the decarbonization scenarios) (L. Gill *et al.*, 2021), which is comparable to the initial capacity additions (1.67 GW) (US Energy Information Administration (EIA), 2021). In comparison, calibrating the model to CEEW's projected trajectories of Rajasthan's solar industry for both the BAU and the decarbonization scenarios requires average annual capacity additions significantly higher than the initial capacity additions (2.35 GW) (MNRE, 2021b, 2021a). The growth trajectories of the operating capacities in the two regions are exactly as expected because the model is calibrated to pre-determined estimates.

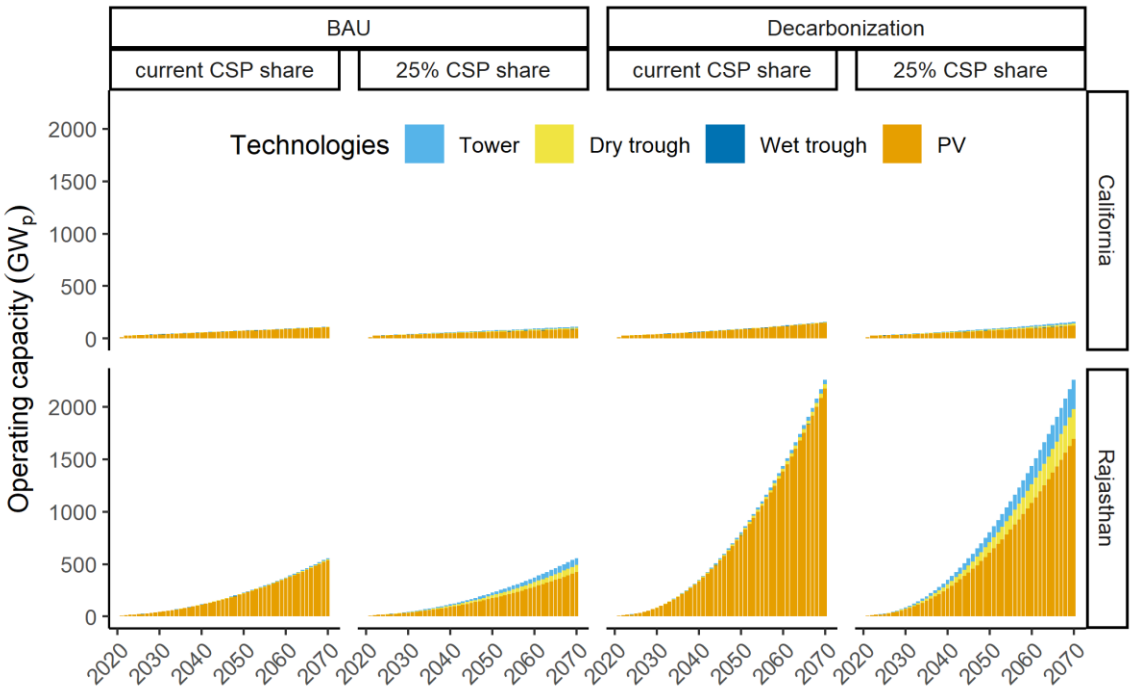

Figure 4.3. Growth trajectory of the operating capacity of utility-scale solar energy under BAU scenarios (left) and under decarbonization scenarios (right) in California (top) and Rajasthan (bottom).

In California, land occupation by USSE never exceeds suitable unused land (Figure 4.4). The low land occupation is caused by the fact that California's estimated USSE projection during the simulation period is much lower than that of Rajasthan's. Under the growth scenarios presented by SB 100 (L. Gill *et al.*, 2021), the land competition between USSE and agriculture is not a concern within the modeling period.

In Rajasthan, USSE will take a larger portion of the land by 2070: the USSE-occupied land exceeds the suitable unused land under the BAU scenario, and the high end of the estimate under the decarbonization scenario exceeds even the total land area in the decarbonization scenario. The high estimates do not consider that multiple USSE facilities will share some portion of roads and transmission infrastructure, so the true sum of land

occupied by the USSE will exist between the lower and the higher estimates. Nonetheless, even the lower estimate of USSE-occupied land in the decarbonized Rajasthan will likely be a significant portion of the sum of unused land and agricultural land, which corroborates previous estimates (van de Ven *et al.*, 2021). The likelihood of the overlap between current agricultural area with future USSE land occupation underscores the importance of co-locating solar energy with agriculture or re-vegetation efforts in the future deployment of USSE. Total soil carbon stock decreases in USSE-occupied lands in all cases of conventional management of USSE sites, whereas the soil carbon stock increased in all cases of co-located USSE deployment (Figure 4.5). Conventional USSE produces a significant impact on soil carbon stock, but this impact can be fully addressed by co-location which leads to a small increase in the soil carbon stock. Proper land management in the solar facilities could improve soil health and increase soil carbon stock over decades of project time.

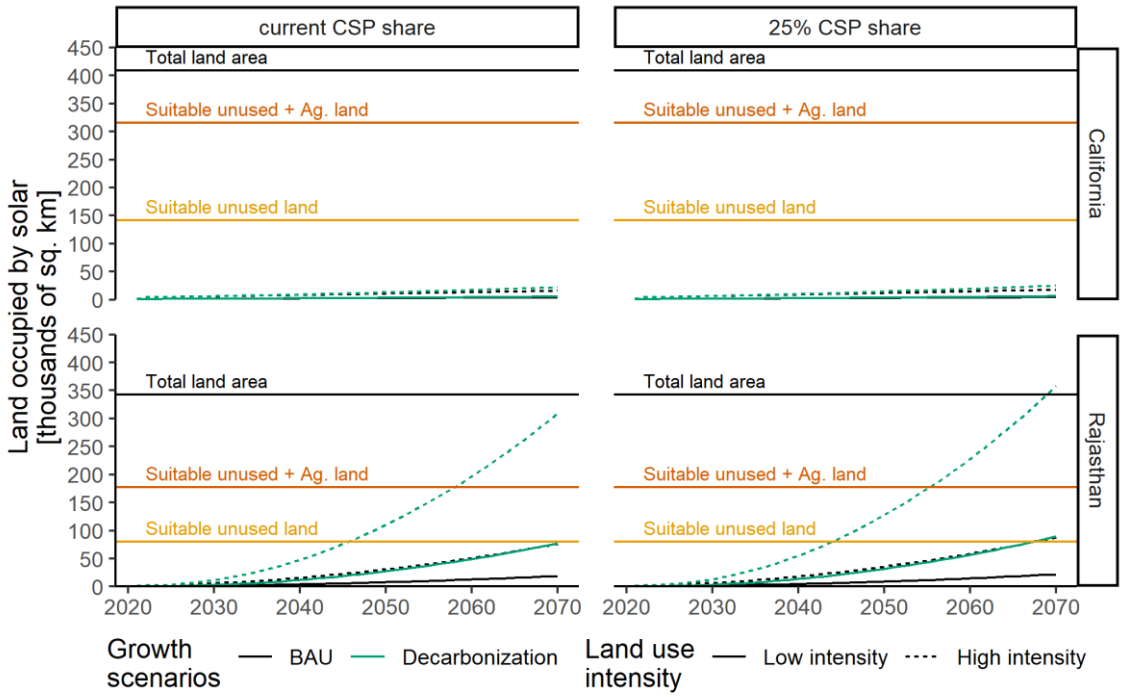

Figure 4.4. Land occupied by solar energy over the modeling period. The yellow line represents suitable unused land, the orange line represents the sum of unused and agricultural lands, and the black line is the total area of respective state. The solid lines represent the estimation of solar-occupied land area using only the direct land-occupation

by solar, and the dotted lines represent the estimation made using the land-use factor of solar modules and transmission infrastructures (Deshmukh *et al.*, 2019).

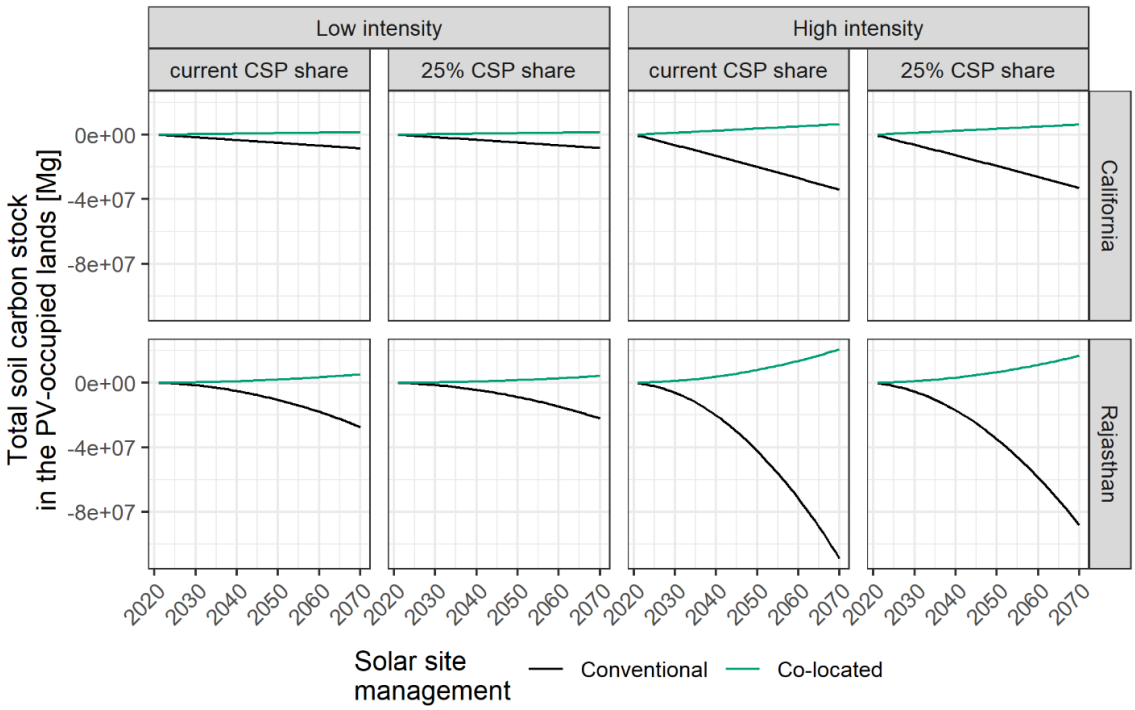

Figure 4.5. Total soil carbon stock in the solar-occupied lands over the modeling period in the decarbonization scenarios

In Rajasthan, water consumption by the USSE under the BAU scenario increases from 6.5 MT yr^{-1} in 2021 to 114.2 MT yr^{-1} with current technology share, and from 7.0 to 171.4 MT yr^{-1} with a CSP share of 25% (Figure 4.6). Under the decarbonization scenario, the water consumption by the USSE increases from 6.5 to 461.5 MT yr^{-1} with the current technology share and from 7.0 to 697.0 MT yr^{-1} with a 25% CSP share.

In California, water consumption by the USSE under the BAU scenario increases from 8.1 MT yr^{-1} in 2021 to 26.2 MT yr^{-1} in 2070 with the current technology share and from 8.5 to 35.2 MT yr^{-1} with a 25% CSP share (Figure 4.6). Under the decarbonization scenario, the water consumption increases from 8.1 to 35.5 MT yr^{-1} with the current technology share and from 8.5 to 49.3 MT yr^{-1} with a 25% CSP share. As a fraction of the

estimated water consumption for thermoelectricity in California in 2015 (148.89 MT) (U.S. Geological Survey (USGS), 2022), the 2070 estimates with current technology share (and a 25% CSP share) under the BAU scenarios is 17.5% (23.6%) and 23.8% (33.1%) under the decarbonization scenario. California's grid is expected to consist mostly of solar and wind power at 100% RPS (Gill *et al.*, 2021), and wind power's water consumption factor is virtually nonexistent (Spang *et al.*, 2014). Therefore, overall water consumption for electricity generation will be less than the current water consumption for electricity by 2070.

In 2015, consumptive use for irrigation is 4.00×10^4 MT yr^{-1} in Rajasthan (Hooda, 2017) and 24395.36 MT yr^{-1} in California (U.S. Geological Survey (USGS), 2022). While the water consumption for USSE was less than 2% of the agricultural water use in both regions under both scenarios, any additional water use would be less than ideal in these two regions that are already water-stressed (Denen *et al.*, 2007; Faunt *et al.*, 2016; Hooda, 2017). In particular, agriculture in Rajasthan uses less land for agriculture than does California but consumes more water, and some of the inefficient water uses can be attributed to are subsidies and the lack of penalty for overuse, as well as the large portion of the irrigated land that uses open surface irrigation instead of sprinkler or drip irrigation (Hooda, 2017; Jain *et al.*, 2019). The inefficiencies in irrigation present an opportunity for on-site power generation from co-located USSE to power sprinkler or drip irrigation. Sprinkler irrigation's water-use efficiency ranges from 50 – 60% and that of drip irrigation ranges from 80 – 90%, compared to 30 – 35% of surface irrigation (Jain *et al.*, 2019). While not explicitly modeled in this study, the abated water consumption from total transition from surface irrigation to sprinkler or drip irrigation may be as much as 2.77×10^4 MT yr^{-1},

which is two-thirds of Rajasthan's consumptive use for irrigation in 2015 and more than 300% of Rajasthan's water deficit (9.0×10^4 MT yr^{-1}) (Hooda, 2017) in 2015. This abatement is two magnitudes larger than the projected consumptive water use of USSE in 2070 (Figure 4.6).

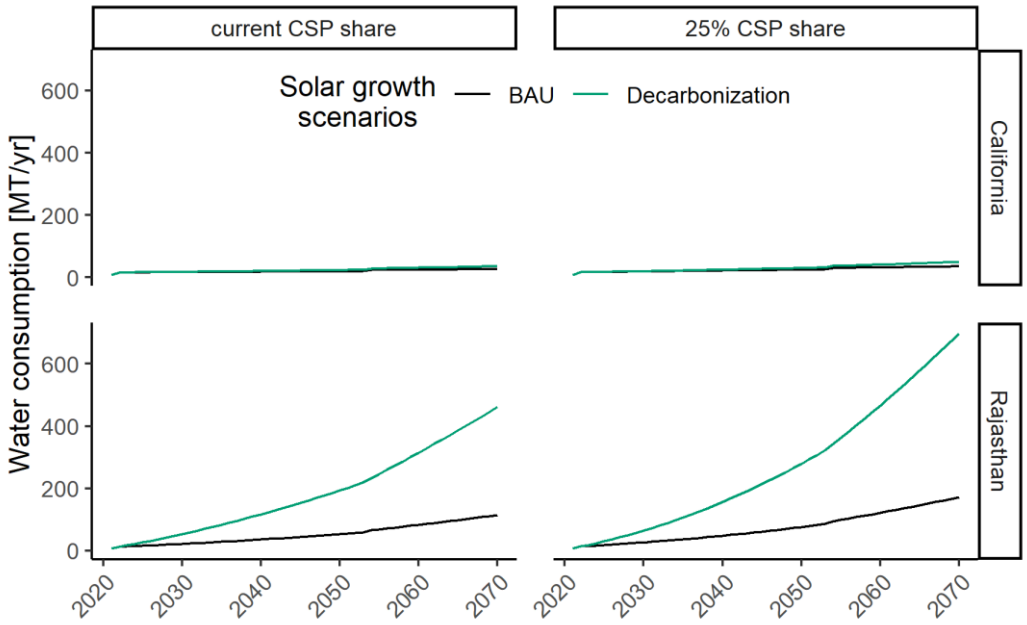

Figure 4.6. Total water consumption by the solar industry

4.6. Conclusion

This study uses the existing projection of solar energy growth to analyze the potential land use, carbon, and water consequences of decarbonizing Rajasthan and California's power grids. This mode of dynamic recursive simulation requires fewer inputs and allows for a rapid and modular adaptation of existing energy transition scenarios for sanity testing to aid policy developments.

While Rajasthan currently has a smaller USSE capacity than does California, its USSE capacity is projected to grow to approximately twenty times that of California's.

Thus, the impacts and the benefits of decarbonization is magnified in Rajasthan compared to its counterpart: whereas USSE may never occupy a significant portion of California, it may stretch Rajasthan's land resources to its limit and have a potential to replace a significant portion of the agricultural land use. Conventional site management of the added USSE facilities may also reduce the soil carbon stock over the USSE-occupied lands and put additional strain on the local water resources that are already scarce. However, Rajasthan may deploy the future USSE capacities as co-located systems to avoid the loss of agricultural lands and its soil carbon stock. Additionally, statewide adoption of co-located systems in Rajasthan may cause significant water savings by allowing use of sprinkler and drip irrigation instead of open surface irrigation, and these water savings would be magnitudes larger than the co-located USSE system themselves would require.

CHAPTER 5. SUMMARY

Achieving food and energy security while minimizing land degradation is a global assignment inextricably linked to our survival amid the effects of rapid climate change. The ongoing growth of large-scale solar PV deployments in the US has raised concerns over the perceived risk of land degradation and loss of farmlands. Addressing these concerns presents an opportunity to co-locate low-carbon energy production with enhancement of ecosystem services through re-establishment of native vegetation. Detailed field studies show it is possible to successful combine power generation while maintain or improving soil quality, ecosystem services, and managing competing needs for water. The model for the growth of solar to decarbonize the power grid, shows how co-location can work at scale to accomplish these goals while supporting electrification, decarbonization of power grides, and support economic growth. But outcomes depend on both the local environment and the economic system.

Like many ecological processes, the environmental co-benefits that can be achieved by a co-located system likely depends on the local climate and other physical factors such as soil characteristics and hydrology that will have strong influence on the nature and the magnitude of microclimatic interaction between the PV arrays, the underlying plants, and the soil. Currently, the research on this topic is largely limited to pilot-scale systems, while the share of utility-scale PV systems constitutes two-thirds of the cumulative solar capacity in the US and is projected to grow (Barbose *et al.*, 2023). Therefore, more research of utility-scale co-located systems is critical to understanding the location-specific suite of environmental co-benefits that can be achieved across varying climates and landscapes

which will determine the overall environmental outcome of wide-spread adoption of the co-location scheme.

The novel research presented in this dissertation explores the microclimatic interaction within a utility-scale co-located system and whether the components of the co-located system can benefit from each other's presence. Our findings from the field studies directly address the hypotheses and research objectives regarding the microclimatic influence of photovoltaic (PV) arrays and the potential for co-located PV-vegetation system to mitigate it as well as the growing effects of the climate change. To determine the impacts of PV array on the underlying soil and vegetation, I performed a multi-year study of the microclimate, hydrology, and soil physico-chemical response to vegetating a utility-scale PV facility. We concluded that the underlying vegetation was not able to divert enough sensible heat to latent heat in a humid environment to cause any statistically significant cooling of the PV panels and increase PV efficiency. We also determined that vegetation removal and land grading activities during PV installation and operation could result in decreased potential for the soil to store nutrients and carbon, and that this effect is the largest in soils with small clay fraction. However, we also saw that the PV arrays and vegetation may provide compounding protection against soil erosion and the increase in soil temperature resulting from global climate change. In deploying PV arrays, vegetation removal should be avoided, and land grading should be minimized. Since not all theorized environmental co-benefits are attainable in a single co-located system, a case-by-case investigation of local climate, soil and ecology need to be performed to identify and maximize achievable environmental co-benefits for a given development location. Finally, the system dynamic model developed from the findings of our field study showed that the

land-use impact of future solar development for meeting renewable energy development targets in Rajasthan may not be significant compared to the current land-use impacts of existing agriculture in the region, especially if the additional solar developments were to be distributed over a large area instead of being concentrated in one division or locale. Lastly, wide adoption of co-location for the new PV additions in Rajasthan could result in positive net soil carbon sequestration and contribute to India's effort to decarbonize its electrical grid.

BIBLIOGRAPHY

Adeh, E. H., Selker, J. S., & Higgins, C. W. (2018). Remarkable agrivoltaic influence on soil moisture, micrometeorology and water-use efficiency. *PLOS ONE*, *13*(11), e0203256. https://doi.org/10.1371/journal.pone.0203256

Adeh, E. H., Good, S. P., Calaf, M., & Higgins, C. W. (2019). Solar PV Power Potential is Greatest Over Croplands. *Scientific Reports*, *9*(1), 11442. https://doi.org/10.1038/s41598-019-47803-3

Al-Khatib, K., & Paulsen, G. M. (1999). High-Temperature Effects on Photosynthetic Processes in Temperate and Tropical Cereals. *Crop Science*, *39*(1), 119–125. https://doi.org/10.2135/cropsci1999.0011183X003900010019x

Aldous, D. E., & Kaufmann, J. E. (1979). Role of Root Temperature on Shoot Growth of Two Kentucky Bluegrass Cultivars. *Agronomy Journal*, *71*(4), 545–547. https://doi.org/10.2134/agronj1979.00021962007100040006x

Allen, R. G., Pereira, L. S., Raes, D., & Smith, M. (1998). *Crop evapotranspiration: Guidelines for computing crop water requirements* (FAO Irrigation and Drainage Paper No. 56). Rome: FAO.

Allen, R. G. ., Walter, I. A. ., Elliot, R., Howell, T., Itenfisu, D., & Jensen, M. (2005). *The ASCE standardized reference evaporation equation*. Reston, VA: ASCE.

Allen, Richard G., Pruitt, W. O., Raes, D., Smith, M., & Pereira, L. S. (2005). Estimating Evaporation from Bare Soil and the Crop Coefficient for the Initial Period Using Common Soils Information. *Journal of Irrigation and Drainage Engineering*, *131*(1), 14–23. https://doi.org/10.1061/(ASCE)0733-9437(2005)131:1(14)

Allen, Richard G, Pereira, L. S., Smith, M., Raes, D., & Wright, J. L. (2005). FAO-56 dual crop coefficient method for estimating evaporation from soil and application extensions. *Journal of Irrigation and Drainage Engineering*, *131*(1), 2–13. https://doi.org/10.1061/(ASCE)0733-9437(2005)131:1(2)

Andres, C., Ruben, C., David, G., Pavel, B., Patrizio, M., Miro, Z., & Olindo, I. (2023). Time-varying, ray tracing irradiance simulation approach for photovoltaic systems in complex scenarios with decoupled geometry, optical properties and illumination conditions. *Progress in Photovoltaics: Research and Applications*, *31*(2), 134–148. https://doi.org/10.1002/pip.3614

Armstrong, A., Waldron, S., Whitaker, J., & Ostle, N. J. (2014). Wind farm and solar park effects on plant-soil carbon cycling: uncertain impacts of changes in ground-level microclimate. *Global Change Biology*, *20*(6), 1699–1706. https://doi.org/10.1111/gcb.12437

Armstrong, A., Ostle, N. J., & Whitaker, J. (2016). Solar park microclimate and vegetation management effects on grassland carbon cycling. *Environmental Research Letters*, *11*(7), 074016. https://doi.org/10.1088/1748-9326/11/7/074016

Baer, S. G., Meyer, C. K., Bach, E. M., Klopf, R. P., & Six, J. (2010). Contrasting ecosystem recovery on two soil textures: implications for carbon mitigation and grassland conservation. *Ecosphere*, *1*(1), art5. https://doi.org/10.1890/ES10-00004.1

Baer, Sara G., Collins, S. L., Blair, J. M., Knapp, A. K., & Fiedler, A. K. (2005). Soil Heterogeneity Effects on Tallgrass Prairie Community Heterogeneity: An Application of Ecological Theory to Restoration Ecology. *Restoration Ecology*, *13*(2), 413–424. https://doi.org/10.1111/j.1526-100X.2005.00051.x

Baer, Sara G., Adams, T., Scott, D. A., Blair, J. M., & Collins, S. L. (2020). Soil heterogeneity increases plant diversity after 20 years of manipulation during grassland restoration. *Ecological Applications*, *30*(1), 1–15. https://doi.org/10.1002/eap.2014

Barbose, G., Darghouth, N., O'Shaughnessy, E., & Forrester, S. (2023). *Tracking the Sun: Pricing and Design Trends for Distributed Photovoltaic Systems in the United States* (2023 Editi). Berkeley, California, USA: Lawrence Berkely National Laboratory.

Barron-Gafford, G. A., Minor, R. L., Allen, N. A., Cronin, A. D., Brooks, A. E., & Pavao-Zuckerman, M. A. (2016). The Photovoltaic Heat Island Effect: Larger solar power plants increase local temperatures. *Scientific Reports*, *6*(1), 35070. https://doi.org/10.1038/srep35070

Barron-Gafford, G. A., Pavao-Zuckerman, M. A., Minor, R. L., Sutter, L. F., Barnett-Moreno, I., Blackett, D. T., *et al.* (2019). Agrivoltaics provide mutual benefits across the food–energy–water nexus in drylands. *Nature Sustainability*, *2*(9), 848–855. https://doi.org/10.1038/s41893-019-0364-5

Bashagaluke, J. B., Logah, V., Opoku, A., Sarkodie-Addo, J., & Quansah, C. (2018). Soil nutrient loss through erosion: Impact of different cropping systems and soil amendments in Ghana. *PLOS ONE*, *13*(12), e0208250. https://doi.org/10.1371/journal.pone.0208250

Beatty, B., Macknick, J., Mccall, J., Braus, G., Buckner, D., Beatty, B., *et al.* (2017). *Native Vegetation Performance under a Solar PV Array at the National Wind Technology Center*. Golden, Colorado. https://doi.org/10.2172/1357887

Beckman, J., & Xiarchos, I. M. (2013). Why are Californian farmers adopting more (and larger) renewable energy operations? *Renewable Energy*, *55*, 322–330. https://doi.org/10.1016/j.renene.2012.10.057

Boligner, M., Seel, J., & Robson, D. (2019). *Empirical Trends in Project Technology, Cost, Performance, and PPA Pricing in the United States*. Retrieved from https://emp.lbl.gov/utility-scale-solar

BP Energy. (2020). *Energy Outlook*. British Petroleum (BP). Retrieved from https://www.bp.com/content/dam/bp/business-sites/en/global/corporate/pdfs/energy-economics/energy-outlook/bp-energy-outlook-2020.pdf

Breazeale, J. F. (1930). *Maintenance of Moisture Equilibrium and Nutrition of Plans at and Below the Wilting Percentage Item type text; Book*. Tucson, AZ. Retrieved from http://hdl.handle.net/10150/190618

Breyer, C., Bogdanov, D., Aghahosseini, A., Gulagi, A., Child, M., Oyewo, A. S., *et al.* (2018). Solar photovoltaics demand for the global energy transition in the power sector. *Progress in Photovoltaics: Research and Applications*, *26*(8), 505–523. https://doi.org/10.1002/pip.2950

Bronick, C. J., & Lal, R. (2005). Soil structure and management: A review. *Geoderma*, *124*(1–2), 3–22. https://doi.org/10.1016/j.geoderma.2004.03.005

Bukhary, S., Ahmad, S., & Batista, J. (2018). Analyzing land and water requirements for solar deployment in the Southwestern United States. *Renewable and Sustainable Energy Reviews*. https://doi.org/10.1016/j.rser.2017.10.016

Bureau of Economic Analysis. (2021). Regional Data: GDP and Personal Income. Retrieved February 7, 2022, from https://apps.bea.gov/iTable/index_regional.cfm

Bureau of Land Management (BLM), & US Department of Energy (USDOE). (2012). *Final Programmatic Environmental Impact Statement (PEIS) for Solar Energy Development in Six Southwestern States, Volume 1*. Washington, D.C.: US Department of Energy (USDOE). Retrieved from https://www.energy.gov/nepa/downloads/eis-0403-final-programmatic-environmental-impact-statement

Capellán-Pérez, I., de Castro, C., & Arto, I. (2017). Assessing vulnerabilities and limits in the transition to renewable energies: Land requirements under 100% solar energy scenarios. *Renewable and Sustainable Energy Reviews*, *77*(September 2016), 760–782. https://doi.org/10.1016/j.rser.2017.03.137

Chaney, K., & Swift, R. S. (1984). The influence of organic matter on aggregate stability in some British soils. *Journal of Soil Science*, *35*(2), 223–230. https://doi.org/10.1111/j.1365-2389.1984.tb00278.x

Chaturvedi, V., & Malyan, A. (2021). *Implications of a Net-Zero Target for India's Sectoral Energy Transitions and Climate Policy*. Retrieved from https://www.ceew.in/sites/default/files/ceew-study-on-implications-of-net-zero-target-for-indias-sectoral-energy-transitions-and-climate-policy.pdf

Chenu, C., Le Bissonnais, Y., & Arrouays, D. (2000). Organic Matter Influence on Clay Wettability and Soil Aggregate Stability. *Soil Science Society of America Journal*, *64*(4), 1479–1486. https://doi.org/10.2136/sssaj2000.6441479x

Choi, C. S. (2019). *Combined land use of solar infrastructure and agriculture for socioeconomic and environmental co-benefits in the tropics*. Temple University.

Choi, C. S., Cagle, A. E., Macknick, J., Bloom, D. E., Caplan, J. S., & Ravi, S. (2020). Effects of Revegetation on Soil Physical and Chemical Properties in Solar Photovoltaic Infrastructure. *Frontiers in Environmental Science*, *8*(August), 1–10. https://doi.org/10.3389/fenvs.2020.00140

Choi, C. S., Ravi, S., Siregar, I. Z., Dwiyanti, F. G., Macknick, J., Elchinger, M., & Davatzes, N. C. (2021). Combined land use of solar infrastructure and agriculture for socioeconomic and environmental co-benefits in the tropics. *Renewable and*

Sustainable Energy Reviews, *151*(September), 111610. https://doi.org/10.1016/j.rser.2021.111610

Choi, C. S., Macknick, J., Li, Y., Bloom, D., McCall, J., & Ravi, S. (2023). Environmental Co-Benefits of Maintaining Native Vegetation With Solar Photovoltaic Infrastructure. *Earth's Future*, *11*(6), 1–12. https://doi.org/10.1029/2023EF003542

Cook, L. M., & McCuen, R. H. (2013). Hydrologic Response of Solar Farms. *Journal of Hydrologic Engineering*, *18*(5), 536–541. https://doi.org/10.1061/(ASCE)HE.1943-5584.0000530

Cozzi, L. (International E. A., & Gould, T. (International E. A. (2021). *World Energy Outlook 2021*. Retrieved from www.iea.org/weo

Cramer, M. D., Barger, N. N., & Tschinkel, W. R. (2017). Edaphic properties enable facilitative and competitive interactions resulting in fairy circle formation. *Ecography*, *40*(10), 1210–1220. https://doi.org/10.1111/ecog.02461

Dale, M., & Benson, S. M. (2013). Energy Balance of the Global Photovoltaic (PV) Industry - Is the PV Industry a Net Electricity Producer? *Environmental Science & Technology*, *47*(7), 3482–3489. https://doi.org/10.1021/es3038824

Denen, B., Larson, D., Lee, C., Lee, J., & Tellinghuisen, S. (2007). *California's Energy-Water Nexus: Water Use in Electricity Generation*. University of California, Santa Barbara.

Deshmukh, R., Wu, G. C., Callaway, D. S., & Phadke, A. (2019). Geospatial and techno-economic analysis of wind and solar resources in India. *Renewable Energy*, *134*, 947–960. https://doi.org/10.1016/j.renene.2018.11.073

Diffenbaugh, N. S., & Barnes, E. A. (2023). Data-driven predictions of the time remaining until critical global warming thresholds are reached. *Proceedings of the National Academy of Sciences*, *120*(6, e2207183120). https://doi.org/10.1073/pnas.2207183120

Dingman, S. L. (2015). *Physical hydrology*. (D. Rosso, Ed.) (3rd ed.). Long Grove, IL: Waveland Press.

Dupont, S., Bergametti, G., & Simoëns, S. (2014). Modeling aeolian erosion in presence of vegetation. *Journal of Geophysical Research: Earth Surface*, *119*(2), 168–187. https://doi.org/10.1002/2013JF002875

Dupraz, C., Marrou, H., Talbot, G., Dufour, L., Nogier, A., & Ferard, Y. (2011). Combining solar photovoltaic panels and food crops for optimising land use: Towards new agrivoltaic schemes. *Renewable Energy*, *36*(10), 2725–2732. https://doi.org/10.1016/j.renene.2011.03.005

Edenhofer, O., Pichs-Madruga, R., Sokona, Y., Seyboth, K., Eickemeier, P., Matschoss, P., *et al.* (2011). *IPCC, 2011: Summary for Policymakers. In: IPCC Special Report on Renewable Energy Sources and Climate Change Mitigation*. *Cambridge University Press*. https://doi.org/10.5860/CHOICE.49-6309

Elamri, Y., Cheviron, B., Mange, A., Dejean, C., Liron, F., & Belaud, G. (2018). Rain concentration and sheltering effect of solar panels on cultivated plots. *Hydrology and Earth System Sciences*, *22*(2), 1285–1298. https://doi.org/10.5194/hess-22-1285-2018

Elamri, Y., Cheviron, B., Lopez, J. M., Dejean, C., & Belaud, G. (2018). Water budget and crop modelling for agrivoltaic systems: Application to irrigated lettuces. *Agricultural Water Management*, *208*(October 2017), 440–453. https://doi.org/10.1016/j.agwat.2018.07.001

Ellabban, O., Abu-Rub, H., & Blaabjerg, F. (2014). Renewable energy resources: Current status, future prospects and their enabling technology. *Renewable and Sustainable Energy Reviews*, *39*, 748–764. https://doi.org/10.1016/j.rser.2014.07.113

Employment Development Department (EDD). (2021). Agricultural Employment in California. Retrieved February 7, 2022, from https://www.labormarketinfo.edd.ca.gov/data/ca-agriculture.html

ESMAP. (2021a). *Global Solar Atlas v2.6*. Washington, D.C. Retrieved from https://globalsolaratlas.info/

ESMAP. (2021b). *Global Solar Atlas v2.6*. Washington, D.C. Retrieved from https://globalsolaratlas.info/

Evans, D. L., & Florschuetz, L. W. (1978). Terrestrial concentrating photovoltaic power system studies. *Solar Energy*, *20*(1), 37–43. https://doi.org/10.1016/0038-092X(78)90139-1

Faunt, C. C., Sneed, M., Traum, J., & Brandt, J. T. (2016). Water availability and land subsidence in the Central Valley, California, USA. *Hydrogeology Journal*, *24*(3), 675–684. https://doi.org/10.1007/s10040-015-1339-x

Federer, C. A., Vörösmarty, C., & Fekete, B. (1996). Intercomparison of Methods for Calculating Potential Evaporation in Regional and Global Water Balance Models. *Water Resources Research*, *32*(7), 2315–2321. https://doi.org/10.1029/96WR00801

Feldhake, C. ., & Boyer, D. . (1986). Effect of soil temperature on evapotranspiration by C3 and C4 grasses. *Agricultural and Forest Meteorology*, *37*(4), 309–318. https://doi.org/10.1016/0168-1923(86)90068-7

De Freitas, P. L., Zobel, R. W., & Snyder, V. A. (1999). Corn root growth in soil columns with artificially constructed aggregates. *Crop Science*, *39*(3), 725–730. https://doi.org/10.2135/cropsci1999.0011183X003900030020x

Fthenakis, V. (2009). Sustainability of photovoltaics: The case for thin-film solar cells. *Renewable and Sustainable Energy Reviews*, *13*(9), 2746–2750. https://doi.org/10.1016/j.rser.2009.05.001

Fthenakis, V., & Kim, H. C. (2009). Land use and electricity generation: A life-cycle analysis. *Renewable and Sustainable Energy Reviews*, *13*(6–7), 1465–1474. https://doi.org/10.1016/j.rser.2008.09.017

Fthenakis, V., & Kim, H. C. (2010). Life-cycle uses of water in U.S. electricity generation. *Renewable and Sustainable Energy Reviews*, *14*(7), 2039–2048. https://doi.org/10.1016/j.rser.2010.03.008

Fthenakis, V. M., & Kim, H. C. (2011). Photovoltaics: Life-cycle analyses. *Solar Energy*, *85*(8), 1609–1628. https://doi.org/10.1016/j.solener.2009.10.002

Genuchten, M. T. van. (1980). A closed-form equation for predicting the hydraulic conductivity of unsaturated soils. *Soil Science Society of America Journal*, *44*, 892–898. https://doi.org/10.2136/sssaj1980.03615995004400050002x

van Genuchten, M. T. (1980). A Closed-form Equation for Predicting the Hydraulic Conductivity of Unsaturated Soils. *Soil Science Society of America Journal*, *44*(5), 892–898. https://doi.org/10.2136/sssaj1980.03615995004400050002x

Gill, B. A., & Meydbray, J. (n.d.). The Problem of Mass Grading for Solar : Why and How the Practice Must Stop.

Gill, L., Gutierrez, A., & Weeks, T. (2021). *Achieving 100 Percent Clean Electricity in California: An Initial Assessment*. *SB 100 Joint Agency Report*.

Goetzberger, A., & Zastrow, A. (1982). On the Coexistence of Solar-Energy Conversion and Plant Cultivation. *International Journal of Solar Energy*, *1*(1), 55–69. https://doi.org/10.1080/01425918208909875

Gonzales, H. B., Ravi, S., Li, J., & Sankey, J. B. (2018). Ecohydrological implications of aeolian sediment trapping by sparse vegetation in drylands. *Ecohydrology*, *11*(7), 1–11. https://doi.org/10.1002/eco.1986

Graham, M., Ates, S., Melathopoulos, A. P., Moldenke, A. R., DeBano, S. J., Best, L. R., & Higgins, C. W. (2021). Partial shading by solar panels delays bloom, increases floral abundance during the late-season for pollinators in a dryland, agrivoltaic ecosystem. *Scientific Reports*, *11*(1), 7452. https://doi.org/10.1038/s41598-021-86756-4

Grout, T., & Ifft Charles, J. H. (2018). Approaches to Balancing Solar Expansion and Farmland Preservation: A Comparison across Selected States. Charles H. Dyson School of Applied Economics and Management. Retrieved from https://dyson.cornell.edu/wp-content/uploads/sites/5/2019/02/Cornell-Dyson-eb1804.pdf

Gulati, M. P., Priya, S., & Bresnyan, E. W. (2020). *Grow Solar, Save Water, Double Farmer Income*. *Grow Solar, Save Water, Double Farmer Income*. Washington, D.C.: World Bank, Washington, DC. https://doi.org/10.1596/33375

Guswa, A. J. (2012). Canopy vs. Roots: Production and Destruction of Variability in Soil Moisture and Hydrologic Fluxes. *Vadose Zone Journal*, *11*(3), vzj2011.0159. https://doi.org/10.2136/vzj2011.0159

Gutiérrez, J. M., Jones, R. G., Narisma, G. T., Alves, L. M., Amjad, M., Gorodetskaya, I. V., *et al.* (2021). *Climate Change 2021: The Physical Science Basis. Contribution of Working Group I to the Sixth Assessment Report of the Intergovernmental Panel on*

Climate Change. (V. Masson-Delmotte, P. Zhai, A. Pirani, S. L. Connors, C. Péan, S. Berger, *et al.*, Eds.). Cambridge University Press. Retrieved from http://interactive-atlas.ipcc.ch/

Hernandez, R. R., Easter, S. B., Murphy-Mariscal, M. L., Maestre, F. T., Tavassoli, M., Allen, E. B., *et al.* (2014). Environmental impacts of utility-scale solar energy. *Renewable and Sustainable Energy Reviews*, *29*, 766–779. https://doi.org/10.1016/j.rser.2013.08.041

Hernandez, R. R., Hoffacker, M. K., & Field, C. B. (2014). Land-Use Efficiency of Big Solar. *Environmental Science & Technology*, *48*(2), 1315–1323. https://doi.org/10.1021/es4043726

Hernandez, R. R., Hoffacker, M. K., & Field, C. B. (2015). Efficient use of land to meet sustainable energy needs. *Nature Climate Change*, *5*(4), 353–358. https://doi.org/10.1038/nclimate2556

Hernandez, R. R., Hoffacker, M. K., Murphy-Mariscal, M. L., Wu, G. C., & Allen, M. F. (2015). Solar energy development impacts on land cover change and protected areas. *Proceedings of the National Academy of Sciences of the United States of America*, *112*(44), 13579–84. https://doi.org/10.1073/pnas.1517656112

Hevia, G. G., Mendez, M., & Buschiazzo, D. E. (2007). Tillage affects soil aggregation parameters linked with wind erosion. *Geoderma*, *140*(1–2), 90–96. https://doi.org/10.1016/j.geoderma.2007.03.001

Hoffacker, M. K., Allen, M. F., & Hernandez, R. R. (2017). Land-Sparing Opportunities for Solar Energy Development in Agricultural Landscapes: A Case Study of the Great Central Valley, CA, United States. *Environmental Science & Technology*, *51*(24), 14472–14482. https://doi.org/10.1021/acs.est.7b05110

Hooda, S. M. (2017). *India - Rajasthan water assessment and potential for private sector interventions*. New Delhi, India.

Hooker, M. A., & Alexander, W. E. (1998). Estimating the demand for irrigation water in the Central Valley of California. *Journal of the American Water Resources Association*, *34*(3), 497–505. https://doi.org/10.1111/j.1752-1688.1998.tb00949.x

Hsu, D. D., O'Donoughue, P., Fthenakis, V., Heath, G. A., Kim, H. C., Sawyer, P., *et al.* (2012). Life Cycle Greenhouse Gas Emissions of Crystalline Silicon Photovoltaic Electricity Generation. *Journal of Industrial Ecology*, *16*(SUPPL.1), S122–S135. https://doi.org/10.1111/j.1530-9290.2011.00439.x

IEA. (2020). Solar PV. Retrieved September 3, 2021, from https://www.iea.org/reports/solar-pv

IRENA. (2018). *Global Energy Transformation: A Roadmap to 2050*. *Global Energy Transformation. A Roadmap to 2050*. https://doi.org/Doi 10.1002/(Sici)1097-0029(19990915)46:6<398::Aid-Jemt8>3.0.Co;2-H

Iturbide, M., Fernández, J., Gutiérrez, J. M., Bedia, J., Cimadevilla, E., Díez-Sierra, J., *et al.* (2021). Repository supporting the implementation of FAIR principles in the IPCC-

WG1 Atlas. https://doi.org/10.5281/zenodo.3691645

Ivanov, V. Y., Fatichi, S., Jenerette, G. D., Espeleta, J. F., Troch, P. A., & Huxman, T. E. (2010). Hysteresis of soil moisture spatial heterogeneity and the "homogenizing" effect of vegetation. *Water Resources Research*, *46*(9), 1–15. https://doi.org/10.1029/2009WR008611

Jacobson, M. Z. (2009). Review of solutions to global warming, air pollution, and energy security. *Energy & Environmental Science*, *2*, 148–173. https://doi.org/10.1039/B809990C

Jain, R., Kishore, P., & Singh, D. K. (2019). Irrigation in India: Status, challenges and options. *Journal of Soil and Water Conservation*, *18*(4), 354. https://doi.org/10.5958/2455-7145.2019.00050.X

Kannenberg, S. A., Sturchio, M. A., Venturas, M. D., & Knapp, A. K. (2023). Grassland carbon-water cycling is minimally impacted by a photovoltaic array. *Communications Earth and Environment*, *4*(1). https://doi.org/10.1038/s43247-023-00904-4

Katul, G., Todd, P., Pataki, D., Kabala, Z. J., & Oren, R. (1997). Soil water depletion by oak trees and the influence of root water uptake on the moisture content spatial statistics. *Water Resources Research*, *33*(4), 611–623. https://doi.org/10.1029/96WR03978

Kazem, H. A., & Chaichan, M. T. (2015). Effect of humidity on photovoltaic performance based on experimental study. *International Journal of Applied Engineering Research*, *10*(23), 43572–43577.

Kelliher, F. M., Leuning, R., Raupach, M. R., & Schulze, E.-D. (1995). Maximum conductances for evaporation from global vegetation types. *Agricultural and Forest Meteorology*, *73*(1–2), 1–16. https://doi.org/10.1016/0168-1923(94)02178-M

Kim, B., Kim, C., Han, S. U., Bae, J. H., & Jung, J. (2020). Is it a good time to develop commercial photovoltaic systems on farmland? An American-style option with crop price risk. *Renewable and Sustainable Energy Reviews*, *125*(February), 109827. https://doi.org/10.1016/j.rser.2020.109827

Kläring, H. P., Schonhof, I., & Krumbein, A. (2001). Modelling yield and product quality of broccoli as affected by temperature and irradiance. *Acta Horticulturae*, *566*, 85–90. https://doi.org/10.17660/ActaHortic.2001.566.8

Kubásek, J., Urban, O., & Šantrůček, J. (2013). C 4 plants use fluctuating light less efficiently than do C 3 plants: a study of growth, photosynthesis and carbon isotope discrimination. *Physiologia Plantarum*, *149*(4), 528–539. https://doi.org/10.1111/ppl.12057

Larney, F. J., Olson, B. M., Janzen, H. H., & Lindwall, C. W. (2000). Early Impact of Topsoil Removal and Soil Amendments on Crop Productivity. *Agronomy Journal*, *92*(5), 948–956. https://doi.org/10.2134/agronj2000.925948x

Larney, F. J., Li, L., Janzen, H. H., Angers, D. A., & Olson, B. M. (2016). Soil quality attributes, soil resilience, and legacy effects following topsoil removal and one-time

amendments. *Canadian Journal of Soil Science*, *96*(2), 177–190. https://doi.org/10.1139/cjss-2015-0089

Latunussa, C. E. L., Ardente, F., Blengini, G. A., & Mancini, L. (2016). Life Cycle Assessment of an innovative recycling process for crystalline silicon photovoltaic panels. *Solar Energy Materials and Solar Cells*, *156*. https://doi.org/10.1016/j.solmat.2016.03.020

Leccisi, E., Raugei, M., & Fthenakis, V. (2016). The energy and environmental performance of ground-mounted photovoltaic systems - A timely update. *Energies*, *9*(8). https://doi.org/10.3390/en9080622

Leung, A. K., Garg, A., & Ng, C. W. W. (2015). Effects of plant roots on soil-water retention and induced suction in vegetated soil. *Engineering Geology*, *193*, 183–197. https://doi.org/10.1016/j.enggeo.2015.04.017

Li, Bin Bin, Li, P. P., Zhang, W. T., Ji, J. Y., Liu, G. Bin, & Xu, M. X. (2021). Deep soil moisture limits the sustainable vegetation restoration in arid and semi-arid Loess Plateau. *Geoderma*, *399*(May 2020), 115122. https://doi.org/10.1016/j.geoderma.2021.115122

Li, Bonan, Wang, L., Kaseke, K. F., Li, L., & Seely, M. K. (2016). The impact of rainfall on soil moisture dynamics in a foggy desert. *PLoS ONE*, *11*(10). https://doi.org/10.1371/journal.pone.0164982

Li, J., Okin, G. S., Alvarez, L., & Epstein, H. (2007). Quantitative effects of vegetation cover on wind erosion and soil nutrient loss in a desert grassland of southern New Mexico, USA. *Biogeochemistry*, *85*(3), 317–332. https://doi.org/10.1007/s10533-007-9142-y

Li, J., Okin, G. S., Alvarez, L., & Epstein, H. (2008). Effects of wind erosion on the spatial heterogeneity of soil nutrients in two desert grassland communities. *Biogeochemistry*, *88*(1), 73–88. https://doi.org/10.1007/s10533-008-9195-6

Li, R., Zhang, H., Wang, H., Tu, Q., & Wang, X. (2019). Integrated hybrid life cycle assessment and contribution analysis for CO2 emission and energy consumption of a concentrated solar power plant in China. *Energy*, *174*, 310–322. https://doi.org/10.1016/j.energy.2019.02.066

Li, X. R., Ma, F. Y., Xiao, H. L., Wang, X. P., & Kim, K. C. (2004). Long-term effects of revegetation on soil water content of sand dunes in arid region of Northern China. *Journal of Arid Environments*, *57*(1), 1–16. https://doi.org/10.1016/S0140-1963(03)00089-2

Li, Y.-T., Luo, J., Liu, P., & Zhang, Z.-S. (2021). C4 species utilize fluctuating light less efficiently than C3 species. *Plant Physiology*, *187*(3), 1288–1291. https://doi.org/10.1093/plphys/kiab411

Lin, C. H., McGraw, R. L., George, M. F., & Garrett, H. E. (1998). Shade effects on forage crops with potential in temperate agroforestry practices. *Agroforestry Systems*, *44*(2–3), 109–119. https://doi.org/10.1023/A:1006205116354

Lo, M., & Famiglietti, J. S. (2013). Irrigation in California's Central Valley strengthens the southwestern U.S. water cycle. *Geophysical Research Letters*, *40*(2), 301–306. https://doi.org/10.1002/grl.50108

Lovich, J. E., & Ennen, J. R. (2011). Wildlife Conservation and Solar Energy Development in the Desert Southwest, United States. *BioScience*, *61*(12), 982–992. https://doi.org/10.1525/bio.2011.61.12.8

Luo, W., Khoo, Y. S., Kumar, A., Low, J. S. C., Li, Y., Tan, Y. S., *et al.* (2018). A comparative life-cycle assessment of photovoltaic electricity generation in Singapore by multicrystalline silicon technologies. *Solar Energy Materials and Solar Cells*, *174*. https://doi.org/10.1016/j.solmat.2017.08.040

Macknick, J., Newmark, R., Heath, G., & Hallett, K. C. (2012). Operational water consumption and withdrawal factors for electricity generating technologies: a review of existing literature. *Environmental Research Letters*, *7*(4), 045802. https://doi.org/10.1088/1748-9326/7/4/045802

Macknick, Jordan, Beatty, B., & Hill, G. (2013). *Overview of Opportunities for Co-Location of Solar Energy Technologies and Vegetation*. Golden, Colorado. Retrieved from http://www.nrel.gov/docs/fy14osti/60240.pdf

Macknick, Jordan, Hartmann, H., Barron-gafford, G., Beatty, B., Burton, R., Seok, C., *et al.* (2022). *The 5 Cs of Agrivoltaic Success Factors in the United States : Lessons From the InSPIRE Research Study The 5 Cs of Agrivoltaic Success Factors in the United States : Lessons From the InSPIRE Research Study*. Golden, CO (United States): National Renewable Energy Laboratory.

Majumdar, D., & Pasqualetti, M. J. (2018). Dual use of agricultural land: Introducing 'agrivoltaics' in Phoenix Metropolitan Statistical Area, USA. *Landscape and Urban Planning*, *170*(October), 150–168. https://doi.org/10.1016/j.landurbplan.2017.10.011

Majumdar, D., & Pasqualetti, M. J. (2019). Analysis of land availability for utility-scale power plants and assessment of solar photovoltaic development in the state of Arizona, USA. *Renewable Energy*, *134*, 1213–1231. https://doi.org/10.1016/j.renene.2018.08.064

Maltais, K. (2019, September 23). Struggling Farmers See Bright Spot in Solar. *The Wall Street Journal*. Retrieved from https://www.wsj.com/articles/struggling-farmers-see-bright-spot-in-solar-11569242733

De Marco, A., Petrosillo, I., Semeraro, T., Pasimeni, M. R., Aretano, R., & Zurlini, G. (2014). The contribution of Utility-Scale Solar Energy to the global climate regulation and its effects on local ecosystem services. *Global Ecology and Conservation*, *2*(October), 324–337. https://doi.org/10.1016/j.gecco.2014.10.010

Marrou, H., Dufour, L., & Wery, J. (2013). How does a shelter of solar panels influence water flows in a soil-crop system? *European Journal of Agronomy*, *50*, 38–51. https://doi.org/10.1016/j.eja.2013.05.004

Marrou, H., Guilioni, L., Dufour, L., Dupraz, C., & Wery, J. (2013). Microclimate under

agrivoltaic systems: Is crop growth rate affected in the partial shade of solar panels? *Agricultural and Forest Meteorology*, *177*, 117–132. https://doi.org/10.1016/j.agrformet.2013.04.012

Marrou, H., Wery, J., Dufour, L., & Dupraz, C. (2013). Productivity and radiation use efficiency of lettuces grown in the partial shade of photovoltaic panels. *European Journal of Agronomy*, *44*, 54–66. https://doi.org/10.1016/j.eja.2012.08.003

Matus, F. J. (2021). Fine silt and clay content is the main factor defining maximal C and N accumulations in soils : a meta - analysis. *Scientific Reports*, 1–17. https://doi.org/10.1038/s41598-021-84821-6

McGeehan, S. L., & Naylor, D. V. (1988). Automated instrumental analysis of carbon and nitrogen in plant and soil samples. *Communications in Soil Science and Plant Analysis*, *19*(4), 493–505. https://doi.org/10.1080/00103628809367953

McLauchlan, K. K. (2006). Effects of soil texture on soil carbon and nitrogen dynamics after cessation of agriculture. *Geoderma*, *136*(1–2), 289–299. https://doi.org/10.1016/j.geoderma.2006.03.053

Mekonnen, M. M., Gerbens-Leenes, P. W., & Hoekstra, A. Y. (2015). The consumptive water footprint of electricity and heat: A global assessment. *Environmental Science: Water Research and Technology*, *1*(3), 285–297. https://doi.org/10.1039/c5ew00026b

MNRE. (2021a). *Annual report 2020-2021*.

MNRE. (2021b). Solar capacity breakdown.

Monteith, J. (1965). Evaporation and environment. Symposia of the Society for Experimental Biology. *Symposia of the Society for Experimental Biology*, (19), 205–234.

Munson, S. M., Belnap, J., & Okin, G. S. (2011). Responses of wind erosion to climate-induced vegetation changes on the Colorado Plateau. *Proceedings of the National Academy of Sciences of the United States of America*, *108*(10), 3854–3859. https://doi.org/10.1073/pnas.1014947108

Nelson, D. W., & Sommers, L. E. (1996). Total carbon, Organic Carbon, and Organic Matter. In M. E. S. D.L. Sparks, J.M. Bartels, D.L. Sparks, A.L. Page, P.A. Helmke, R.H. Loeppert, P.N. Soltanpour, M.A, Tabatabai, C.T. Johnston (Ed.), *Methods of soil analysis: Part 3 Chemical methods* (3rd ed., pp. 961–1010). Madison, WI: Soils Science Society of America, Inc. and American Society of Agronomy, Inc.

Nir, S. M. (2020, March 18). He Set Up a Big Solar Farm. His Neighbors Hated It. *The New York Times*. Retrieved from https://www.nytimes.com/2020/03/18/nyregion/solar-energy-farms-ny.html

Nóia Júnior, R. de S., do Amaral, G. C., Pezzopane, J. E. M., Toledo, J. V., & Xavier, T. M. T. (2018). Ecophysiology of C3 and C4 plants in terms of responses to extreme soil temperatures. *Theoretical and Experimental Plant Physiology*, *30*(3), 261–274. https://doi.org/10.1007/s40626-018-0120-7

Nugent, D., & Sovacool, B. K. (2014). Assessing the lifecycle greenhouse gas emissions from solar PV and wind energy: A critical meta-survey. *Energy Policy*, *65*. https://doi.org/10.1016/j.enpol.2013.10.048

O'Shaughnessy, P., & Cavanaugh, J. E. (2015). Performing T-tests to Compare Autocorrelated Time Series Data Collected from Direct-Reading Instruments. *Journal of Occupational and Environmental Hygiene*, *12*(11), 743–752. https://doi.org/10.1080/15459624.2015.1044603

Oliver, S. A., Oliver, H. R., Wallace, J. S., & Roberts, A. M. (1987). Soil heat flux and temperature variation with vegetation, soil type and climate. *Agricultural and Forest Meteorology*, *39*, 257–269.

Ong, S., Campbell, C., Denholm, P., Margolis, R., & Heath, G. (2013). *Land-Use Requirements for Solar Power Plants in the United States*. *NREL/TP-6A20-56290*. Golden, Colorado. Retrieved from http://www.nrel.gov/docs/fy13osti/56290.pdf

Pregitzer, K. S., & King, J. S. (2005). Chapter 10: Effects of Soil Temperature on Nutrient Uptake. *Ecological Studies, Vol. 181: Nutrient Acquisition by Plants: An Ecological Perspective*, *181*(1991), 277–310.

Quinton, J. N., Govers, G., Van Oost, K., & Bardgett, R. D. (2010). The impact of agricultural soil erosion on biogeochemical cycling. *Nature Geoscience*, *3*(5), 311–314. https://doi.org/10.1038/ngeo838

Rafferty, N. E. (2017). Effects of global change on insect pollinators: multiple drivers lead to novel communities. *Current Opinion in Insect Science*, *23*, 22–27. https://doi.org/10.1016/j.cois.2017.06.009

Raghavan, G. S. V., McKyes, E., Baxter, R., & Gendron, G. (1979). Traffic-soil-plant (maize) relations. *Journal of Terramechanics*, *16*(4), 181–189. https://doi.org/10.1016/0022-4898(79)90027-2

Raven, P. H., & Wagner, D. L. (2021). Agricultural intensification and climate change are rapidly decreasing insect biodiversity. *Proceedings of the National Academy of Sciences*, *118*(2), 1–6. https://doi.org/10.1073/pnas.2002548117

Ravi, S., Lobell, D. B., & Field, C. B. (2014). Tradeoffs and synergies between biofuel production and large solar infrastructure in deserts. *Environmental Science and Technology*, *48*(5), 3021–3030. https://doi.org/10.1021/es404950n

Ravi, S., Macknick, J., Lobell, D., Field, C., Ganesan, K., Jain, R., *et al.* (2016). Colocation opportunities for large solar infrastructures and agriculture in drylands. *Applied Energy*, *165*, 383–392. https://doi.org/10.1016/j.apenergy.2015.12.078

Ringler, C., Bhaduri, A., & Lawford, R. (2013). The nexus across water, energy, land and food (WELF): potential for improved resource use efficiency? *Current Opinion in Environmental Sustainability*, *5*(6), 617–624. https://doi.org/https://doi.org/10.1016/j.cosust.2013.11.002

Ritchie, J. T. (1972). Model for predicting evaporation from a row crop with incomplete cover. *Water Resources Research*, *8*(5), 1204–1213.

https://doi.org/10.1029/WR008i005p01204

Rivero, R. M., Ruiz, J. M., García, P. C., López-Lefebre, L. R., Sánchez, E., & Romero, L. (2001). Resistance to cold and heat stress: accumulation of phenolic compounds in tomato and watermelon plants. *Plant Science*, *160*(2), 315–321. https://doi.org/10.1016/S0168-9452(00)00395-2

Rosales, M. A., Cervilla, L. M., Sánchez-Rodríguez, E., Rubio-Wilhelmi, M. del M., Blasco, B., Ríos, J. J., *et al.* (2011). The effect of environmental conditions on nutritional quality of cherry tomato fruits: Evaluation of two experimental Mediterranean greenhouses. *Journal of the Science of Food and Agriculture*, *91*(1), 152–162. https://doi.org/10.1002/jsfa.4166

Ross, D., & Kettering, Q. (2011). Recommended methods for determining soil cation exchange capacity. In J. T. Sims & A. Wolf (Eds.), *Recommended Soil Testing Procedures for the Northeasten United States. Cooperative Bulletin No. 493* (2nd ed., pp. 75–86). Newark, Delaware: University of Delaware. Retrieved from http://extension.udel.edu/lawngarden/files/2012/10/CHAP9.pdf (accessed: February 2013)

Sanderman, J., Hengl, T., & Fiske, G. J. (2017). Soil carbon debt of 12,000 years of human land use. *Proceedings of the National Academy of Sciences*, *114*(36), 9575–9580. https://doi.org/10.1073/pnas.1706103114

Schlenker, W., & Roberts, M. J. (2009). Nonlinear temperature effects indicate severe damages to U.S. crop yields under climate change. *Proceedings of the National Academy of Sciences*, *106*(37), 15594–15598. https://doi.org/10.1073/pnas.0906865106

Schulze, E.-D., Kelliher, F. M., Körner, C., Lloyd, J., & Leuning, R. (1994). RELATIONSHIPS AMONG MAXIMUM STOMATAL CONDUCTANCE, ECOSYSTEM SURFACE CONDUCTANCE, CARBON ASSIMILATION RATE, AND PLANT NITROGEN NUTRITION: A Global Ecology Scaling Exercise. *Annual Review of Ecology and Systematics*, *25*(1), 629–662. https://doi.org/10.1146/annurev.es.25.110194.003213

Sharpley, A. N. (1985). The Selection Erosion of Plant Nutrients in Runoff. *Soil Science Society of America Journal*, *49*(6), 1527–1534. https://doi.org/10.2136/sssaj1985.03615995004900060039x

Singh Rajput, A., Sharma, L., Shekhawat, P. S., & Pawariya, V. (2022). Estimation of seasonal surplus labour in agriculture in different agro-climatic regions of Rajasthan. *Environment Conservation Journal*, *23*(1&2), 55–64. https://doi.org/10.36953/ECJ.021873-2142

Sinha, P. (2013). Life cycle materials and water management for CdTe photovoltaics. *Solar Energy Materials and Solar Cells*, *119*, 271–275. https://doi.org/10.1016/j.solmat.2013.08.022

Sinha, P., Hoffman, B., Sakers, J., & Althouse, L. (2018). Best Practices in Responsible Land Use for Improving Biodiversity at a Utility-Scale Solar Facility. *Case Studies in*

the Environment, *2*(1), 1–12. https://doi.org/10.1525/cse.2018.001123

Solar Energy Industries Association. (2022). Solar Market Insight Report 2022 Q4. Retrieved from https://www.seia.org/research-resources/solar-market-insight-report-2022-q4

SolarPower Europe. (2018). *Global Market Outlook For Solar Power 2018–2022*. Brussels, Belgium. Retrieved from www.africa-eu-renewables.org

Spang, E. S., Moomaw, W. R., Gallagher, K. S., Kirshen, P. H., & Marks, D. H. (2014). The water consumption of energy production: an international comparison. *Environmental Research Letters*, *9*(10), 105002. https://doi.org/10.1088/1748-9326/9/10/105002

Stewart, J. . (1988). Modelling surface conductance of pine forest. *Agricultural and Forest Meteorology*, *43*(1), 19–35. https://doi.org/10.1016/0168-1923(88)90003-2

Sturchio, M. A., Macknick, J. E., Barron-Gafford, G. A., Chen, A., Alderfer, C., Condon, K., *et al.* (2022). Grassland productivity responds unexpectedly to dynamic light and soil water environments induced by photovoltaic arrays. *Ecosphere*, *13*(12), 1–14. https://doi.org/10.1002/ecs2.4334

Tang, L., Zeng, G., Nourbakhsh, F., & Shen, G. L. (2009). Artificial Neural Network Approach for Predicting Cation Exchange Capacity in Soil Based on Physico-Chemical Properties. *Environmental Engineering Science*, *26*(1), 137–146. https://doi.org/10.1089/ees.2007.0238

Trainor, A. M., McDonald, R. I., & Fargione, J. (2016). Energy Sprawl Is the Largest Driver of Land Use Change in United States. *PLOS ONE*, *11*(9), e0162269. https://doi.org/10.1371/journal.pone.0162269

Tsoar, H. (2005). SAND DUNES. In *Encyclopedia of Soils in the Environment* (Vol. 4, pp. 462–471). Elsevier. https://doi.org/10.1016/B0-12-348530-4/00410-0

Turner, C. L., & Knapp, A. K. (1996). Responses of a C 4 Grass and Three C 3 Forbs to Variation in Nitrogen and Light in Tallgrass Prairie. *Ecology*, *77*(6), 1738–1749. https://doi.org/10.2307/2265779

Turney, D., & Fthenakis, V. (2011). Environmental impacts from the installation and operation of large-scale solar power plants. *Renewable and Sustainable Energy Reviews*, *15*(6), 3261–3270. https://doi.org/10.1016/j.rser.2011.04.023

U.S. Department of Energy. (2012). *SunShot Vision Study*. *U.S. Department of Energy*. https://doi.org/SunShot, Energy Efficiency and Renewable Energy, U.S. Department of Energy. NREL Report No. BK5200-47927; DOE/GO-102012-3037

U.S. Geological Survey (USGS). (2022). USGS Water Data for USA. Retrieved from https://waterdata.usgs.gov/nwis?

US Census Bureau. (2021). QuickFacts: California. Retrieved February 7, 2022, from https://www.census.gov/quickfacts/fact/table/CA/PST045221

US Department of Energy. (n.d.). Farmer's Guide to Going Solar. Retrieved January 27, 2022, from https://www.energy.gov/eere/solar/farmers-guide-going-solar

US Department of Energy Solar Energy Technologies Office. (2021). *Solar Futures Study*. Washington, D.C.

US Energy Information Administration. (2022, January 10). Solar power will account for nearly half of new U.S. electric generating capacity in 2022. Retrieved January 27, 2022, from https://www.eia.gov/todayinenergy/detail.php?id=50818#:~:text=In 2022%2C we expect 46.1,%25 and wind at 17%25.

US Energy Information Administration (EIA). (2021). Electricity Data Browser. Retrieved October 10, 2021, from https://www.eia.gov/electricity/data/browser/

Veldhuis, A. J., & Reinders, A. H. M. E. (2012). Real-time irradiance simulation for PV products and building integrated PV in a virtual reality environment. *IEEE Journal of Photovoltaics*, *2*(3), 352–358. https://doi.org/10.1109/JPHOTOV.2012.2189937

van de Ven, D.-J., Capellan-Peréz, I., Arto, I., Cazcarro, I., de Castro, C., Patel, P., & Gonzalez-Eguino, M. (2021). The potential land requirements and related land use change emissions of solar energy. *Scientific Reports*, *11*(1), 2907. https://doi.org/10.1038/s41598-021-82042-5

Walston, L. J., Mishra, S. K., Hartmann, H. M., Hlohowskyj, I., McCall, J., & Macknick, J. (2018). Examining the Potential for Agricultural Benefits from Pollinator Habitat at Solar Facilities in the United States. *Environmental Science & Technology*, *52*(13), 7566–7576. research-article. https://doi.org/10.1021/acs.est.8b00020

Walston, L. J., Li, Y., Hartmann, H. M., Macknick, J., Hanson, A., Nootenboom, C., *et al.* (2021). Modeling the ecosystem services of native vegetation management practices at solar energy facilities in the Midwestern United States. *Ecosystem Services*, *47*(December 2020), 101227. https://doi.org/10.1016/j.ecoser.2020.101227

Wang, A.-P., Li, F.-H., & Yang, S.-M. (2011). Effect of Polyacrylamide Application on Runoff, Erosion, and Soil Nutrient Loss Under Simulated Rainfall. *Pedosphere*, *21*(5), 628–638. https://doi.org/10.1016/S1002-0160(11)60165-3

Warren, R., Price, J., Graham, E., Forstenhaeusler, N., & VanDerWal, J. (2018). The projected effect on insects, vertebrates, and plants of limiting global warming to 1.5°C rather than 2°C. *Science*, *360*(6390), 791–795. https://doi.org/10.1126/science.aar3646

Whitaker, M. B., Heath, G. A., Burkhardt, J. J., & Turchi, C. S. (2013). Life cycle assessment of a power tower concentrating solar plant and the impacts of key design alternatives. *Environmental Science and Technology*, *47*(11), 5896–5903. https://doi.org/10.1021/es400821x

Wick, A. F., Stahl, P. D., Ingram, L. J., & Vicklund, L. (2009). Soil aggregation and organic carbon in short-term stockpiles. *Soil Use and Management*, *25*(September), z. https://doi.org/10.1111/j.1475-2743.2009.00227.x

De Wild-Scholten, M. J. (2013). Energy payback time and carbon footprint of commercial

photovoltaic systems. *Solar Energy Materials and Solar Cells*, *119*, 296–305. https://doi.org/10.1016/j.solmat.2013.08.037

Wolff, X. Y., & Coltman, R. R. (1990a). Productivity of Eight Leafy Vegetable Crops Grown Under Shade in Hawaii. *Journal of the American Society for Horticultural Science*, *115*(1), 182–188. https://doi.org/10.21273/JASHS.115.1.182

Wolff, X. Y., & Coltman, R. R. (1990b). Productivity Under Shade in Hawaii of Five Crops Grown as Vegetables in the Tropics. *Journal of the American Society for Horticultural Science*, *115*(1), 175–181. https://doi.org/10.21273/JASHS.115.1.175

Wu, X., Shao, L., Chen, G., Han, M., Chi, Y., Yang, Q., *et al.* (2021). Unveiling land footprint of solar power: A pilot solar tower project in China. *Journal of Environmental Management*, *280*(December 2020), 111741. https://doi.org/10.1016/j.jenvman.2020.111741

Yavari, R., Zaliwciw, D., Cibin, R., & McPhillips, L. (2022). Minimizing environmental impacts of solar farms: a review of current science on landscape hydrology and guidance on stormwater management. *Environmental Research: Infrastructure and Sustainability*, *2*(3), 032002. https://doi.org/10.1088/2634-4505/ac76dd

Zhang, B., Yang, Y., & Zepp, H. (2004). Effect of vegetation restoration on soil and water erosion and nutrient losses of a severely eroded clayey Plinthudult in southeastern China. *Catena*, *57*(1), 77–90. https://doi.org/10.1016/j.catena.2003.07.001

Zhang, G. H., Liu, G. Bin, Wang, G. L., & Wang, Y. X. (2011). Effects of Vegetation Cover and Rainfall Intensity on Sediment-Bound Nutrient Loss, Size Composition and Volume Fractal Dimension of Sediment Particles. *Pedosphere*, *21*(5), 676–684. https://doi.org/10.1016/S1002-0160(11)60170-7

Zhang, R. (1997). Determination of Soil Sorptivity and Hydraulic Conductivity from the Disk Infiltrometer. *Soil Science Society of America Journal*, *61*(4), 1024. https://doi.org/10.2136/sssaj1997.03615995006100040005x

Zibilske, L. M., & Bradford, J. M. (2007). Soil Aggregation , Aggregate Carbon and Nitrogen , and Moisture Retention Induced by Conservation Tillage, *71*(3), 793–802. https://doi.org/10.2136/sssaj2006.0217

Zougmoré, R., Mando, A., & Stroosnijder, L. (2009). Soil Nutrient and Sediment Loss as Affected By Erosion Barriers and Nutrient Source in Semi-Arid Burkina Faso. *Arid Land Research and Management*, *23*(1), 85–101. https://doi.org/10.1080/15324980802599142

APPENDIX A

SUPPLEMENTAL INFORMATION FOR CHAPTER 2

The supporting information provides more information on the study sites, model parameters for evapotranspiration model, statistical analysis, and additional references.

Text A.1 Study Site

The study area was a 2.9-acre portion of a 9.5-MW PV plant (located at 45.451148, -92.907255) in Chisago City, Minnesota, USA, that started operating in October of 2016 (Enel Green Power North America (EGP-NA) (**Figure A.1 a & b**). Prior to the construction of the PV facility, approximately 74% of the land area was agricultural, and 17% was temperate forest. The remaining portion of the land was categorized as developed/urban (approximately 6%), recently disturbed/modified (approximately 2%), flooded and swamp forest (approximately 1%), and boreal forest (< 1%). To retain the land's ability to cultivate crops after the decommissioning of the facility, land grading or any other construction techniques that would remove a significant portion of the topsoil were avoided during the construction of the facility. Native flora was planted on the intact soil in a portion of the facility following the construction. Sensor towers in their respective treatments are shown in **Figure A.2**.

The vegetated site was seeded with pollinator friendly native seed mix consisting of Anise hyssop, American water plantain, Brown eyed susan, Blue grama, Blue joint grass, Bishop's cap, Butterfly milkweed, Bottlebrush sedge, Bebb's oval sedge, Boneset, Bottlebrush sedge, Canada milkvetch, Canada wild rye, Common milkweed, Culver's root, Calico aster, Cream wild indigo, Foxglove beardtongue, Fowl bluegrass, Fox sedge,

Fragrant giant hyssop, Fringed loosestrife, Golden alexanders, Great blue lobelia, Greater straw sedge, Gray goldenrod, Hoary vervain, Junegrass, Little bluestem, Long-headed coneflower, Mountain mint, Marsh betony, Narrow leaved coneflower, New England aster, Ox-eye sunflower, Partridge pea, Prairie brome, Prairie coreopsis, Prairie dropseed, Purple prairie clover, Porcupine sedge, Purple meadow rue, Riddell's goldenrod, Showy goldenrod, Side-oats grama, Silk wild rye, Sky blue aster, Spotted bee balm, Stiff goldenrod, Swamp milkweed, Slender wheat grass, Tussock sedge, Turtle head, Turtlehead, Virginia wild rye, White prairie clover, White wild indigo, Wild bergamot , Wool grass, White prairie clover, Wild bergamot, Wood betony, Wild licorice, Yellow coneflower, Yarrow.

Text A2. Distribution of Air Temperature and Relative Humidity

Distribution of daily minimum and maximum air temperature and relative humidity was virtually identical across all three treatments (**Figure A2 a & b**).

Text A3. Panel Efficiency Analysis

Enel Green Power North America provided the time series data of electricity production from the inverters connected to the PV arrays in the veg PV and the bare PV treatments. Each treatment consisted of 14.5 arrays that each consisted of 72 modules. Each solar module was 1.956-m-long and 0.992-m-wide.

To examine the variation in operation efficiency of the solar panels under different weather conditions, we normalized hourly average of DC power output (kW) from each treatment with the total area of PV modules (m^2) and the net shortwave radiation intensity (W m^{-2}) measured in the Control treatment. We limited the analysis to 10 am to 5 pm and excluded the normalized DC output above the 95th percentile that resulted from shading of the solar pyranometer by nearby transmission towers.

While PV output was negatively correlated to the panel temperature as expected (**Figure A.3**), it did not strongly correlate with either air temperature (**Figure A.4**) or relative humidity (**Figure A.5**).

Text A4. Evapotranspiration Model

Evaporation from Bare Soil and Vegetated Surfaces

The theoretical framework for the mechanistic relationship between the soil-vegetation complex and the PV arrays will be used to create the model to estimate the effectiveness of potential evapotranspiration-driven cooling of the PV arrays by the understory vegetation. The estimation of reference evapotranspiration over a vegetated area uses the Penman-Monteith model, which is one of the most widely used approaches to estimating ET from land surfaces: (Monteith, 1965)

$$\boldsymbol{ET_o} = \frac{\Delta\cdot(\boldsymbol{K}+\boldsymbol{L})+\boldsymbol{\rho_a}\cdot\boldsymbol{c_a}\cdot\boldsymbol{C_{at}}\cdot\boldsymbol{e_a}^*\cdot[\boldsymbol{1}-\boldsymbol{RH}(\boldsymbol{z_m})]}{\boldsymbol{\rho_w}\cdot\boldsymbol{\lambda_v}\cdot[\Delta+\boldsymbol{\gamma}\cdot(\boldsymbol{1}+\boldsymbol{C_{at}}/\boldsymbol{C_{can}})]} \quad \text{Eq. 1}$$

Where Δ is the slope of the saturation-vapor-pressure curve (kPa/°C), K is the net solar radiation (MJ m^{-2} day^{-1}), L is the net longwave radiation (MJ m^{-2} day^{-1}), ρ_a is air density (kg m^{-3}), c_a is the specific heat of air (MJ kg^{-1} $°C^{-1}$), e_a^* is the saturation vapor

pressure (kPa), $RH(z_m)$ is the relative humidity (unitless), ρ_w is the water density (kg m^{-3}), λ_v is the latent heat of vaporization (MJ kg^{-1}), γ is the psychromatic constant (kPa °C^{-1}), C_{at} is the atmospheric conductance (m day^{-1}), and C_{can} is the canopy conductance (m day^{-1}). **Eq. 2** accounts for different vegetation types with C_{can}, which is defined as follows:(Dingman, 2015)

$$\boldsymbol{C_{can} = k_s \cdot LAI \cdot C_{leaf}}, \text{ Eq. 2}$$

where k_s is a shelter factor that ranges from 0.5 to 1; LAI, or leaf area index, is the total area of leaf surface above ground area A divided by A; and C_{leaf} is leaf conductance that is determined as follows (Dingman, 2015):

$$\boldsymbol{C_{leaf} = C^*_{leaf} \cdot f_K(K_{in}) \cdot f_\rho(\Delta\rho_v) \cdot f_T[T(z_m)] \cdot f_\theta(\Delta\theta)}, \qquad \text{Eq. 2}$$

where C^*_{leaf} is the maximum value of leaf conductance, K_{in} is incident shortwave radiation flux, $\Delta\rho_v$ is the difference between the saturated and actual absolute humidity of the air, $T(z_m)$ is air temperature at the measurement height, and $\Delta\theta$ is the difference between the field capacity and the actual water content of the root zone. ET_o is then multiplied by the crop coefficient to take into account various soil and vegetation conditions in calculating potential evaporation and crop evaporation (R. G. Allen *et al.*, 1998).

Stewart model of leaf conductance (non-linear functions) and the Penman–Monteith model was used to compare the transpiration rate from the canopy for soil-moisture deficits (Δθ) of 0 cm (wet soil) and 8.0 cm (dry soil). Even though the leaf

conductance nonlinear functions for environmental controls on canopy conductance (incident short-wave radiation, specific humidity deficit, air temperature and soil moisture deficit) used in this example are not specifically for grassland species, it's instructive to visualize the significance of water limitations and temperature on evapotranspiration. Each term of the leaf conductance equation is defined below.

Leaf conductance nonlinear functions (Stewart, 1988)

Light, Incident solar radiation, K_{in} (MJ m^{-2} day^{-1}):

$$f_k(K_{in}) = \frac{12.78.K_{in}}{11.57.K_{in} + 104.4}, \qquad \textbf{Eq. 3}$$

$$0 \leq K_{in} \geq 86.5 \text{ MJ m}^{-2} \text{ day}^{-1}$$

Absolute humidity deficit (Kg m^{-3}):

$$f_p(\Delta\rho_v) = 1 - 66.6\,\Delta\rho_v, \quad 0 \leq \Delta\rho_v \leq 0.01152\ Kgm^{-3}; \qquad \textbf{Eq. 4}$$

$$f_p(\Delta\rho_v) = 0.233, \quad 0.01152\ Kgm^{-3} \leq \Delta\rho_v$$

Air temperature, $T(z_m)$ (°C):

$$f_T[T(z_m)] = \frac{T(z_m) \cdot [40 - T(z_m)]^{1.18}}{691}, \qquad \textbf{Eq. 5}$$

$$0 \leq T(z_m) \leq = 40℃$$

Soil moisture deficit, Δθ (cm):

$$f_\theta(\Delta\theta) = 1 - 0.00119 \cdot \exp(0.81 \cdot \Delta\theta), \qquad \textbf{Eq. 6}$$

$$\leq \Delta\theta \leq 0.01152\ Kg\ m^{-3}$$

Bare soil evaporation

Evaporation from bare soil is often described as having two stages (Ritchie, 1972): Stage 1 and Stage 2. During Stage 1, E_s is limited by energy availability at the soil surface,

rather than water availability. During Stage 2, water supply to the soil surface is unable to keep up with the potential evaporation rate, and a portion of the evaporation occurs in the subsurface. Because the rainfall events in the study area occur every one to two days during the growing season, the soil surface stays in Stage 1 most of the time.(Richard G. Allen *et al.*, 2005) In this case, potential soil water evaporation from a wet soil (E_{so}) surface can be calculated as follows(Richard G. Allen *et al.*, 2005):

$$E_{so} = K_{c\ ini} ET_o \qquad \textbf{Eq. 7}$$

where $K_{c\ ini}$ is the initial crop coefficient that is used during the initial stages of crop growth when the area of ground covered by vegetation is less than or equal to 10% (functionally bare). $K_{c\ ini}$ is calculated as follows:

$$K_{c\ ini} = \frac{TEW - (TEW - REW) exp\left(\frac{t_w \cdot 1.15 ET_o - REW}{TEW - REW}\right)}{t_w ET_o} \qquad \textbf{Eq. 8}$$

Where REW and TEW are readily evaporable water and total evaporable water (mm) and t_w is the average time between wetting events in days. This equation applies for periods when t_w exceeds the duration of Stage 1. Details on estimating TEW, REW, and the duration of Stage 1 can be found in Allen, 2005 (Richard G. Allen *et al.*, 2005). If t_w is smaller than the duration of Stage 1, $K_{c\ ini}$ is defined as:

$$K_{c\ ini} = 1.15 \qquad \textbf{Eq. 9}$$

Eqs. 9 and **10** serve as the basis for the estimation of $K_{c\ ini}$ shown in Fig. 3.4a. In comparison to $K_{c\ ini}$, crop coefficient for vegetated surface K_c varies between 0.7 to 1.15 depending on the type of vegetation, growth stage, and maximum growth height (R. G.

Allen *et al.*, 1998). The Basal crop coefficient range non stressed grazing pastures (0.85 – 1.05) in subhumid climates (for use with the FAO Penman-Monteith ET_0) are from Allen *et al.* (1998).

Text A5. Statistical analysis

Kolmogorov-Smirnov (KS) tests for comparison of soil and microclimatic variables across relative position and vegetation treatments.

Two-sample KS tests ($\alpha = 0.05$) were performed to compare the distributions of soil moisture and soil temperature among all the relative position within the bare PV and the veg PV treatments to examine the spatial variability within each treatment. Distributions of soil moisture, soil temperature, air temperature, relative humidity, wind speed, panel temperature, and power production between the two treatments were also compared to study the effect of vegetation on these variables.

Within each treatment, the distributions of soil moisture and soil temperature were significantly different among all the relative positions (**Table A.2**). Between treatments, the distributions of soil moisture, soil temperature, and wind speed were all significantly different (**Table A.2**). However, the p-values for the KS-test for the distributions of air temperature, relative humidity, panel temperature, and power production were much larger than those of the other variables, and the D-statistics for these variables were an order of magnitude less than those of the other variables as well.

Tables

Table A.1 Parameter used for the ET model (Penman Monteith with Stewart model)

NO.	PARAMETER	VALUE	SOURCE/REMARKS
1.	Heigh of vegetation (h) m	0.6	Field observation from site (tall grass)
2.	Wind speed (u) ms^{-1}	4	From field data
3.	Displacement height (z_d)	0.7h	Dingman, 2015
4.	Roughness length (z_0)	0.1h	Dingman, 2015
5.	Air temperature (T_{air}) ^oC	25	From field data
6.	Relative humidity RH (%)	60 %	
7.	Specific heat capacity of air (KJ Kg^{-1} K^{-1})	1.005	
8.	Density of water (Kg m^{-3})	996	
9.	Density of air (Kg m^{-3})	1.20	
10.	Latent heat of vaporization (MJ Kg^{-1})	2.45	
11.	Psychrometric constant (kPa K^{-1})	0.067	
12.	Global irradiance ($MJm^{-2}Day^{-1}$)	24	Daily Net Radiation is calculated based on the methods in Allen *et al.*, 2005b
13.	Albedo	0.11	(Dingman, 2015)
14.	Maximum daily temperature ($T_{a\ max}$) ^oC	30.8	From field data
15.	Minimum daily temperature ($T_{a\ min}$) ^oC	17	From field data
16.	Elevation m	282	Site location
17.	Latitude	45.5^o	Site location
18.	Maximum leaf stomatal conductance (mm s^{-1})	8	(Federer *et al.*, 1996; Kelliher *et al.*, 1995; Schulze *et al.*, 1994)
19.	Shelter factor (K_s)	0.60	(Dingman, 2015)
20.	Leaf Area Index (LAI)	1.8	(Federer *et al.*, 1996; Kelliher *et al.*, 1995; Schulze *et al.*, 1994)
21	Soil moisture deficit ($\Delta\theta$)	0 and 8 cm	0 – near field capacity 8 – Dry soil

Table A.2 KS test to compare the soil properties among the relative positions within each treatment

	Soil Moisture			Soil Temperature		
Treatment	**Relative position**	**D**	**p-value**	**Relative position**	**D**	**p-value**
Bare PV	BP - EE	0.87737	<2.2e-16	BP - EE	0.13135	<2.2e-16
	BP - IS	0.71756	<2.2e-16	BP - IS	0.22493	<2.2e-16
	BP - WE	0.3584	<2.2e-16	BP - WE	0.14685	<2.2e-16
	EE - IS	0.28489	<2.2e-16	EE - IS	0.09519	<2.2e-16
	EE - WE	0.91709	<2.2e-16	EE - WE	0.2998	4.92E-05
	IS - WE	0.74805	<2.2e-16	IS - WE	0.082571	<2.2e-16
Veg PV	BP - EE	0.23577	<2.2e-16	BP - EE	0.17785	<2.2e-16
	BP - IS	0.71104	<2.2e-16	BP - IS	0.24949	<2.2e-16
	BP - WE	0.71468	<2.2e-16	BP - WE	0.11187	<2.2e-16
	EE - IS	0.50161	<2.2e-16	EE - IS	0.081978	<2.2e-16
	EE - WE	0.50195	<2.2e-16	EE - WE	0.077066	<2.2e-16
	IS - WE	0.075965	<2.2e-16	IS - WE	0.14744	<2.2e-16

Table A.3 KS tests among the treatments

Variable	*Treatment*	*Relative position*	*D-statistic*	*p-value*
Soil moisture	Bare PV - veg PV	BP	0.82597	<2.2e-16
	Bare PV - veg PV	EE	0.39668	<2.2e-16
	Bare PV - veg PV	IS	0.88897	<2.2e-16
	Bare PV - veg PV	WE	0.99483	<2.2e-16
Soil temperature	Bare PV - veg PV	BP	0.1438	<2.2e-16
	Bare PV - veg PV	EE	0.08833	<2.2e-16
	Bare PV - veg PV	IS	0.1543	<2.2e-16
	Bare PV - veg PV	WE	0.16463	<2.2e-16
Air temperature	Bare PV - veg PV	N/A	0.022273	0.005715
	Bare PV - control	N/A	0.01689	0.0689
	Veg PV - control	N/A	0.021666	0.007835
Relative humidity	Bare PV - veg PV	N/A	0.034553	1.51E-06
	Bare PV - control	N/A	0.027215	0.000318
	Veg PV - control	N/A	0.017269	0.05913
Wind speed				
	Bare PV - veg PV	N/A	0.064787	<2.2e-16
Max	Bare PV - control	N/A	0.74767	<2.2e-16
	Veg PV - control	N/A	0.74674	<2.2e-16
	Bare PV - veg PV	N/A	0.069275	<2.2e-16
Min	Bare PV - control	N/A	0.74166	<2.2e-16
	Veg PV - control	N/A	0.74293	<2.2e-16
	Bare PV - veg PV	N/A	0.075711	<2.2e-16

Mean	Bare PV - control	N/A	0.16902	<2.2e-16
	Veg PV - control	N/A	0.12422	<2.2e-16
Panel temperature				
All daylight hours	Bare PV – veg PV	N/A	0.016938	0.06758
Hours 10 – 15	Bare PV – veg PV	N/A	0.32182	0.09402
Before 10 and after 15	Bare PV – veg PV	N/A	0.022696	0.02088
Power production				
All daylight hours	Bare PV – veg PV	N/A	0.016938	0.06758
Hours 10 – 15	Bare PV – veg PV	N/A	0.32182	0.09402
Before 10 and after 15	Bare PV – veg PV	N/A	0.022696	0.02088

Figures

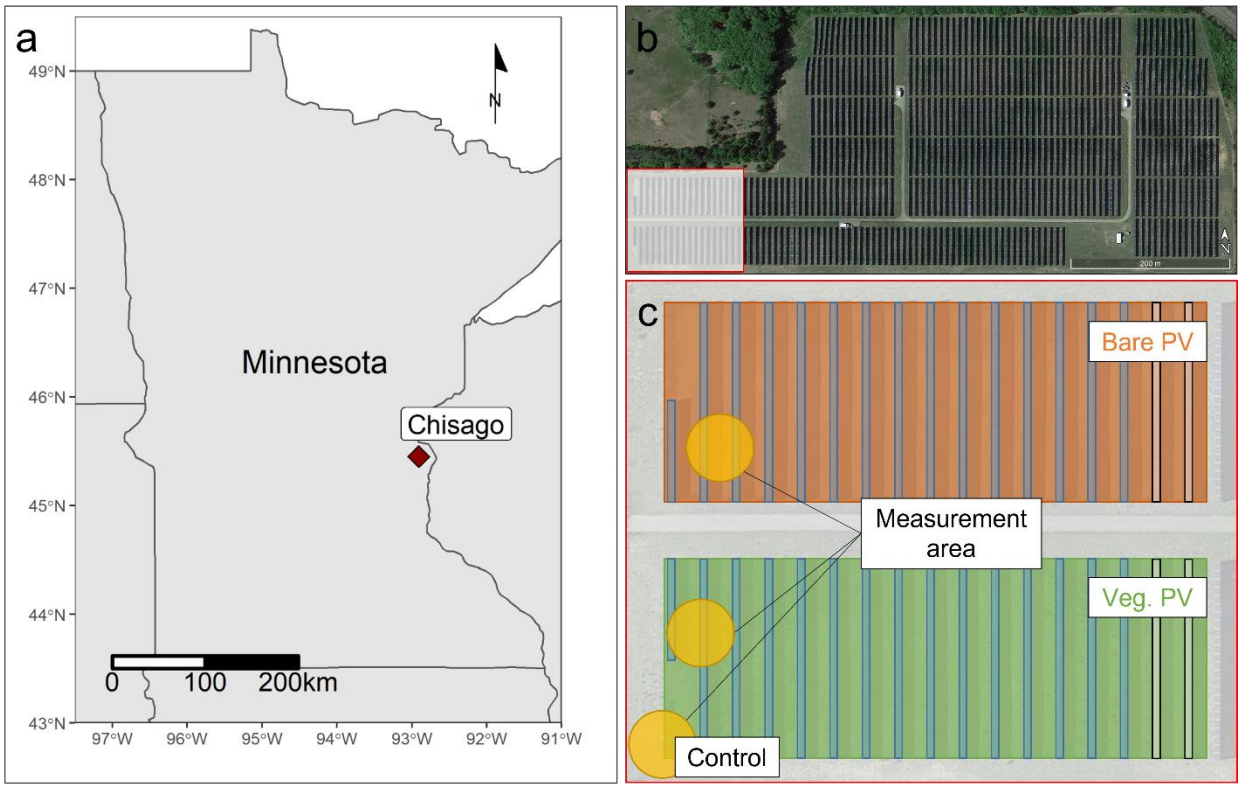

Figure A.1 a. location of the study site in Minnesota; b. complete extent of the PV plant in Chisago with the study area outlined in the red rectangle; c. Zoom-in of the study area utlined in b; the electricity production data analyzed were from the PV arrays that are highlighted in blue.

Figure A.2 Sensor towers in a. bare PV treatment; b. veg PV treatment; and c. Control.

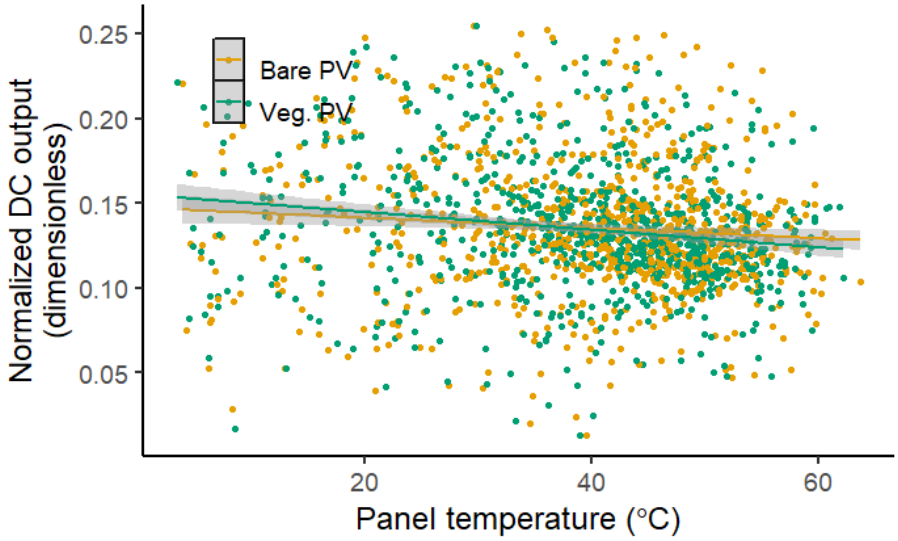

Figure A.3 The effect of panel temperature on the power output. The shaded area represents a 95% confidence interval.

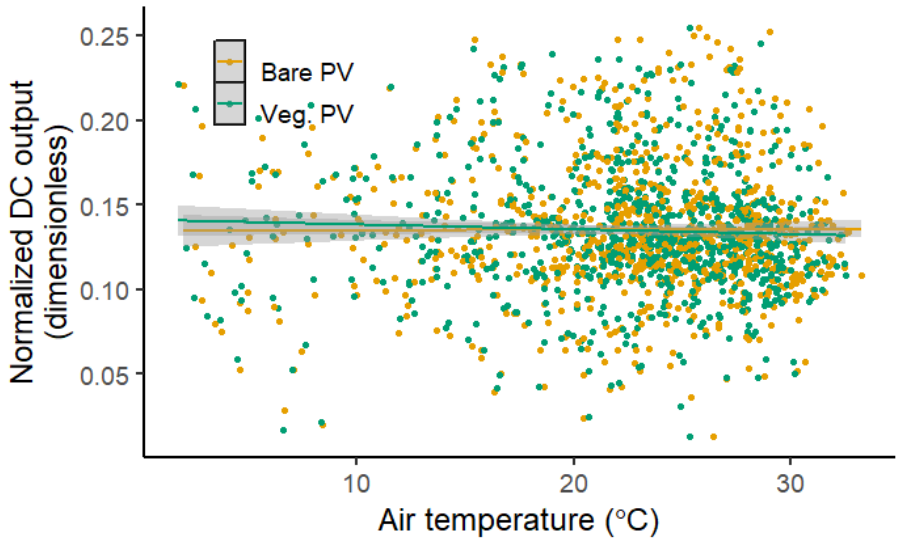

Figure A.4 The effect of air temperature on the power output. The shaded area represents a 95% confidence interval.

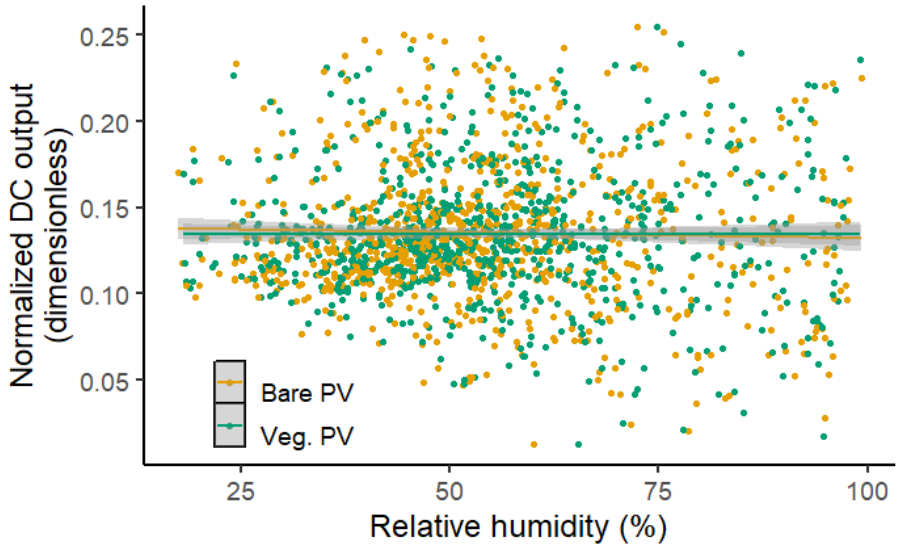

Figure A.5 The effect of relative humidity on power output. The shaded area represents a 95% confidence interval.

References

Allen, R. G., Pereira, L. S., Raes, D., and Smith, M., (1998), *Crop evapotranspiration: Guidelines for computing crop water requirements: FAO Irrigation and Drainage Paper 56*. Rome, Italy. Retrieved from https://www.fao.org/3/x0490e/x0490e00.htm

Allen, R. G., Pruitt, W. O., Raes, D., Smith, M., and Pereira, L. S., (2005a), Estimating evaporation from bare soil and the crop coefficient for the initial period using common soils information. *Journal of Irrigation and Drainage Engineering*, *131*, 14–23, https://doi.org/10.1061/(ASCE)0733-9437(2005)131:1(14).

Allen, R. G., Walter, I. A., Elliot, R., Howell, T., Itenfisu, D., and Jensen, M., (2005b), The ASCE standardized reference evaporation equation. *Watershed Management and Operations Management 2000*, *2000*, 1-11, https://doi.org/10.1061/40499(2000)126

Dingman, S.L., (2015), *Physical hydrology* (D. Rosso, Ed.): Long Grove, IL, Waveland Press.

Federer, C. A., Vörösmarty, C., and Fekete, B., (1996), Intercomparison of methods for calculating potential evaporation in regional and global water balance models: *Water Resources Research*, *32*(7), 2315–2321, https://doi.org/10.1029/96WR00801.

Kelliher, F. M., Leuning, R., Raupach, M. R., and Schulze, E. -D., (1995), Maximum conductances for evaporation from global vegetation types. *Agricultural and Forest Meteorology*, *73*(1-2), 1–16, https://doi.org/10.1016/0168-1923(94)02178-M.

Monteith, J., (1965), Evaporation and environment. *Symposia of the Society for Experimental Biology*, *19*, 205–234.

Ritchie, J. T., (1972), Model for predicting evaporation from a row crop with incomplete cover: Water Resources Research, v. 8, p. 1204–1213, doi:10.1029/WR008i005p01204.

Schulze, E.-D., Kelliher, F.M., Körner, C., Lloyd, J., and Leuning, R., (1994), Relationships among maximum stomatal conductance, ecosystem surface conductance, carbon assimilation rate, and plant nitrogen nutrition: a global ecology scaling exercise: Annual Review of Ecology and Systematics, v. 25, p. 629–662, doi:10.1146/annurev.es.25.110194.003213.

Stewart, J., (1988), Modelling surface conductance of pine forest: Agricultural and Forest Meteorology, v. 43, p. 19–35, doi:10.1016/0168-1923(88)90003-2.

APPENDIX B

SUPPLEMENTAL INFORMATION FOR CHAPTER 3

Table B.1 Details of the three study sites in Minnesota, USA.

Site	Capacity (MW-AC)	Facility area (ha)	County	Latitude (degrees)	Longitude (degrees)	Prior land uses
Atwater	4	16.23	Kandiyohi	45.140815	-94.769841	97.7% agricultural, 2.3 % medium- and low- intensity development
Chisago	6.5	25.25	Chisago	45.451238	-92.907242	83.3% agricultural, 11.6% forest and grasslands, 5.1% developed open space
Eastwood	5.5	20.11	Blue Earth	44.15568	-93.914649	93.0% agriculture, 4.0% developed area, 3.0% forest and grasslands

Table B.2 Measured microclimate variables and the measurement locations.

Variable	Treatments	Instrument	Notes
Wind speed and direction	Veg PV, Bare PV, Control	Campbell Scientific, USA: 03002 Wind Sensor	Positioned 1.5 meters above ground; Averaged over a 15-minute interval
Relative humidity and air temperature	Veg PV, Bare PV, Control	Campbell Scientific, USA: EE181 Temperature and Relative humidity probe	0.5 meter above ground; 15-minute interval
Soil water content and temperature	Veg PV, Bare PV, Control	Campbell Scientific, USA: CS655 Water Content Reflectometers	25 cm below ground; Four locations in bare PV and veg PV; two locations in Control; 15-minute interval
Back-of-the-panel temperature	veg PV and bare PV	Campbell Scientific, USA: CS240	One per treatment; 15-minute interval
Precipitation depth	Control	Campbell Scientific, USA: TE525 Tipping Bucket Rain Gage	Summed over a 15-minute interval
Radiation intensity	Control	Campbell Scientific, USA: CS320 Thermopile Pyranometer	Averaged over a 1-hour interval

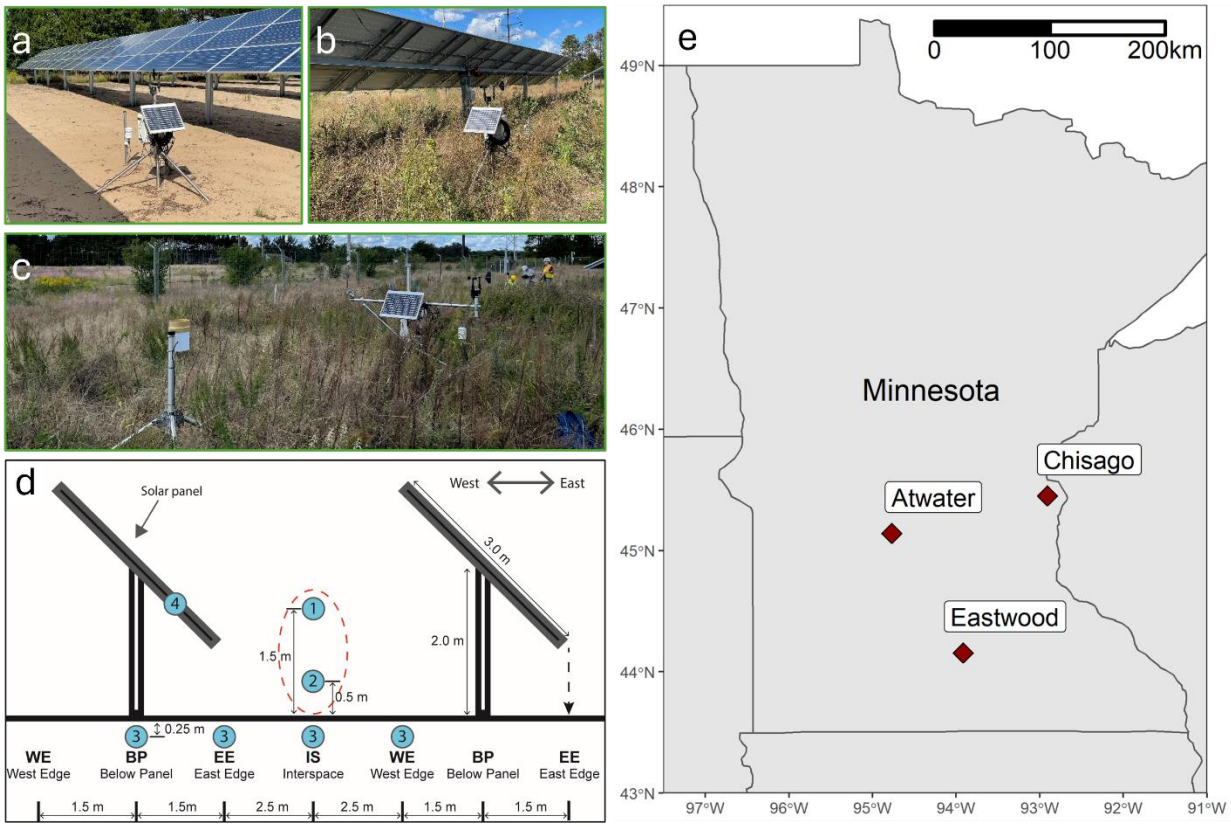

Figure B.1 a. Vegetated PV site (veg PV); b. Bare PV site (bare PV); c. Adjacent site with native vegetation and no solar (Control); d. Instrument setup in the veg PV and bare PV; e. Location of the studied solar facilities in Minnesota

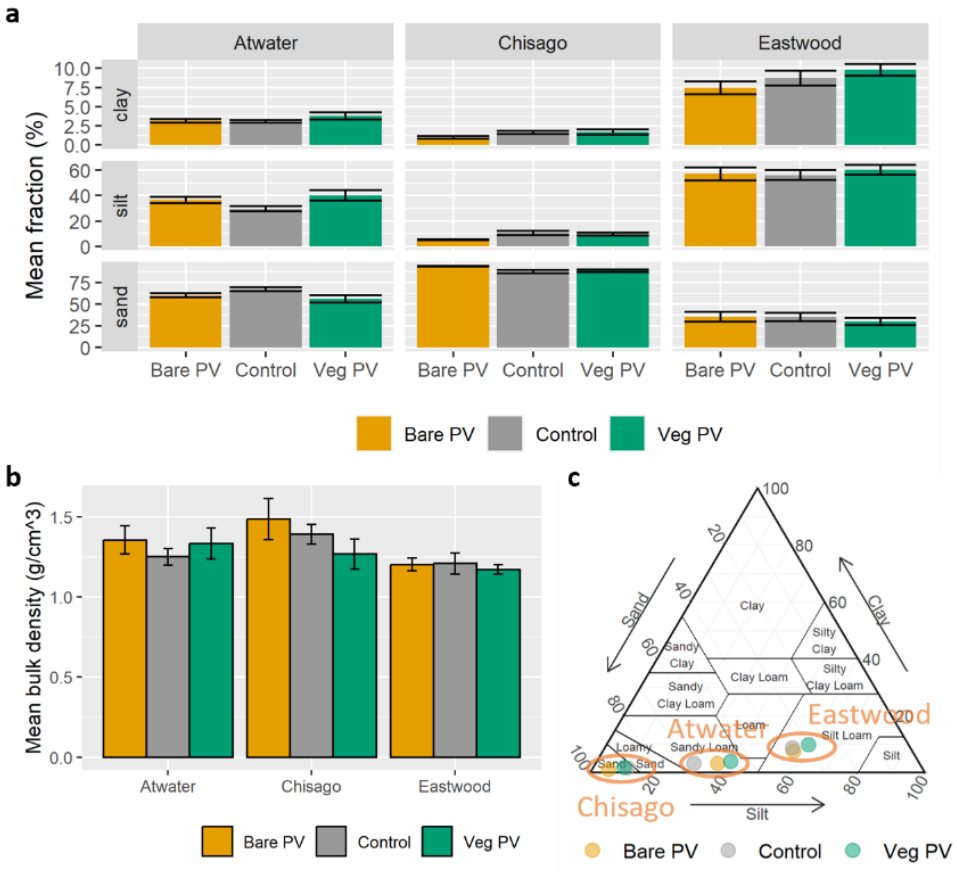

Figure B.2 a. Relative abundance of sand, silt, and clay size fractions of the soil samples from Atwater, Chisago, and Eastwood; b. Mean bulk densities; c. Classification of the mean texture of soil samples of each treatment from all three facilities.

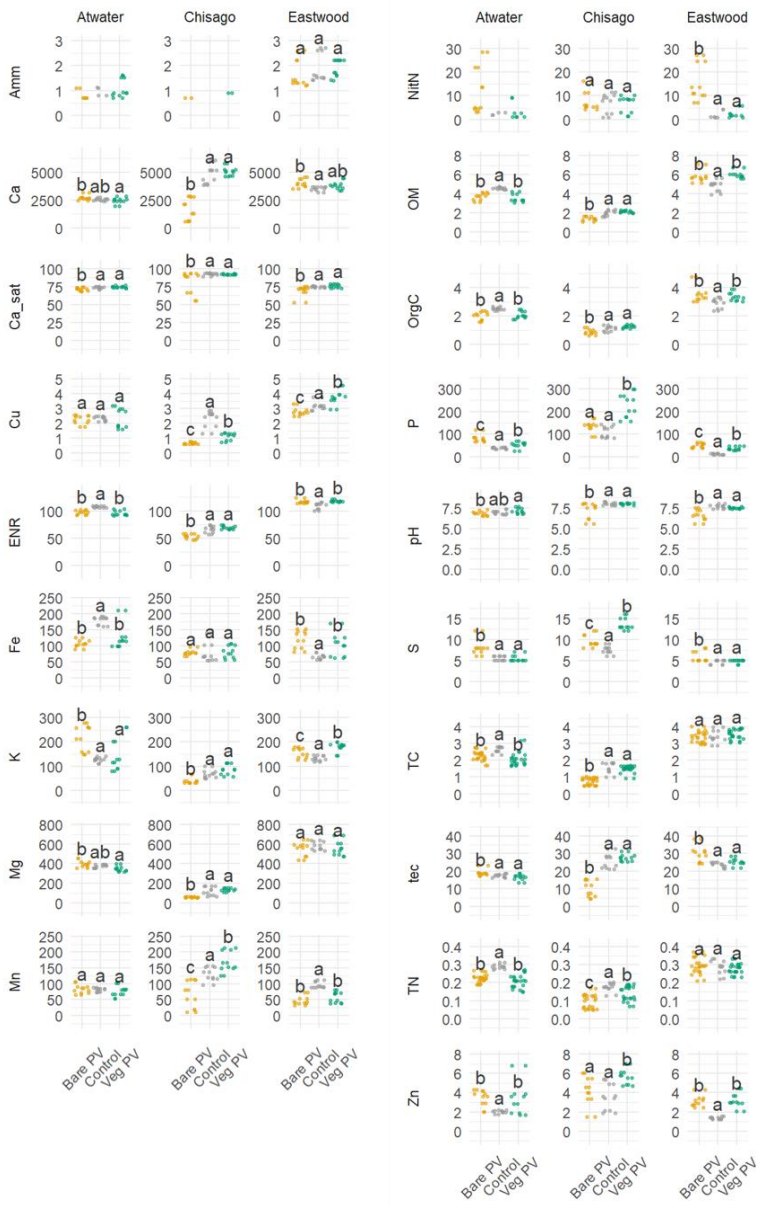

Figure B.3 Comparison of soil nutrient contents using ANOVA and Tukey Honestly Significant difference. Amm = ammonia, TotC = total carbon, OrgC = organic carbon, TotN = total nitrogen, NitN = Nitrate-nitrogen, Amm = Ammoniacal nitrogen, P = phosphorus, K = potassium, Ca = calcium, Ca_sat = calcium base saturation percentage, Cu = copper, S = sulfur, Mg = magnesium, Fe = iron, Mn = manganese, B = boron, and Zn = zinc.

APPENDIX C

COPYRIGHT PERMISSIONS

A version of Chapter 2 is published in Wiley journal *Earth's Future*. The citation is as follows:

Choi, C. S., Macknick, J., Li, Y., Bloom, D., McCall, J., & Ravi, S. (2023). Environmental Co-Benefits of Maintaining Native Vegetation With Solar Photovoltaic Infrastructure. *Earth's Future*, *11*(6), 1–12. https://doi.org/10.1029/2023EF003542

Permission is granted by Wiley to reproduce articles in dissertation and theses:

https://www.wiley.com/en-us/network/publishing/research-publishing/trending-stories/how-to-clear-permissions-for-a-thesis-or-dissertation on their website.